



**The Development of Dimple Shape Dry Powder Carrier for Ethambutol
Dihydrochloride and Its Antituberculosis Evaluation**

Md Iftekhar Ahmad

**A Thesis Submitted in Fulfillment of the Requirements for the Degree of
Doctor of Philosophy in Pharmaceutical Sciences**

Prince of Songkla University

2014

Copyright of Prince of Songkla University

This is to certify that the work here submitted is the result of the candidate's own investigations. Due acknowledgement has been made of any assistance received.

.....

(Assoc. Prof. Dr. Teerapol Srichana)

.....

(Md Iftekhar Ahmad)

I hereby certify that this work has not been accepted in substance for any other degree, and is not being currently submitted in candidature for any degree.

.....

(Md Iftekhar Ahmad)

Thesis Title The Development of Dimple Shape Dry Powder Carrier for
Ethambutol Dihydrochloride and Its Antituberculosis
Evaluation

Author Mr. Md Iftekhar Ahmad

Major Program Doctor of Philosophy (Pharmaceutical Sciences)

Academic Year 2014

Major Advisor

.....
(Assoc. Prof. Dr. Teerapol Srichana)

Examining Committee

.....Chairperson
(Assoc. Prof. Dr. Suwipa Ungphaiboon)

.....
(Assoc. Prof. Dr. Teerapol Srichana)

.....
(Assist. Prof. Dr. Kwunchit Oungbho)

.....
(Dr. Prapasri Sinsawat)

The Graduate School, Prince of Songkla University, has approved this thesis as fulfillment of the requirements for the Doctor of Philosophy Degree in Pharmaceutical Sciences.

.....
(Assoc. Prof. Dr. Teerapol Srichana)
Dean of Graduate School

Thesis Title	The Development of Dimple Shape Dry Powder Carrier for Ethambutol Dihydrochloride and Its Antituberculosis Evaluation
Author	Mr. Md Iftekhar Ahmad
Major Program	Doctor of Philosophy (Pharmaceutical Sciences)
Academic Year	2014

ABSTRACT

The aim of this study was to develop the dry powder inhaler formulations of micro size chitosan (CS) and nano size ethambutol dihydrochloride to target the alveoli and to check its toxicity on the respiratory cell lines.

Ethambutol dihydrochloride (EDH) is primarily a bacteriostatic and anti-tuberculosis agent that is used in combination with other first-line anti-tuberculosis agents mainly because of its synergy with other first-line drugs. The oral dose of EDH is 20 mg/kg and this produces peak plasma levels of 3 to 5 µg/mL. Due to this relatively high oral dose, ethambutol causes visual impairment, if used consistently over a long time. The side-effects of the EDH are dose and time dependent. The studies have shown consistent decrease in the case of visual impairment with decrease in the dose. If EDH could be administered in an aerosol form with a dry powder inhaler (DPI), perhaps the dose of EDH could be dramatically reduced and the side effects of ethambutol could be better controlled.

The micro size chitosan was prepared by spray drying and later its particle size, shape, surface area, porosity, degree of deacetylation, and angle of repose were determined. The nanosize drug was obtained by nanospray drying and later five formulations were developed by physically mixing the CS and EDH. The developed formulations were characterized for its aerosol property, melting point, functional group,

and deaggregation. The developed formulations were further monitored for its cell toxicity, bioactivity, and permeability through lipid bilayers.

The nano size EDH (260 nm), spherical with smooth surface was obtained by nano spray drying and micro size chitosan (CS) (1.2 μm) was prepared by spray drying at specific condition. The degree of deacetylation of CS before spray drying (56%) was lower than after spray drying (58%). Five formulations i.e. 1:2, 1:2.5, 1:3.3, 1:5, and 1:10 w/w of the EDH to chitosan carrier namely formulation #1 to #5 were prepared by physical mixing. Chitosan formed dimple surface over its body after spray drying at specific conditions. This dimpled surface provided shallow cavities to which the drug was bound, both within its grooves as well as on its surface. The EDH had shown sharp melting point at 203°C while the carrier had a very low crystallinity and was highly amorphous. The formulations showed low crystallinity at a low temperature but later showed amorphous nature. The FTIR spectra showed interaction between the chitosan carrier and the EDH. The prepared formulations had a uniform drug content of the labeled amount. The prepared formulations had a uniform drug content of the labeled amount. The median adhesion force (50% of drug detachment) for formulations # 1 to # 5 was between 122 – 993 μN . The mass median aerodynamic diameter of the EDH was within the range (2.3-2.7 μm) to target alveoli, having fine particle fractions (aerosolized particles less than 4.4 μm) of 32-42% of the nominal dose. The developed formulations have shown % viability of more than 80% and were not toxic to the A549, Calu-3, and NR8383 cell lines. The potency of formulations has increased to two-fold due to the chitosan in formulation. The permeability through lipid bilayer was between 56-71%. The formulations were completely engulfed by the macrophage cell after 30 min.

In conclusion, EDH DPI is a promising formulation for controlling the tuberculosis especially in minimizing the risk of multidrug resistant tuberculosis.

ACKNOWLEDGEMENTS

My journey to obtain a PhD degree ends with the successful completion of this thesis. In this journey, I did not travel in vacuum or darkness but were kept on track and been seen through to completion with the support, guidance and encouragement of numerous people including my friends, colleagues, teaching and non-teaching staff of this faculty. At the end of my thesis, I would like to express my deep and sincere gratitude to all those who contributed in many ways for successful completion of this study and to make it an unforgettable experience for me.

First and foremost, I would like to express my honest, sincere, and heartfelt gratitude to my advisor Associate Professor Dr. Teerapol Srichana, Faculty of Pharmaceutical Sciences and Dean of Graduate School, Prince of Songkla University, who gave me the opportunity to study Ph.D program. I am thankful for his continuous support during Ph.D study, research, patience, motivation, inspiration, enthusiasm, and immense knowledge. His tutelage helped me all the time during research work and in writing manuscript and thesis. I could not have imagined having a better advisor or mentor for my Ph.D study than him. I am short of words to express adequately my appreciation and gratitude to him.

I extend my thanks to Associate Professor Dr. Suwipa Ungphaiboon, Department of Pharmaceutical Technology, Faculty of Pharmaceutical Sciences, Prince of Songkla University, for her support and guidance in research and manuscript editing.

I take this opportunity to sincerely acknowledge the Graduate School, Prince of Songkla University, Songkhla, Thailand, for providing financial assistance in the form of scholarship which buttressed me to perform my lab work and in attending the conference, comfortably. I would also like to thank Department of Pharmaceutical Technology, Faculty of Pharmaceutical Sciences, and Prince of Songkla University for providing me all the assistance related with the Ph.D. thesis.

I would also like to appreciate the Nanotec-PSU Excellence Center on Drug Delivery System, Faculty of Pharmaceutical Sciences, Prince of Songkla University, for providing their facilities and scholarship over whole duration of study.

I gratefully acknowledge the staff and scientist (Ms. Kornkamon Petyord, Ms. Supreede Songkarak, Ms. Titpawan Nakpheng, Ms. Wilaiporn Buatong, Mr. Ekawat Thawithong and Mr. Vikrom Changarn) of Nanotec-PSU Excellence Center on Drug Delivery System, Faculty of Pharmaceutical Sciences, Prince of Songkla University for teaching the cell culture techniques and training me to operate the various equipment. I thank them all for their help, without them, it was difficult for me to finish my Ph.D thesis work.

I owe a great deal of appreciation and gratitude to Dr. Brian Hodgson for editing the manuscript and offering suggestion for improvement.

I acknowledge Miss Panisara Boonsanong, education service officer of Faculty of Pharmaceutical Sciences, Prince of Songkla University, who keeps on coordinating and updating the information of academic process through mails.

I would like to extend my heartfelt thanks to my seniors, Dr. Wipaporn Kajornwongwattana, Dr Neelam Balekar and Dr Gangadhar Katkam for their guidance and encouragement in beginning of my study.

I am also strongly indebted to my Ph.D and M.Pharm colleagues during my study period, Dr Somchai Sawatdee, Mr. Tan Suwandecha, Mr. Janewit Dechraksa, Ms Janjira, Ms. Kanogwan, Ms Teerarat and Ms Anongtip for helping in experiments, data analysis and general discussion, without their help my research work would not have been possible.

I would like to extend huge and warm thanks to my special friends Ms Kirti Arora, Ms Kausar Jahan and Ms Pang HP, for their constant moral and emotional support during whole period of study.

I expand my special thanks to all friends, Syed Haris Omar, Dr. Lily Jaiswal, Dr. Nilesh Nirmal, Dr. Tanaji Kudre, Dr. Kartikeyan, Dr. Yasir Arafat, Dr. Mustafa, Mr. Yasir Khan, Mr. Ahmer, Mr. Waqar, Mr. Naveen, Mr. Kashif-ur-Rahman,

Mr. Prasad, and Ms Aparna for their moral support and for stimulating a fun filled environment during stay in Prince of Songkla University.

I am strongly indebted to the Prince of Songkla University, Hatyai, Thailand, for providing an excellent infrastructure for extracurricular activities, sports facilities, libraries, laboratories, journals and best healthcare facilities which truly makes life easy in campus.

Last but not least, I would like to pay high regards to my Parents and my all family members for their sincere encouragement and inspiration throughout my research work and lifting me uphill this phase of life. I owe everything to them.

In conclusion, this research would not have been possible without the financial assistance by various granting agencies. I would like to thank (1) Graduate School, Prince of Songkla University, (2) National Research University, (3) Nanotec-PSU Excellence Center on Drug Delivery System and (4) Faculty of Pharmaceutical Sciences, Prince of Songkla University. The grants include thesis fund, monthly salary and for participating in conference, during whole study period.

The author alone bears the responsibility for discussion and conclusions of this thesis and owns any errors it contains.

Md Iftekhar Ahmad

CONTENTS

	Page
ABSTRACT	v
ACKNOWLEDGEMENTS	vii
CONTENTS	x
LIST OF TABLES	xiv
LIST OF ILLUSTRATIONS	xv
LIST OF ABBREVIATION	xvii
CHAPTERS	
1. INTRODUCTION	1
1.1 Rationale	1
1.2 Objectives	7
2. REVIEW OF LITERATURE	8
2.1 Pulmonary route	8
2.2 Inhalation therapy	10
2.3 Dry powder inhaler (DPI)	11
2.3.1 Principles of DPI	11
2.3.2 Advantages of DPI	12
2.3.3 DPI deposition in the lung	15
2.3.3.1. Inertial impaction	16
2.3.3.2. Sedimentation	17
2.3.3.3. Diffusion	17
2.4 Chitosan (CS)	17
2.5 Ethambutol dihydrochloride (EDH)	22
2.6 Tuberculosis	24
2.6.1. Pathogenesis	24
2.6.2. Clinical manifestation	25
2.6.2.1. Systemic effects of tuberculosis	25
2.6.2.2. Pulmonary tuberculosis	25
2.6.2.3. Treatment of tuberculosis	26

CONTENTS (continued)

	Page
2.6.2.3.1. Prevention of drug resistance	26
2.6.2.3.2. Early bactericidal activities	26
2.6.2.3.3. Sterilizing activity	26
3. MATERIALS AND METHODS	29
3.1 Materials	29
3.2 Methods	29
3.2.1 Optimization of spray drying process of EDH	29
3.2.2 Spray drying of CS	30
3.2.3 Molecular weight determination of CS solutions	31
3.2.4 Determination of degree of deacetylation (DD) using nuclear magnetic resonance (NMR)	31
3.2.5 Determination of particle size, surface area, porosity, and flowability of CS	32
3.2.6 Preparation of the EDH formulations by physically mixing EDH with different ratios of CS	33
3.2.7 EDH, CS and EDH formulations imaged by SEM	33
3.2.8 Characterization of EDH, CS and EDH formulations by DSC	33
3.2.9 Characterization of EDH,CS and EDH formulations by FTIR	34
3.2.10 Determination of uniformity of the drug contents in each dose of various formulations	34
3.2.11 Determination of detachment force for EDH from the CS surface by using ultracentrifugation	34
3.2.12 <i>In-vitro</i> deposition of the EDH formulation in an Andersen cascade impactor (ACI)	37

CONTENTS (continued)

	Page
3.3 Cell cultures	37
3.3.1 Human bronchial epithelial cell lines (Calu3)	37
3.3.2 Human lung adenocarcinoma cell lines (A549)	38
3.3.3 Alveolar macrophage cell line (NR8383)	38
3.4 Determination of cytotoxicity of EDH, CS, and EDH formulations.	38
3.5 Determination of cytokine response to EDH formulations	39
3.5.1 Nitric Oxide (NO) by the Griess reaction assay	39
3.6 Assesment of antimycobacterial activity of EDH formulations	39
3.6.1 Culture of <i>M. bovis</i>	39
3.6.2 Determination of MIC against <i>M.bovis</i>	40
3.7 Determination of cell permeability with EDH formulations	40
3.7.1 Lipid bilayers	40
3.7.2 Preparation of lipid bilayers	41
3.7.3 Preparation of electrodes	41
3.7.4 Preparation of transport media	42
3.7.5 Sample collections from Ussing chamber	42
3.7.6 Functioning of Ussing chamber	42
3.8 Phagocytosis of EDH formulations by macrophage cells	43
3.9 Statistical analysis	44
4. Results and Discussions	45
4.1 Optimization of the spray drying process of EDH	45
4.2 Physicochemical properties of CS	47
4.3 Physicochemical properties EDH formulations	51
4.4 Content uniformity of different EDH formulations	54
4.5 Drug carrier deaggregation by ultracentrifugation	55
4.6 ACI evaluation of EDH formulations	56
4.7 Cytotoxicity of EDH, CS and EDH formulations	57

CONTENTS (continued)

	Page
4.8 NO release by AM on interaction with EDH formulations	58
4.9 MIC determination of EDH, CS and EDH formulations on <i>M. bovis</i>	59
4.10 Determination of cell permeability through lipid bilayers	60
4.11 Phagocytosis of EDH formulations by macrophage cells	61
4.12 Discussion	64
4.12.1 Optimization of nano spray drying of EDH	64
4.12.2 Physicochemical characterization of CS	64
4.12.3 Physicochemical characterization of EDH formulations	66
4.12.4 Cytotoxicity and bioactivity of EDH, CS and EDH formulations	67
4.12.5 Cumulative permeation of EDH and EDH formulations through lipid bilayers	68
5. CONCLUSIONS	70
BIBLIOGRAPHY	71
APPENDICES	84
VITAE	92

LIST OF ABBREVIATIONS

α	Alpha
β	Beta
ω	Angular velocity
K	Kelvin
% RSD	Percentage of relative standard deviation
$^{\circ}\text{C}$	Degree Celsius
μg	Microgram
$\mu\text{g/mL}$	Microgram per milliliter
μL	Microliter
μm	Micrometer
μN	Micro newton
%	Percentage
AIDS	Acquired immunodeficiency syndromes
AM	Alveolar macrophage
ACI	Andersen Cascade Impactor
ATCC	American Type Cell Culture
BCG	Bacilli Calmette-Guérin
cm	Centimeter
CI	Carr's Index
CFU	Colony Forming Unit
CS	Chitosan
d_{ae}	Aerodynamic diameter
DD	Degree of deacetylation
DMSO	Dimethylsulfoxide
DPI	Dry powder inhaler
DSC	Differential scanning calorimetry
DE	Device
ED	Emitted dose
EDH	Ethambutol dihydrochloride
FBS	Fetal bovine serum

LIST OF ABBREVIATIONS (continued)

FDC	Fixed-dose combination
FPF	Fine particle fraction
FT-IR	Fourier transform-infrared spectroscopy
f_c	Centrifugation frequency
g	Gram
g/ml	Gram/milliliter
GSD	Geometric standard deviation
h	Hour
HPLC	High performance liquid chromatography
IL-1 β	Interleukin-1 β
IR	Infrared
J/g	Joule/gram
kV	Kilovolt
kPa	Kilopascal
kDa	Kilodalton
L	Liter
L/min	Litre/minute
L/h	Litre/hour
LOD	limit of detection
LOQ	limit of quantitation
LPS	lipopolysaccharide
m	Particle mass
mg/mL	Milligram per milliliter
m	Mole
m ³ /h	Cubic meter per hour
M7H9	Middlebrook 7H9
MDR-TB	Multidrug-resistance tuberculosis
mg	Milligram
MIC	Minimum inhibitory concentrations

LIST OF ABBREVIATIONS (continued)

mL	Milliliter
mL/min	Milliliter per minute
mm	Millimeter
MMAD	Mass median aerodynamic diameter
mmole	Millimole
m/s ²	Meter per second square
MTT	3-(4,5-dimethylthiazol-2-yl)-2,5-diphenyltetrazolium bromide
mN	Milli newton
n	Number of sample
ng	Nanogram
nm	Nanometer
NO	Nitric oxide
NMR	Nuclear magnetic resonance
OADC	Oleic acid-albumin-dextrose catalase
PBS	Phosphate buffer solution
PDI	Polydispersity index
PS	Preseparator
pg/mL	Picogram/milliliter
R	R configuration
RSD	Relative standard deviation
r ²	Correlation coefficient
rad/s	Radian per second
S	S configuration
S	Stage
s	Second
SD	Standard deviation
SEM	Scanning electron microscope

LIST OF ABBREVIATIONS (continued)

TB	Tuberculosis
TNF- α	Tumor necrosis factor- α
U	Unit
UK	United kingdom
USA	United states of America
UV	ultraviolet
v/v	volume/volume
w/w	weight/weight
w/v	weight/volume
WHO	World Health Organization
XDR-TB	extensively drug-resistant tuberculosis

LIST OF ILLUSTRATIONS

Figure		Page
1.1	Ninety-six high burden TB countries	2
2.1	Diagram of pulmonary airways	8
2.2	Schematic branching of human pulmonary airways	9
2.3	Principles of DPI device	12
2.4	Mechanisms of particle deposition in lungs	16
2.5	Structures of chitin and chitosan	18
2.6	Preparation of chitosan from chitin by alkali deacetylation	19
2.7	Structure of EDH	22
2.8	Schematic diagram to show the EDH mechanism of action	23
3.1	Preparation of ultracentrifuge tube: The sieves were sandwiched between two stainless steel tubes and kept inside the plastic centrifuge tube which rotates under different rotational centrifugal force (RCF) after loading the dry powder formulation (a), Position of centrifuge tube under rotation and the separation of drug from the carrier (b)	36
3.2	Schematic diagram of (a) Ussing chamber fitted with lipid bilayer membrane, (b) transwell	41
4.1	SEM images of EDH at 50,000X after nano spray drying at 110°C inlet temperature and 80% spray rate	45
4.2	Optimization of EDH % yield at different inlet temperature (90°, 100°, and 110°) and spray rate conditions (80, 90, and 100%)	47
4.3	NMR spectra of CS (a) before spray drying and (b) after spray drying	49
4.4	SEM images of CS particles at 50,000X (1-6) from spraying of a= 0.1 % (Control/sphere) at 80°C, b=0.2%, c=0.3%, d=0.4%, e=0.5%, f=1% CS solution at 150°C with feeding rate of 3 mL/min	50

LIST OF ILLUSTRATIONS (continued)

Figure		Page
4.5	SEM images of CS and EDH formulations of 1:2 (a), 1:2.5 (b), 1:3.3 (c), 1: 5 (d), 1:10 (e) and CS only (f)	52
4.6	DSC thermograms of EDH, CS, and EDH formulations at different ratios. EDH (a), CS (b), and EDH formulations at various ratios of 1:2 (c), 1:2.5 (d), 1:3.3 (e), 1:5 (f) and 1:10 (g)	53
4.7	FT-IR spectra of EDH (a), CS (b) and EDH formulations at different ratios of 1:2 (c), 1:2.5 (d), 1:3.3 (e), 1:5 (f) and 1:10 (g)	53
4.8	The % detachment of EDH from formulations at various centrifugal forces, 1:2, 1:2.5, 1:3.3, 1:5 and 1:10	56
4.9	Cell viability of A549 (A), Calu 3 (B), NR8383 cell (C) after exposing with different concentrations of EDH, CS and EDH formulations of 1:10, 1:5, 1:3.3, 1:2.5 and 1:2	58
4.10	Nitric oxide (NO) production by macrophage cells after incubating it with EDH, CS and EDH formulations of 1:10, 1:5, 1:3.3, 1:2.5 and 1:2	59
4.11	Cumulative transport showing permeability of EDH, and EDH formulations of 1:10, 1:5, 1:3.3, 1:2.5 and 1:2 across the lipid bilayers	61
4.12	Formulation I treated with Lumidot [®] 640	62
4.13	Phargocytosis of NR8383 cell incubated with EDH formulation I at 2 min (a) and 30 min (b) after staining with Lumidot [®] 640	63

LIST OF TABLES

Table		Page
2.1	Example of commercially available DPIs in the market	13
2.2	Groups of antituberculosis drugs with abbreviation according to the WHO	27
2.3	Different phases for anti-tubercular drug administration	28
4.1	Nano spray drying optimization parameters	45
4.2	Particle size and surface area of chitosan powders obtained from spray drying process of a chitosan solutions.	48
4.3	Physicochemical properties of EDH-chitosan dry powder formulations.	53
4.4	Percent recovery and RSD for accuracy and precision of EDH.	54
4.5	Adhesion forces at 50% drug detachment for different formulations	55
4.6	MIC values of EDH, chitosan and various formulations	59

CHAPTER 1

1.1 Rationale

Tuberculosis (TB) is an infectious bacterial disease characterized by the growth of nodules (tubercles) in the tissues, especially the lungs. Tuberculosis has shown its presence since ancient times i.e. Greece, Rome, Egypt. The early evidence of tuberculosis presence goes back to thousand years back when tubercular decay was found in the spines of Egyptian mummies and Neolithic. Tuberculosis was also known as phthisis by earlier scientist because the body starts waning. A French scientist Rene Laennec (1781-1826), in his observation found that the tubercle lesions present in lungs were also present in the spine, intestine, and lymph glands on autopsy. In 1882 the German bacteriologist Robert Koch (1843–1910), announced his discovery of the tubercle bacillus i.e. *Mycobacterium tuberculosis* (*M. tuberculosis*). The discovery of causative agent had not brought any advancement in tuberculosis treatment. It was being treated by same old method; sanatoria rest, restorative diet, keeping healthy away from the sick, air treatment and by artificially collapsing the lung until the body halts the disease progression (Medcalf et al., 2013). In 1920 BCG vaccine development and discovery of antibacterial in late twentieth century brought some rapid changes in the treatment of tuberculosis.

Tuberculosis is currently an endemic to developing countries and show resurgence in both developing and developed world with high rates of human immunodeficiency (HIV) infection (Grenfell et al., 2013). Tuberculosis has become a significant opportunistic disease among population with a high incidence of acquired immunodeficiency syndrome (AIDS). Globally, 8.6 million people get manifested with tuberculosis disease to which 1.1 million died and additional 0.35 million died with HIV-associated TB (WHO, 2013). TB is considered as the most opportunistic disease associated with AIDS, around 20-25% of AIDS patients suffer from tuberculosis (Ghebreyesus et al., 2010). HIV-infected patients with *M. tuberculosis* infection are 100 times more likely to develop active extra pulmonary tuberculosis than normal hosts due to the immunosuppression (Kwan et al., 2011).

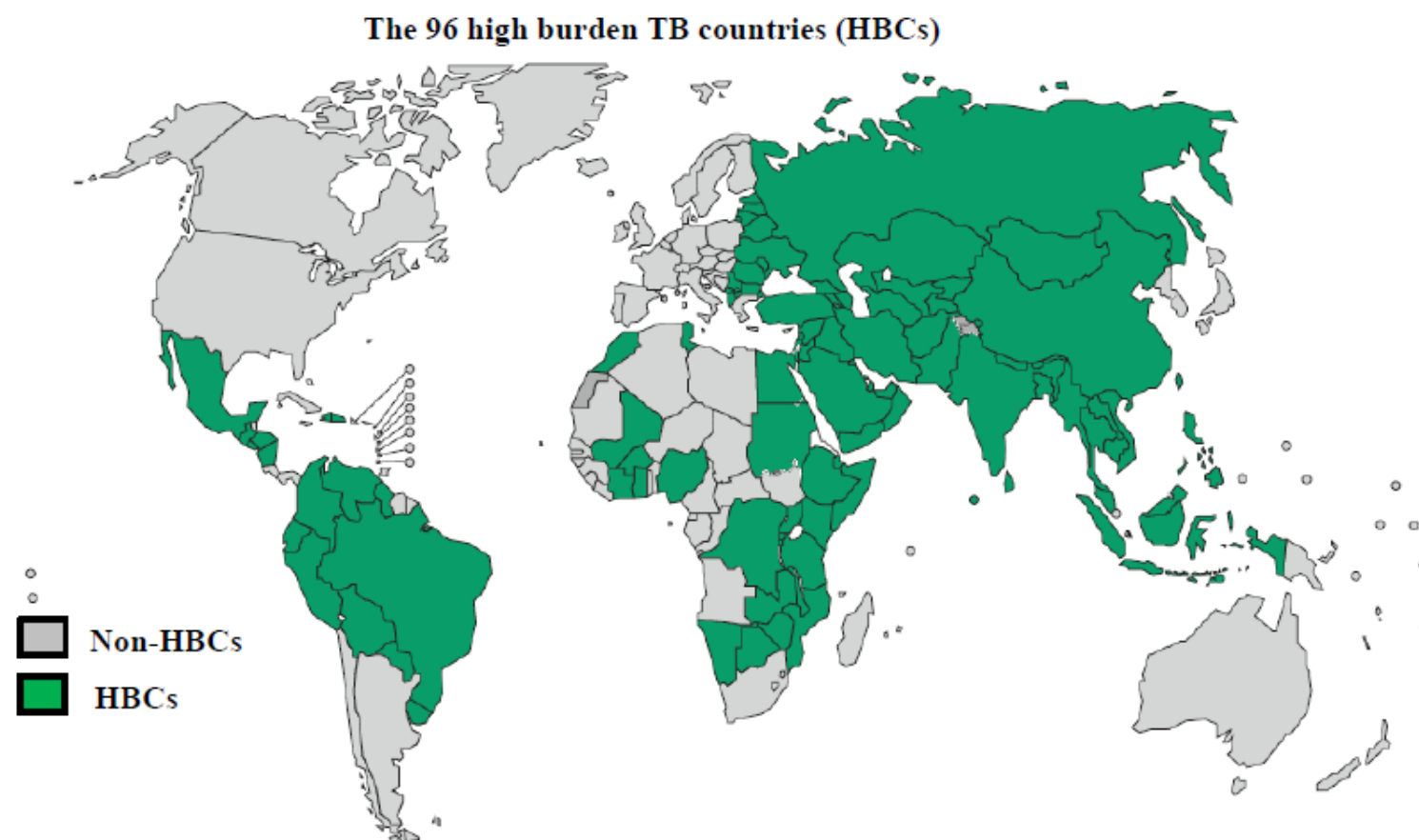


Figure 1.1 Ninety-six high burden TB countries (WHO, 2013).

There has been tremendous growth in case related with multidrug resistance tuberculosis (MDR-TB), extensively drug resistance tuberculosis (XDR) in confluence with HIV epidemic, which turned tuberculosis into a global public health crisis (Lawn et al., 2011). MDR-TB is caused by *M. tuberculosis* that is resistant to at least isoniazid and rifampicin, and XDR-TB is caused by MDR-TB tuberculosis strains that are also resistant to any fluoroquinolone and one of three injectable aminoglycosides (capreomycin, kanamycin, and amikacin). Ninety-six high burden TB countries including Thailand are shown in Figure 1.1 (WHO, 2013). Being a contagious disease, it spreads through air and infects healthy people on an average of 10-15 people each year.

M. tuberculosis is an obligate intracellular pathogen. It is acid-fast, aerobic, non-motile, non-capsulated, non-sporing pathogen, slightly curved bacilli (1-4 μm long). *M. tuberculosis* grows very slow in culture media and takes 2-8 weeks for growth due to presence of mycolic acid over its surface. *M. tuberculosis* grows in Lowenstein Jensen (LJ) medium. *M. tuberculosis* bacilli get killed at 60°C in 15-20 minutes, microbes in sputum survive for 20-30 h. Lungs are the primary site for the pulmonary tuberculosis which comprises more than 80% of all cases, extra-pulmonary TB makes up the remaining 20% (Hunter, 2011). TB spread through the inhalation of droplet from one person to another. When a person with TB of the lung, coughs, sneezes, talks or even sings, the bacteria sprayed out into the air as infectious droplets. These droplets dry up rapidly and the smallest of them remain suspended in the air for several hours. People may inhale these bacteria and become infected. Most TB infections are acquired by continued exposure rather than casual contact because respiratory defense mechanisms can kill small numbers of mycobacteria. TB bacilli can remain viable in the body without spread from one person to another; this phase is called primary tuberculosis. Only 10% of primary tuberculosis develops to post-primary tuberculosis that spread from one person to another (Dube et al., 2014). Antituberculosis drugs are divided into two groups; first and second line medication. First line medication drugs include isoniazid, rifampicin, pyrazinamide, ethambutol, streptomycin, having high therapeutic efficacy. The second line medication includes ethionamide, cycloserine, para-amino-salicylic acid (PAS), capreomycin, levofloxacin, gatifloxacin and moxifloxacin. World health organization (WHO)

recommends short course drug therapy for new infected TB into two phases. Initial phase is an intensive course; the patients have to take three to four drugs (isoniazid, rifampicin, pyrazinamide, ethambutol, and streptomycin) for at least two months. The continuous phase, two drugs are used together for at least four months (usually isoniazid and rifampicin) (Rojanarat et al., 2012).

The main cause of drug resistance in patient is due to the non-adherence to the prescribed drug regimen, poor patient management, or absence of effective policy to control the tuberculosis. The first line medication drugs have high therapeutic efficacy but administering it for long time (at least six months) leads to the ocular, liver and renal toxicity. In addition, by skipping dose, develops drug resistant tuberculosis especially MDR-TB. The chemical agent present in drug may cause severe toxicity and hepatotoxicity to an infected site over a prolonged use which might lead to premature termination of chemotherapy (Chernyaeva et al., 2013). To reduce the menace of tuberculosis, there is urgent need to minimize the duration of drug regimen by targeting the specific organs to kill the tubercle bacilli. The management of MDR, XDR requires high skill, care, and new generation antibiotics. The new generation antibiotics are highly expensive, relatively weak in action and exhibit many side effects to the body.

The development of new anti-tuberculosis drug with great efficacy, less side-effects and economic is likely to be far from satisfactory (Mehanna et al., 2014). Therefore it is the necessity of time to improve the existing drugs therapeutic efficacy by employing suitable drug delivery system. Since pulmonary tuberculosis comprises of more than 80% of TB worldwide, the use of novel inhalable drug delivery systems has received considerable attention in the last few years (Mehanna et al., 2014). Tuberculosis generally affecting the lungs which is characterized by the involvement of alveolar macrophages (AMs), which harbors large amount of *M. tuberculosis* (Maretti et al., 2014). The tubercle bacilli invade AMs and replicate inside it before translocating to other parts of body and causing tuberculosis (Orme, 2014). AM is a type of white blood cell found in the alveoli of lungs. AM acts as a first line of defense. After ingestion of mycobacteria by macrophage, the mycobacteria start replicating intracellularly as a parasite by modulating phagosomal compartment.

The failure in eradicating the initial *M. tuberculosis* microbes leads to the primary disease. Targeting alveolar macrophage by anti-TB drugs by using dry powder inhaler (DPI) to the lungs can bypass the first-pass metabolism, enhance the bioavailability of the drugs at the site of action with large absorptive surface area and at the same time reduce systemic side-effects (Chernyaeva et al., 2013). On the other hand, oral drug therapy for treatment of TB is a lengthy process involving combination of antibiotics with severe side-effects and fails to penetrate the alveolar macrophage. The major reason for limited action of antibiotics to target intracellular infection is the poor drug penetration and bioavailability of anti-tuberculosis drug through oral route (Misra et al., 2011). So, the main task for tuberculosis management should be to make available the sufficient amount of antibiotics intracellularly to kill the tubercles (Parikh et al., 2014).

The reasons for the attention that pulmonary delivery receiving now are due to: (i) the increasing numbers of therapeutic peptide and protein pharmaceuticals being developed with their associated difficulties in conventional oral delivery, (ii) recognition that the rate of absorption from the lung can provide improved pharmacokinetic profiles and (iii) continued interest in respiratory targeting of drugs for lung disorders.

DPI formulation would help to target lungs for killing the bacilli tubercles inside the alveolar macrophage precisely. DPI reduces the dose frequency and shorten treatment period, compared to standard oral or systemic treatment regimen (Chan et al., 2013).

EDH is primarily a bacteriostatic and anti-tuberculosis agent that is used in combination with other first-line antituberculosis agents mainly because of its synergy with other first line drugs. EDH itself inhibits the arabinosyl transferase enzyme that is responsible for arabinogalactan biosynthesis. EDH causes an increased permeability in the mycobacterial cell wall and inhibits its growth. The oral dose of EDH is 20 mg/kg and this produces peak plasma levels of 3–5 mg/mL. Due to high oral dose, EDH can cause serious side-effects to various organs if used for a long time. The most serious side-effect of EDH is a visual impairment. The side-effects of the EDH are dose and time dependent, studies have reported an incidence of 18% in subjects treated for >2 months with >35 mg/kg/day, 5–6% with 25 mg/kg/day, 3%

with 20 mg/kg/ day and <1% with 15 mg/kg/day (Hasenbosch et al., 2008). The studies have shown a consistent decrease in the cases of visual impairment with a decrease in the dose. Since the dose administered in DPI formulations is comparatively very low compared to the oral dosage form (Kaialy et al., 2012), perhaps the dose of EDH could be dramatically reduced. Hence the side effects of ethambutol could be better controlled without any side effects.

CS is partially deacetylated form of chitin; the second most abundant natural polymer obtained from the shells of crabs and shrimp. It is a polymer of mainly β (1–4)-2 amino-2-deoxy-D-glucose units (Pereda et al., 2012). It is a biodegradable polymer with an excellent potential for pharmaceutical applications due to its biocompatibility, high charge density, non-toxicity and mucoadhesive properties. At present all the evidence supports the usage of CS as a carrier to deliver isoniazid to the lungs from a DPI (Pourshahab et al., 2011). CS has a low cytotoxicity with cell lines of human origin from the airways and the alveolar regions of the pulmonary tract (Grenha et al., 2007; Vllasaliu et al, 2012). It has been reported that chitosan microspheres loaded with protein have been used to deliver the protein drug deeply inside the alveoli (Grenha et al., 2005; Patil-Gadhe et al., 2014).

Physical mixing of EDH with CS powder particles with a Dimple surface has been successfully used to improve the aerosol performance by facilitating the delivery of a drug to the lower respiratory regions of the lung. Rough surface particles are more likely to reduce the van der Waals forces of attraction and increase the aerosolization properties of the powder particles (Tang et al., 2003; Karner et al., 2014). Any smooth surface on the coarse carrier particles can lead to the formation of auto-adhesive layers around the coarser carrier particles, and results in an aggregation of the micronized drug particles and hinders their detachment during inhalation (Podzcek, 1999). The shape, size, morphology, and density of the powder particles depend on the spray-drying conditions (Steckel et al., 2004; Pilcer et al., 2009).

The development of DPI preparation will prove very effective to fight against the tuberculosis bacilli. So, it is hypothesized that the DPI formulation of antituberculosis drug will reduce the dose and increases the therapeutic efficacy and prevents the MDR and XDR.

1.2 Objectives

- 1.2.1. To prepare the dimple shape carrier powder particles and to investigate the factors affecting on its preparation.
- 1.2.2. To study the physico-chemical properties and interaction of ethambutol dihydrochloride with the carriers.
- 1.2.3. To develop ethambutol dihydrochloride dry powders and evaluate the formulation for inhalation.
- 1.2.4. Bioactivity and toxicity study of the ethambutol dihydrochloride dry powder inhaler.
- 1.2.5. To monitor the membrane permeability of drug through the lipid bilayer membranes.
- 1.2.6. To study the phagocytosis of prepared DPI formulations by macrophage cells.

CHAPTER 2

REVIEW OF LITERATURE

2.1 Pulmonary route

The drug delivery through the mouth to target lungs for local/systemic action through aerosol is known as the pulmonary drug delivery system. A pulmonary route constitutes; nose, pharynx, larynx, trachea, bronchus, bronchi, alveoli, and alveolar ducts for local drug action. A pulmonary route is the best available alternative route to deliver the drug, protein, and amino acid for treating the lung disease. The pulmonary airways has a great resemblance to an inverted trees connected with a trunk, are often described as the pulmonary tree. The tree trunk shows similarity to trachea, which bifurcate the airways to form two main bronchi which divides further to form smaller bronchi to form individual lung lobes; three lobes on the right side (right lung) and two on the left side (left lung) (Figure 2.1) .

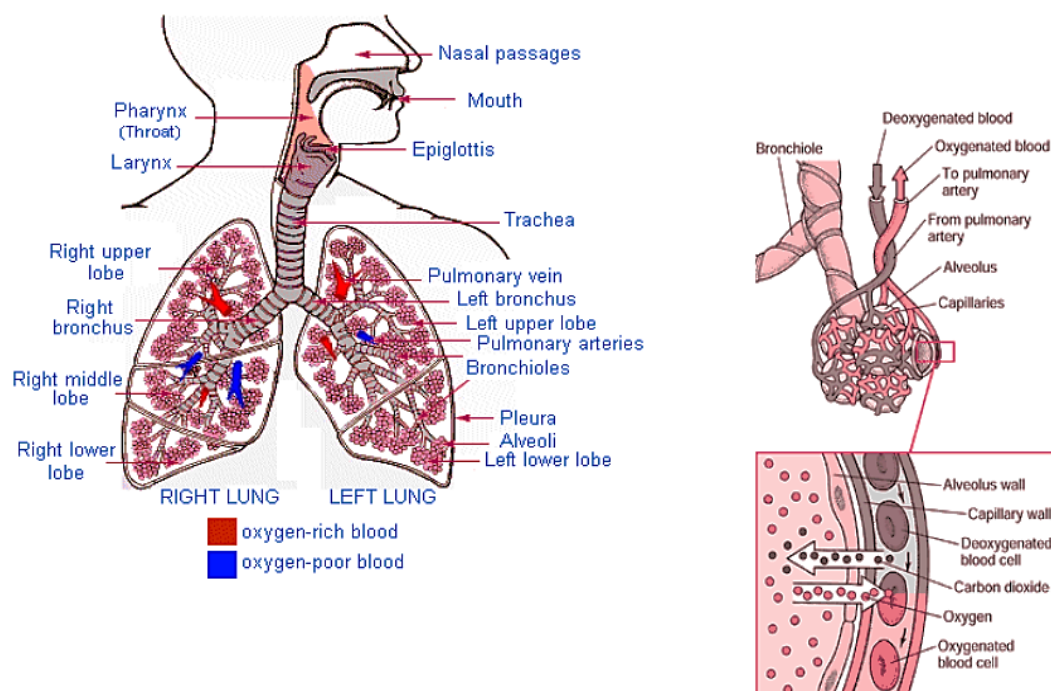


Figure 2.1 Diagram of pulmonary airways (Virginia bioinformatics institute, 2008).

Inside each lobe, the bronchi bifurcate several times to form new generations till reaches to terminal bronchioles (the smallest airway not involved with an alveolus). In the classic model of the airways by Weibel 1963, each airway divides to form two

smaller airways; as a result, the number of airways at each generation gets double to that of the previous generation. The model proposes the existence of 24 airway generations in total, with the trachea being generation 0 and the alveolar sacs being generation 23 (Figure 2.2).

conducting zone	generation		diameter (cm)	length (cm)	number	total cross sectional area (cm ²)	Powder deposition by particle diameter
	trachea	0	1.80	12.0	1	2.54	7 - 10 μm
bronchi	1	1.22	4.8	2	2.33	2 - 10 μm	
	2	0.83	1.9	4	2.13		
	3	0.56	0.8	8	2.00		
	4	0.45	1.3	16	2.48		
	5	0.35	1.07	32	3.11		
bronchioles	16	0.06	0.17	6·10 ⁴	180.0	0.5 - 2 μm and < 0.25 μm	
	terminal bronchioles	17	↓	↓	↓		↓
respiratory bronchioles	18	↓	↓	↓	↓		
	19	0.05	0.10	5·10 ⁵	10 ³		
	20	↓	↓	↓	↓		
alveolar ducts	21	↓	↓	↓	↓		
	22	↓	↓	↓	↓		
alveolar sacs	23	0.04	0.05	8·10 ⁶	10 ⁴		

Figure 2.2 Schematic branching of the human pulmonary airways (Hickey and Thomson, 1992).

Two important physical changes took place in airways while passing from the trachea to the alveolar sacs, which influences the airway function. Firstly, the number of airway caliber decreases with increasing number of generations for e.g. tracheal diameter 1.8 cm versus alveolar diameter 0.04 cm (Figure 2.2) which permits the adequate penetration of air to the lower airways of lungs. Secondly, with each increasing in number of generations, the surface area increases, to such an extent that the total area at the level of the human alveolus is on the order of 140 m². The alveoli is the main place in airways where the exchange of gases took place, with the increased surface area, the diffusion of gas exchange between the alveolar space and the blood in alveolar capillaries get increased. Pulmonary drug delivery research is mainly based on efficient aerosol generation and particle deposition in the lung's alveoli. Aerosol deposition took place when there is a collision of particles (water

droplets) with the lung surface liquids which lines the airway epithelium. The deposition of drug particles deep inside the lungs depend upon the particle aerodynamic diameters; smaller the aerodynamic diameters, deeper they can penetrate into the lung. For effective deposition the particle should also overcome lung geometry as well as lung physiology barrier. Drug particles should also overcome mucociliary clearance, pulmonary surfactant, epithelial tight junctions, immunological cells, and lung lining fluids barrier for drug deposition inside the lungs.

2.2. Inhalation therapy

Drug delivery to the lungs especially in patients with disease like cystic fibrosis, asthma, chronic pulmonary infections, tuberculosis or lung cancer are highly desirable. The main advantages of inhalation therapy are that, it reduces the systemic side effects and higher doses of the applicable medication at the site of drug action. The lungs are an effective place to administer drugs to the bloodstream due to its large surface area available for absorption ($\sim 100\text{m}^2$), thin absorption membrane (0.1–0.2 μm) and the elevated blood flow (5 l/min), which rapidly diffuses the drug throughout the body. The lungs exhibit low enzymatic activity locally and it bypass the first pass hepatic metabolism (Adjei and Gupta, 1997; Wanakule et al., 2012).

There are three main principal devices used for inhaled drug delivery therapy i.e. nebulizers, pressurized metered-dose inhalers (pMDIs) and DPIs each class with its unique strengths and weaknesses. A good pulmonary drug delivery device has to generate an aerosol of suitable size in the range of 0.5–5 μm and provide reproducible drug dosing. Device must also protect the physical and chemical stability of the drug formulation. The ideal inhaled drug delivery device must be a simple, convenient, inexpensive, and portable.

Nebulizers are the devices, developed for inhalation therapy but they have disadvantages such as low efficiency, poor reproducibility, great variability, time consuming (Newhouse et al., 2003). MDIs were developed in 1950s, since then they have been used for chronic obstructive pulmonary disease (COPD) and asthma inhalation therapy. However, concerns have been raised over pMDIs potential drawbacks: harmful effects of environmentally incompatible propellant, Freon to patients and extensive oropharyngeal deposition of the active pharmaceutical

ingredients (APIs) included in the device (Hendeles et al., 2007). Due to pMDIs contribution to ozone depletion from CFC, pharmaceutical companies were forced to find alternative propellants. As a result, hydrofluoroalkane (HFA)-based pMDIs were developed to replace CFCs (Acerbi et al., 2007). However, this replacement strategy has not been much successful due to several disadvantages like potency, high manufacturing cost, and problem in reformulation. Problem with the operational restrictions and performance of pMDIs encouraged to the development DPI.

As a result, many DPIs have been developed and launched in the market. Since the launch of the first single-dose DPI product, the Spinhaler® (Sanofi-Aventis, Holmes Chapel, UK), in the market, many new DPIs with remarkable progress in various aspects such as dose-metering, dose-dispensing, and aerosolization properties of dry powder particles (Smyth et al., 2005). In recent times many attempts have been made to deliver a variety of active pharmaceutical ingredients (APIs) through pulmonary route using novel DPI devices such as Exubra® (Nektar therapeutics, San Carlos, CA, USA), Spiro® (Dura Pharmaceuticals, San Diego, CA, USA), and AIR™ (Alkermes Cambridge, MA, USA).

2.3 Dry powder inhaler (DPI)

DPI device is designed to transport the drug particle deep inside the lung by using inspiratory airflow of patient. DPI requires little or no coordination between actuation and inhalation, which results in better drug delivery in lung than achieved by MDIs

2.3.1 Principles of DPI

DPI works on the principle of generating dispersion and turbulence in static powder bed of DPI aerosol through inspiratory flow of patient which creates shear and movement in device, causes fluidization to the powder bed and static powder blend enters into the patient airways, there the carrier get separated from the drug, drug travel deep inside the lung while the carrier get deposit on the oropharynx and cleared by mucociliary clearance (Telko et al., 2005) (Figure 2.3).

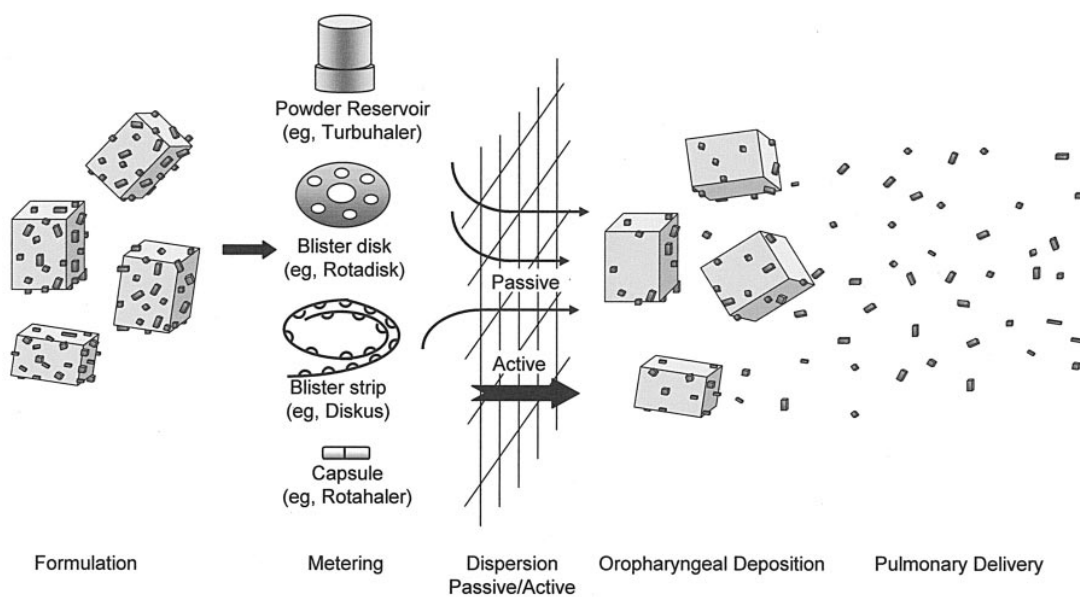


Figure 2.3 Principles of DPI device (Telko and Hickey, 2005).

The deposition of drugs into the lungs is dependent on the patient's variable inspiratory airflow, drug/carrier separation in oral cavity or oropharynx. Various dispersion techniques have been adopted for DPIs but the most commonly used DPIs are the breath activated one, used for aerosol generation. Several power-assisted DPIs are either developed or under development to increase the drug bioavailability in lungs.

2.3.2 Advantages of DPIs

The pulmonary route of administration has many potential advantages for the delivery of APIs over other routes. The major advantage of DPI includes: large surface area for drug absorption, high permeability through a thin alveolar membrane, low enzymatic activity, propellant free, no first pass hepatic metabolism, excellent bioavailability, easy to handle, less systemic side-effects and environment friendly (Labiris et al., 2003; Paranjpe et al., 2014). DPI formulations are considered as stable formulation due to their processing in one phase; solid-particle blend (Pilcer et al., 2010). DPI powders exhibit low energy state which reduces their chemical degradation and reaction with contact surfaces. DPIs got wide acceptance and provided a very attractive platform for drug delivery due to their propellant-free nature, high patient compliance, improved formulation stability, and patient protection

from harmful Freon (Smith et al., 2003). The carrier and drug morphology influenced immensely in the dry powder inhalation system (Larhrib, 2003; Islam et al., 2012). DPIs regarded as a better device for inhaling APIs as they offer better drug deposition in central and peripheral regions of the lung, with minimal oropharyngeal deposition than the pMDI (Borgstorm et al, 1996; Demoly et al., 2014). This might happen due to the differences in the aerosol generation mechanism between delivery devices. DPIs get activated by the patient's inspiratory airflow, which require little or no coordination of actuation and inhalation. Whereas pMDIs get activated by pressurized propellant at high velocity, which may lead to premature drug deposition in the oropharynx. As a result, DPIs are being used widely to treat asthma and COPD. The development of new DPIs has been accelerated for delivering therapeutic proteins and antibiotics through innovative research. Currently around 22 DPIs devices are present in market for use and many devices are under development for delivering a variety of therapeutic agents, for a variety of therapeutic needs. Two types of DPIs are available in the market, commercially: 1) packaged in individual doses (capsules) (single dose or unit-dose devices) and 2) multiple doses (multi-unit and multi-dose devices) (Table 2.1).

Table 2.1 Examples of commercially available DPIs in the market (Islam et al., 2008)

First generation: breath actuated single unit doses					
Device	DPI Type	Company	Delivery method	Drug	Disease
Spinhaler	Single dose	Aventis	Capsule	SC	Asthma
Rotahaler	Single dose	Glaxosmithkline	Capsule	SS, BDP, SS+BDP	Asthma
Inhalator	Single dose	Boehringer- lengeheim	Capsule	Fenoterol	Asthma
Cyclohaler	Single dose	Pharmachemie	Capsule	SS, BDP, IB, BUD	Asthma
Handihaler	Single dose	Boehringer- lengeheim	Capsule	Tiotropium	COPD
Aerolizer	Single dose	Novartis	Capsule	Fomoterol	Asthma

Table 2.1 Examples of commercially available DPIs in the market (continued)

Device	DPI Type	Company	Delivery method	Drug	Disease
Flowcaps	Single-unit dose	Hovione	Capsule	NA	Asthma
Twincaps	Single dose	Hovione	Capsule	Nuraminidase inhibitor	influenza
Second generation: breath actuated multi-unit, multi doses					
Device	DPI Type	Company	Delivery method	Drug	Disease
Turbohaler	Multi dose	Astrazeneca	Reservoir	SS, TS, BUD	Asthma
Diskhaler	Multi- unit dose	Glaxosmithkline	Blister package	SX, BDP, FP, Zanamivir	Asthma, Influenza
Discus/ Accuhaler	Multi- unit dose	Glaxosmithkline	Strip pack	SS, SX, FP, SX+FP	Asthma
Aerohaler	Multi- unit dose	Boehringer- lengeheim	----	IB	Asthma
Easyhaler	Multiple dose	Orion Pharma	Reservoir	SS, BDP	Asthma
Ultrahaler	Multiple dose	Aventis	Reservoir	SS, BDP	Asthma
Pulvinal	Multiple dose	Chiesl	Reservoir	SS, BDP	Asthma
Novelizer	Multiple dose	ASTA	Reservoir cartridge	BUD	Asthma, COPD
MAGhaler	Multiple dose	Boehringer- lengeheim	Reservoir	SS	Asthma
Taifun	Multi- unit dose	LAB Pharma	Reservoir	SS	Asthma
Eclipse	Multi- unit dose	Aventis	Capsule	Sodium chromoglycate	Asthma
Clickhaler	Multiple dose	Innoveta Blomed	Reservoir	SS, BDP	Asthma
Asmanex/ twist haler	Multiple dose	Schering – plough corporation	Reservoir	MF	Asthma

Table 2.1 Examples of commercially available DPIs in the market (continued)

Third generation DPIs: active device					
Device	DPI Type	Company	Delivery method	Drug	Disease
Exubera	Single dose	Pfizer	Blister	Insulin	Diabetes
Almax	Multi dose	Norton Healthcare	Reservoir	Formoterol, BUD	Asthma, COPD

MF: mometasone furoate, SS: salbutamol sulphate, SX: salmeterol xinafoate, FP: fluticasone propionate, BUD: budesonide, TS: terbutaline sulphate, F: fenoterol, formoterol, IB: ipratropium bromide, Ti: tiotropium, SC: sodium cromoglycate, BDP: beclomethasone dipropionate, EFD: eformoterol fumarate dehydrate, COPD: chronic obstructive pulmonary disease.

The dose of DPI is depended on the four interrelated factors: the properties of the drug formulation (powder flow, particle size, shape, surface properties and drug carrier interaction), the performance of the inhaler device (aerosol generation, delivery correct inhalation technique for deposition in the lungs) and the inspiratory flow rate.

2.3.3 DPI deposition in the lung

The respiratory tract act as a filter membrane which filters the powder particle upon inspiration, filtration depends upon the region and trajectory of the respiratory tract (Heyder et al., 1998; Hoppentocht et al., 2014). The effectiveness of the filter depends on particle properties (size, shape, density, and charge), respiratory tract morphology, and the breathing pattern (e.g. airflow rate and tidal volume) (Heyder et al., 1998; Gradon et al., 2013). These above mentioned parameters are responsible for the determination of particles quantity and the region of particle deposition in respiratory tract. The cross sectional areas of airways are inversely proportional to the airflows rate i.e. cross-sectional area increases, the airflow rate decreases which consequently leads to increase in the residence time for particles in lung from the large conducting airways to towards the lung periphery (Tena et al., 2012). The drug particle deposition inside the respiratory tract depends on the three most important mechanisms i.e. inertial impaction, sedimentation, and diffusion (Figure 2. 4).

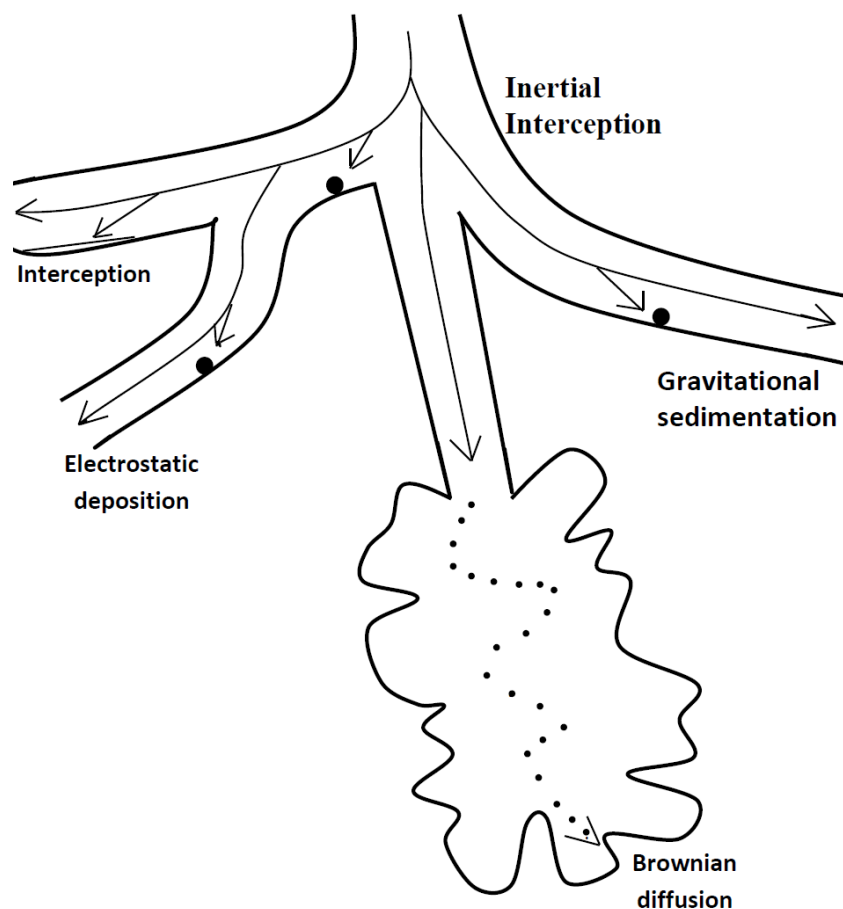


Figure 2.4 Mechanisms of particle deposition in lungs (adapted from Frohlich et al., 2014)

2.3.3.1 Inertial impaction

Inertial impaction is a physical phenomenon which predominantly occurs in the extra-thoracic airways and in the tracheobronchial tree; where the powder particles tend to continue on a trajectory path when travel through the airway, instead of conforming to the curves of the respiratory tract. A particle having large momentum gets affected by centrifugal force at the points where the airflow suddenly changes direction and collides with the airway wall. This generally happens in the first 10 bronchial generations, where the air speed is high with turbulent flow. This phenomenon mainly affects particles larger than $10\ \mu\text{m}$, which are mostly retained in the oropharyngeal region, especially if the drug is administered by DPI or MDI where the airflow velocity is high and rapid changes in airflow direction occurs (Tena et al., 2012).

2.3.3.2 Sedimentation

Sedimentation is a physical phenomenon in which particles with diameter of 0.5-2 μm are deposited due to the force of gravity when they remain in the small airway and alveoli for a sufficient length of time. This mainly happens in the last 5 bronchial generations, where the air speed is slow and the residence time is longer (Tena et al., 2012).

2.3.3.3 Diffusion

Diffusion is the phenomenon in which the drug particles move erratically from one place to another in the airways due to the Brownian motion, having an MMAD smaller than 0.5 μm where the air speed is practically zero into the alveolar spaces (Tena et al., 2012).

2.4 Chitosan (CS)

CS is a partially deacetylated form of chitin; the second most abundant natural polymer obtained from the shells of crab, shrimp. It consists mainly of β (1–4)-2 amino-2-deoxy-D-glucose units (Pereda et al., 2012). CS is a biodegradable natural polymer with great potential for pharmaceutical applications due to its biocompatibility, high charge density, non-toxicity, and mucoadhesive (Pourshahab et al., 2011). CS are natural amino-polysaccharide polymers with unique structures, multi-dimensional properties, highly sophisticated functions and wide ranging applications in biomedical and other industrial areas. CS is considered as a material of great futuristic potential with immense possibilities for structural modifications to impart desired properties, functions, research, and developmental work. The positive characteristics of CS like biocompatibility, biodegradability, ecological safety, low toxicity with versatile biological activities such as antimicrobial activity and low immunogenicity have provided a huge opportunity for drug development (Hejazi and Amiji, 2003; Harris et al., 2013). CS is the N-deacetylated derivative of chitin with a typical DD of less than 0.35, a copolymer composed of glucosamine and N-acetyl glucosamine (Rinaudo, 2008 and Muzarelli, 1990). CS is produced mainly by thermochemical alkaline deacetylation of acetamide group at the C-2 position in the 2-acetamido-2-deoxy- glucopyranose unit of chitin (Figure 2.5). CS can be

synthesized both by acid and alkali deacetylation from chitin, but due to the acid susceptibility to glycosidic bond, generally alkaline de-acetylation is used for CS preparation (Figure 2.6).

There are two methods to prepare CS by alkali treatment; one is the homogeneous alkaline treatment which is performed at lower temperature and longer reaction time, while in heterogeneous alkaline treatment, the reaction is performed at higher temperature for shorter reaction time (Kumar, 2000). The DDs and MWs of prepared chitosan are greatly affected by heterogeneous alkaline treatment, solution to solid ratio, reaction time, and temperature.

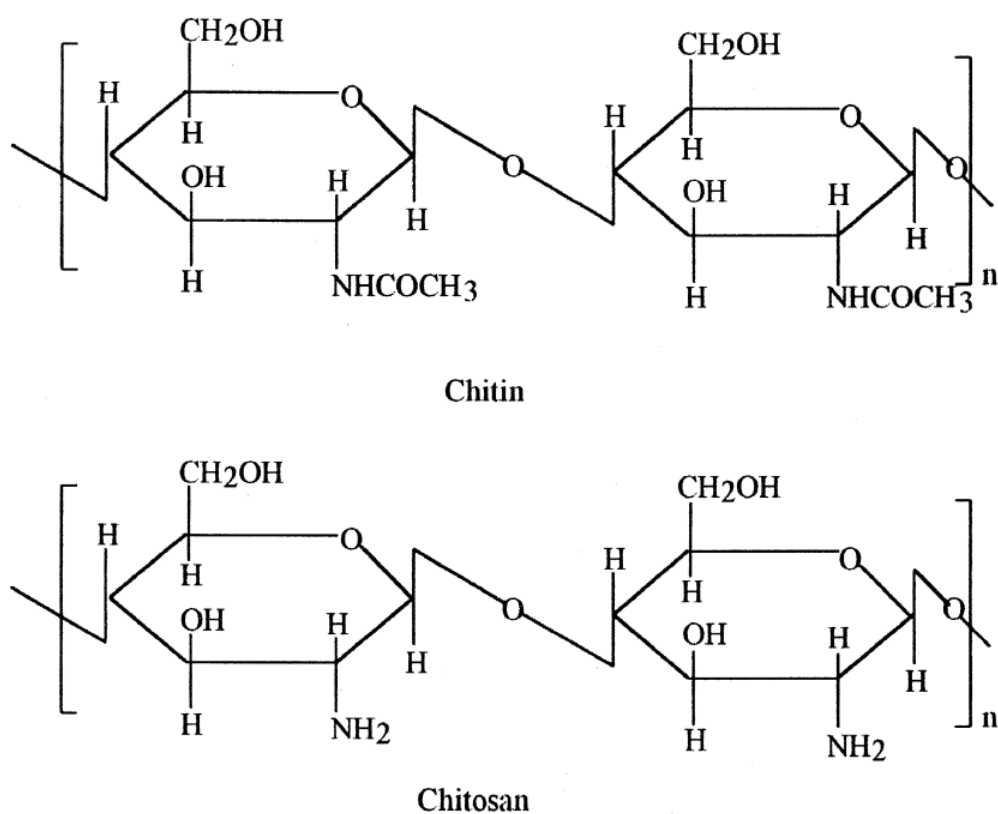


Figure 2.5 Structure of chitin and chitosan.

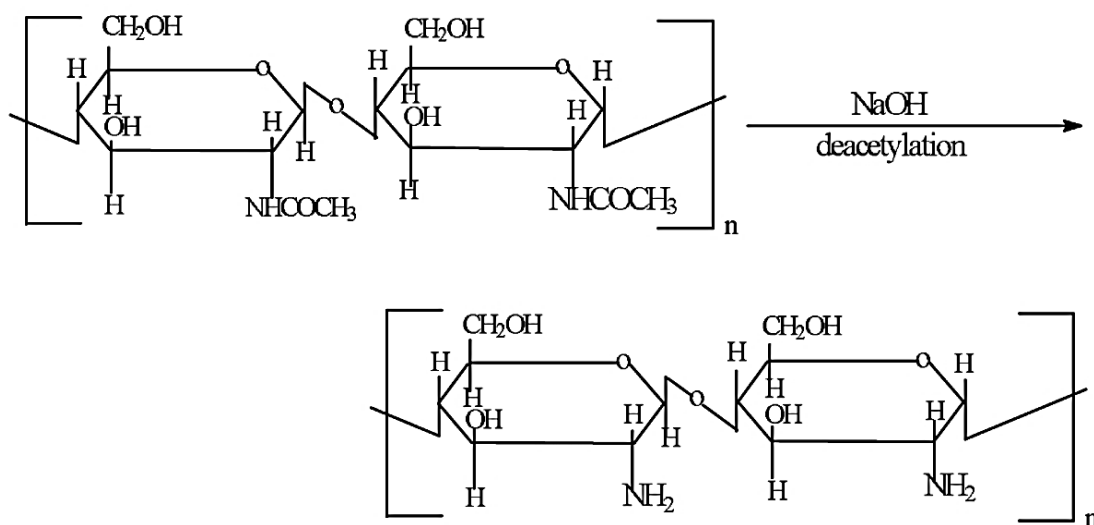


Figure 2.6 Preparation of chitosan from chitin by alkali deacetylation.

The deacetylation reaction gets enhanced rapidly in the presence of higher alkali concentrations as well as higher solution to solid ratio; higher the reaction temperature, higher will be the DD and lower MW of CS (Tsaih et al., 2002; Yang et al., 2014). CS shows aqueous solubility at DD of 50% while acidic aqueous solution at a DD higher than 60%. The physical properties of CS depend on a number of parameters such as the molecular weight (from approximately 10,000 to 1 million Dalton), DD (in the range of 50–95%), sequence of the amino and the acetamido groups and the purity of product (Pillai et al., 2009). CS is an interesting polysaccharide due to the presence of the amino functional groups. It can be suitably modified to impart desired properties and distinctive biological functions including solubility. In acidic medium, the amine groups of CS are protonated resulting in a soluble, positively charged polysaccharide that has a high charge density (one charge for each D-glucosamine unit). The amino group in CS gives rise to chemical reactions such as acetylation, quaternization, reactions with aldehydes and ketones (to give Schiff's base) alkylation, grafting, chelation of metals to provide a variety of products with properties such as antibacterial, anti-fungal, anti-viral, anti-acid, anti-ulcer, non-toxic, non-allergenic, total biocompatibility and biodegradability. Apart from the amino groups, CS has two hydroxyl functionalities for effecting appropriate chemical modifications to enhance solubility. The hydroxyl groups also give various reactions such as *o*-acetylation, H-bonding with polar atoms. The possible reaction sites for CS

are illustrated in Fig 2.6. CS is easily soluble in dilute acidic solutions below pH 6 due to the presence of primary amino group; the amino group cause the pH to substantially alters the charged state and properties of CS (Yi et al., 2005). At low pH, these amines get protonated and become positively charged that makes CS a water-soluble cationic polyelectrolyte and at higher pH above 6, CS's amines become deprotonated and the polymer loses its charge and becomes insoluble. The soluble–insoluble transition occurs at its pKa value between pH 6 and 6.5. CS readily form quaternary nitrogen salts at low pH values and organic acids such as acetic, formic, and lactic acids can dissolve CS (Kim et al., 2006). The most commonly used solvent is 1% acetic acid at about pH 4.0. Attention has been paid to CS with regard to developing derivatives with well-defined macromolecule to meet certain functions such as receptor-mediated gene delivery, cell penetration enhancer, site specific tracking etc. CS can form gels by interacting with different types of divalent and polyvalent (anions) ions (Sinha et al., 2004).

CS is capable of opening the tight junction between epithelial cells of alveoli and help in diffusion of drug to the alveoli. The evidence supports the usage of CS as a carrier to deliver the isoniazid to the lungs as a dry powder inhaler (Pourshahab et al., 2011). CS has low cytotoxicity with cell lines of human origin airways and the alveolar regions of the pulmonary tract (Grenha et al., 2007). It has been reported that CS microspheres loaded with protein have been used to deliver the protein drug deep inside the alveoli (Grenha et al., 2005). The size and shape of chitosan also play an important role in delivering the drug to the lungs. The aerodynamic diameter of chitosan should not be more than 5 μ m, if more than that it will not enter into the alveoli and less than 0.5 μ m will exhale out.

However, powder particles in this size range exhibit strong inter-particulate cohesion, leading to poor powder flow properties (Steckel et al., 2004; Milenkovic et al., 2014). The diameter is an important parameter for considering the chitosan as a carrier. The shape of the chitosan as a carrier are of generally three types like i) donut shape, ii) spherical shape, iii) dimple shape. In spherical shape, the drug binding on the surface of chitosan strongly due to van der Waals forces which decreases its aerosolization property inside alveoli. In donut shape also the van der Waals forces decreases aerosolization property of formulation. The dimple shapes

have grooves all over its body surface so it provides good space for drug to bind over its surface and also there is non-uniformity in van der Waals forces which helps in deaggregation of drug easily and improves the aerosolization property of formulations. Researchers have investigated a number of approaches to improve powder aerosolisation, such as mixing the micronized drug with inert carrier particles, modification of particle morphology, particle surface roughness, particle porosity, or powder density (Learoyd et al., 2007).

An alternative approach to generate dry powders for pulmonary drug delivery is through spray-drying technology. Spray-drying is a one-step constructive process that provides greater control over particle size, particle morphology and powder density. The dimple shape appearance on surface of chitosan is dependent on the inlet temperature, the concentration of chitosan solution and feed rate for spray drying (He et al., 1999). When the solution is sprayed at high inlet temperature (150°C) with low feed rate, the particles which come out through nozzles show shrinkage on their surfaces. This may be due to water evaporation at a high inlet temperature which results in dimple formation on particle surface. Spray-drying produces dried micro-sized CS powders with controlled surface morphology in order to enhance their aerosolization efficiency (Chew et al., 2005). The shapes and surface of the CS play an important role in the delivery of formulations to the lung as they affect CS ability to aggregate and deaggregate with formulation deep inside the lung. Carrier particles with a rough surface have been successfully used to improve the aerosol performance by facilitating the delivery of a drug to the lower respiratory regions of the lung. Van der Waals force plays an important role in aerosolization of powder particles in the lower respiratory region. The rough surface particles are more likely to reduce the van der Waals forces of attraction and increase their aerosolization properties (Tang et al., 2003). The smooth surface on the coarse carrier a particle leads to the formation of auto-adhesive layers around it and results in an aggregation of the micronized drug particles and hinders their detachment during inhalation (Podczek, 1999). CS based nanoparticles are currently being explored for controlling the rate of drug release, prolonging the duration of therapeutic effects, and delivering the drug to the specific sites in body. CS possesses high positive charge on NH_3^+ groups when dissolved in aqueous acidic solution and therefore it is able to

adhere or aggregate with negatively charged lipids and fats (Wydro et al., 2007). The antimicrobial activity of chitosan is dependent on the molecular weight, DD and type of microorganism. CS with a low molecular weight around 50kDa is optimum for antimicrobial activity against the growth of *S. aureus*, *E. coli* and *C. albicans* (Chung and Chen, 2007). The primary amino group plays an important role on microbial activity through the alteration of cell membrane permeability and suppression of biosynthesis and finally led to death (Kim et al., 2005). CS as a dry powder inhaler has shown tremendous potential to deliver the drugs, insulin, nucleic acids to the lungs. An idea behind preparing dimple shaped CS carrier for drug was to increase in number of drug binding on CS surface and grooves for its better aerosolization property (Chew et al., 2005).

2.5 Ethambutol dihydrochloride (EDH)

EDH [(S, S)-2, 20-(ethylenediimino)-di-1-butanol, 1], was first reported by Wilkinson and co-workers of Lederle laboratories in the early 1961 (Wilkinson et al., 1961). EDH is a white, crystalline, freely soluble powder in water, alcohol, methanol but slightly soluble in ether and in chloroform (Martindale, 2009). EDH is a simple diamine molecule that is synthesized by reacting 1, 2- dihaloethane with chirally pure (S)-2- amino 1-butanol (Figure 2.7).

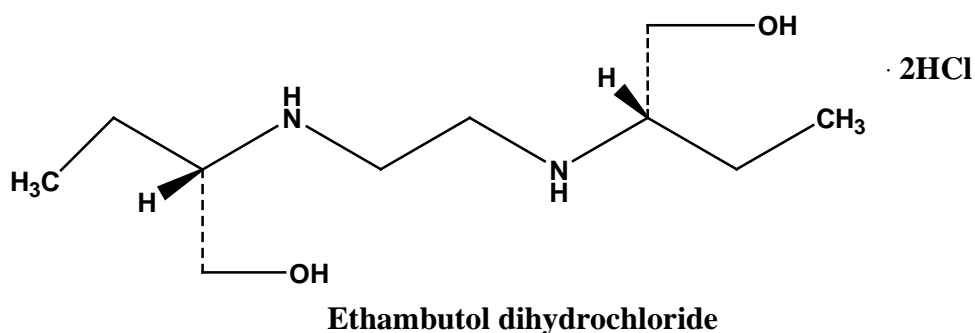


Figure 2.7 Structure of EDH.

Early SAR study indicates that the distance between two nitrogen atoms, the presence of two hydroxyl groups, and the small side chains in the molecule are key pharmacophore elements (Shepherd, et al., 1966). The chirality of the molecule is also very crucial in determining the activity. The (S, S) isomer of EDH is

approximately 200 times more potent than the (R, R) isomer (Bryskier and Grosset, 2005). Ethambutol is primarily a bacteriostatic and anti-tuberculosis agent. EDH is used in combination with other first-line anti-tuberculosis agents mainly due to its synergy with the other first-line drugs. EDH targets the arabinosyl transferases responsible for arabinogalactan biosynthesis; a key component of the unique mycobacterial cell wall hence produces the permeable bacterial cell wall which leads to the inhibition of bacterial growth (Figure 2.8) (Zhang et al., 2007). The oral dose of EDH is 20mg/kg, on administration 70-80% drug get absorbed and peak plasma reached to 3 to 5 $\mu\text{g/ml}$ within 1-2 h of administration (Bryskier and Grosset, 2005). EDH showed the elimination half-life of 6 to 8 hour. The MIC of EDH for *M. tuberculosis*, *M. bovis* and *M. avium* ranges from 0.5-2 $\mu\text{g/ml}$, depending on the media used i.e. liquid medium with Tween-albumin or Lowenstein-Jensen medium (Bryskier and Grosset, 2005). EDH diffuses into whole body including the cerebro spinal fluid (CSF) but in inflamed meninges, concentration reduced to 10-20% of those in serum. Around 40% of the administered dose gets absorbed and rest eliminated through the glomerular filtration after 24 h in parent form.

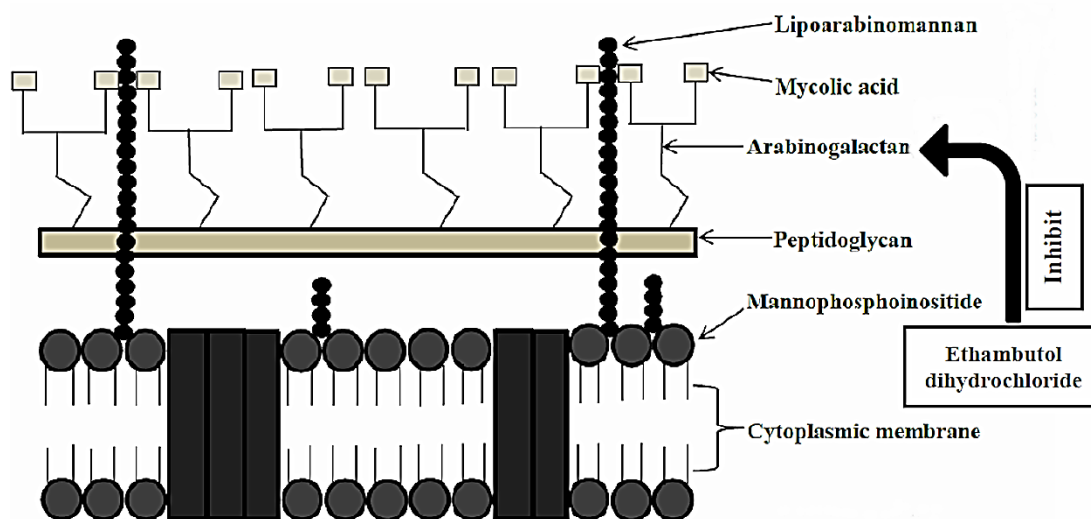


Figure 2.8 Schematic diagrams to show the EDH mechanism of action (adapted from Sreevatsan et al., 1997).

Erythrocytes serve as a storage depot for EDH and show its sustaining release for long time which causes higher intraerythrocytic concentration than serum concentration. Due to its high dose EDH causes serious side-effects to various organs

if used for long time. The most serious side-effects of EDH are visual impairment, if the oral dose of drug is administered consistently or more than 20mg/kg for long time then it will lead to complete blindness. If it is administered in aerosol form as a dry powder inhaler, the dose of EDH dry powder inhaler (DPI) is expected to be reduced drastically. Hence, the side effects of EDH will be easily controlled. Therefore, the DPI formulation of EDH will play a major role in controlling MDR, XDR and TDR tuberculosis. Ethambutol is active against nearly all strains of *M. tuberculosis* and *M. kansasii* as well as a number of strains of *M. avium* (Hall et al., 2011).

2.6 Tuberculosis

2.6.1 Pathogenesis

The macrophages are the innate immunity which destroy the invading mycobacteria and prevent infection (Van Crevel et al., 2002; Ernst, 2012). Macrophages are phagocytic cell which has the capability to combat with many pathogens by several mechanism and macrophage receptors (Nicod et al., 2007). The lipoarabinomannan present in the mycobacterial cell wall provides a key ligand for macrophage receptor (Nicod et al., 2007). The complement system also plays a major role in the phagocytosis of the bacteria. The complement protein C3 binds to the cell wall and enhances recognition of the mycobacteria by macrophages. The phagocytosis starts a cascade of events and its outcome depend upon the strength of host defense and the balance formed between host defenses and invading bacteria (Li et al., 2002; Andersen et al., 2014).

Mycobacteria start multiplying inside the macrophage upon ingestion slowly at every 23-32 hours. The macrophage produces proteolytic enzyme and cytokines in attempt to degrade the bacteria (Li et al., 2002, Ferguson et al., 2004, Andersen et al., 2014). The released cytokines attach with the T lymphocytes to the site; the macrophage exposed the mycobacterial antigens on the surface to T lymphocytes cells. This immune response continues for 2 to 12 weeks and bacteria continue to grow until in sufficient number to get detected by skin test. The next defensive step is the formation of granulomas; these nodular type lesions form an accumulation of T lymphocytes and macrophages which creates a microenvironment

to limit bacterial spread and replication (Ferguson et al., 2004). A person with strong immunity, lesions undergo fibrosis and calcification successfully and bacilli get in dormant phase while in a person with less effective immunity the lesions progress to primary tuberculosis. The infected person upon coughing infects the other person too with their exhaled infected droplets.

2.6.2 Clinical manifestations

Clinical manifestation of tuberculosis depends on a number of factors including age, immune status, immunization status to the bacillus Calmette-Guerin (BCG); virulence of the infecting organism and host-microbe interaction. It has been reported that 85% cases reported were of pulmonary tuberculosis and 15% extrapulmonary tuberculosis. Extrapulmonary tuberculosis case increases with worsening of immune systems in a patient (Robert et al., 2013).

2.6.2.1 Systemic effects of tuberculosis

The infection of tuberculosis in any part of body produces the systemic symptoms. The main symptoms include high body temperature, loss of appetite, weight loss; weakness, night sweats, and malaise are also common. The most common hematological manifestation includes increase in granulocytes in peripheral blood and anemia (De Backer et al., 2006).

2.6.2.2 Pulmonary tuberculosis

Nonproductive cough in beginning and later with sputum results due to tissue necrosis is one of the main manifestations in pulmonary tuberculosis. Hemoptysis results from previous disease and may arise from tuberculous bronchiectasis, rupture of a dilated vessel in the wall of a cavity, bacterial or fungal infection in a cavity or erosion into an airway (broncholithiasis). Pleuritic pain is caused generally due to the inflammation of lung parenchyma cell. The lungs upper lobe and cavitation is common abnormalities due to latent infection.

2.6.2.3 Treatment of tuberculosis

The major goals for treatment of tuberculosis include cure, restoring quality and productivity of life, prevent mortality, relapse from active tuberculosis, reduce transmission and development of drug resistance in patient. Antituberculosis drugs are outlined into three categories based on their therapeutic activity.

2.6.2.3.1 Prevention of drug resistance

The drugs which are highly active in suppressing the growth of tubercle bacilli, to prevent the emergence of mutant resistant to another drug. This activity measured the degree of drug prevention to a treatment failure due to the emergence of multi drug resistance during therapy. Isoniazid and rifampicin shows highest degree of activity in preventing the emergence of drug resistance. The activity of pyrazinamide for TB prevention is poor (Fujiwara et al., 2000).

2.6.2.3.2 Early bactericidal activities

The ability of anti-tubercular drug to kill the actively growing bacilli, rapidly, during initial part of therapy.

2.6.2.3.3 Sterilizing activity

Ability of killing semi-dormant bacilli by anti-tubercular agent and measurement of its speed at which the last few viable bacilli got killed is known as sterilizing activity (Fujiwara et al., 2000). Rifampicin and pyrazinamide is the most potent sterilizing agent (Table 2.2).

Table 2.2 Groups of antituberculosis drugs with abbreviation according to the WHO

Group name	Antituberculosis drugs	Abbreviations
Group 1 First-line of oral agents	Isoniazid	H
	Rifampicin	R
	Pyrazinamide	P
	Ethambutol	E
	Rifabutin	Rfb
Group 2 Injectable agents	Streptomycin	S
	Kanamycin	Km
	Capreomycin	Cm
Group 3 Fluoroquinolones (FQs)	Amikacin	Amk
	Moxifloxacin	Mfx
	Ofloxacin	Ofx
Group 4 Oral bacteriostatic second line anti-tuberculosis drug	Levafloxacin	Lfx
	Ethionamide	Eto
	Prothionamide	Pto
	Cycloserine	CS
Group 5 Drugs with limited data on efficacy and /or long term safety in the treatment of DR-TB	Para-aminosalicylic acid	PAS
	Bedaquiline	Bdq
	Clofazimine	Cfz
	Linezoilid	Lzd
	Amoxicillin / Clavulanic acid	Amx/Clv
	Isoniazid high dose	High dose H
	Thioacetazone	Thz
Imipenem /cilastatin	Ipm/Cln	
Meropenem	Mpm	

To reduce or to avoid the emergence of tuberculosis resistance in patient, it is necessary to administer antitubercular drug in combinations. Treatment regimens for the tuberculosis include the combinations of specific drug and their duration of treatment. The initial, intensive phase comprises of Isoniazid, Rifampicin, Pyrazinamide, and ethambutol for 2 months. In continuation phase isoniazid and rifampicin are administered for 4 months (Table 2. 3).

Table 2.3 Different phases for anti-tubercular drug administration

Phase	Drug	Duration (Months)
Intensive	Isoniazid	2
	Rifampicin	
	Pyrazinamide	
	Ethambutol	
Continuation	Isoniazid	4
	Rifampicin	

CHAPTER 3

Materials and Methods

3.1 Materials

CS (MW:3.2 kDa, 58%:deacetylated) and EDH were from Sigma-Aldrich, St. Louis, USA. Glacial acetic acid was from Baker analyzed reagent, USA. Sodium 1-heptanesulphonate monohydrate was from Aldrich Chemistry, Switzerland. Tetrahydrofuran (HPLC grade) was from RCI, Labscan, Bangkok. Other chemicals were analytical grade and used as received. All solutions (reagent packs) used for the maintenance and culture of human bronchial epithelial cells (Calu-3), Alveolar macrophage cell lines (NR8383) and human lung adenocarcinoma cell line (A549) were acquired from ATCC (Virginia, USA). Samples of 3-(4, 5-dimethylthiazol-2-yl)-2, 5-diphenyltetrazolium bromide (MTT) (were from Sigma-Aldrich. The BCG vaccine of *M. bovis* and Middlebrook 7H9 culture medium was obtained from Queen Saovabha Memorial Institute (Bangkok, Thailand) and Becton Dickinson and Co. (New Jersey, USA), respectively.

3.2 Methods:

3.2.1 Optimization of the spray drying process of EDH

The nanospary drying method allowed adjusting many parameters and it was important to know the process parameters to obtain the desired dried powder with predictable performance. A 2^3 full factorial design and multiple regression analysis were applied to investigate the effect of the main spray drying process variables on the powder characteristics polynomial regression analysis was applied to investigate the effect of the main spray drying process variables on the powder characteristics (Table 3.1). The processing variables were spray rate (X_1) and inlet temperature (X_2), using the Buchi nanospray dryer B-90 (Buchi, Flawil, Switzerland).

To perform this experiment, one gram of EDH was weighed and dissolved in 100 mL of distilled water and sonicated for 15 min. The solution was then filtered through a 0.45 μm polyamide membrane (Sartorius Biotech GmbH, Goettingen, Germany) and nanosprayed by using a nano-spray dryer B-90 at an inlet

temperature of 110°C, and a spray rate of 80%. The EDH powders were collected by scraping from the collecting drum carefully and kept in desiccators until used. The average size and size distribution of the EDH powders were determined using a zetasizer (Malvern, Worcestershire, UK).

Table 3.1. Nano spray drying optimization parameters

Parameter	Low (-)	Medium (1)	High (2)	Unit
Inlet temperature (X_2)	80	100	110	°C
Spray rate (X_1)	80	90	100	%

3.2.2 Spray drying of CS

The CS carrier was developed by spray drying. The CS in 1% acetic acid solution was pumped into an atomizing device where it was broken into small particles. The droplets dried rapidly when they came into contact with a stream of hot air that evaporated the moisture. The dry particles were separated from the moist air in a cyclone by centrifugal action. The dense powder particles were forced towards the cyclone walls while the moist air was directed away through the exhaust pipes. CS was dissolved in 1% acetic acid solution to obtain various concentrations of CS solutions in the range of 0.1-1% with a constant stirring at 500 rpm for 12 h. The solutions were then filtered through a 0.45 μm polyamide membrane. The density of the CS solution was determined using a pycnometer (Weigel International, Bayern, Germany). The solution was sprayed through a 1.5 mm sized nozzle using a mini-spray dryer B-290 (Buchi, Flawil, Switzerland) under different inlet temperatures (80-150°C) and a feeding rate of 3 mL/min. The outlet temperature was recorded, products were separated and collected by the cyclone and then directed into the collecting chamber. The collected powders were then monitored for their molecular weight, degree of deacetylation, size, surface area, flowability and preparation of formulation by mixing physically.

3.2.3 Molecular weight determination of CS solutions

The molecular weight of CS was determined before and after spray drying to monitor any changes. Samples of CS solutions were withdrawn before spray drying at 0, 6, 12, and 24 h to monitor its molecular weight. CS in an aqueous medium was incubated with continuous stirring at 500 rpm and the samples were collected at different time points. The molecular weight of the CS dry powder obtained after spray drying was determined by an electrospray ionization mass spectrometer (ESI-MS, 2690, LCT, Waters, Micromass, UK). Ten microliters were injected directly into the mass spectrometer and the solvent evaporated. The nozzle voltage was increased from 30 to 3200V to cause fragmentation and nebulised with nitrogen. During the ESI-MS, the hexapole were typically scanned from an m/z of 100 to 10,000 at 2s/scan. Calibration was performed using a separate injection of horse myoglobin (16.95 kDa).

3.2.4 Determination of the degree of deacetylation (DD) using nuclear magnetic resonance (NMR)

^1H NMR measurements were performed by a Fourier transform NMR spectrometer 500 MHz (Unity Inova, Varian, Germany) under a static magnetic field of 9.4 T at 70°C. For the ^1H NMR measurement, 5 mg of sample was vacuum dried at 50°C for 2 days. This was then introduced into a 5 mm NMR tube and further vacuum dried at 50°C for 2 days. Then 0.5 mL of a 2 % CD_3COOD in D_2O solution was added, and finally the test tube was kept at 70°C to completely dissolve the polymer. A 45° single pulse sequence was used for accumulation by free induction decay (FID). Pulse widths for the 2 % CD_3COOD in D_2O were 5.8 μs . The pulse repetition delays were 6 s. The spectral width and data points were 6000 Hz and 32 K points, respectively. The ^1H chemical shifts were expressed in ppm downfield from the signal for sodium 3-(trimethylsilyl) propane sulphonate (TSP) used as an external reference. The ^1H spin-lattice relaxation time, T_1 , was measured by means of an inversion recovery ($180^\circ\text{-}\tau\text{-}90^\circ$) pulse sequence. The DD was calculated by using the signal from the protons H_2 , H_3 , H_4 , H_5 , and H_6 (H_{2-6}) of both monomers and the peak of the acetyl group (H-Ac) by using equation 1 as proposed by Hirai et al., 1991.

$$\text{DD (\%)} = \left(1 - \frac{1}{3} \text{ICH}_3 / \frac{1}{6} \text{IH}_{2-6}\right) \times 100 \quad (1)$$

3.2.5 Determination of the particle size, surface area, porosity, and flow ability of the CS carrier

The size distribution of CS dry powder was determined by Zetasizer® (Malvern, Worcestershire, UK). Five hundred milligrams of CS powders were weighed and dissolved in 50 mL of 1% acetic acid solution and sonicated for 10 min and then its particle size was analyzed. The specific surface area of the carrier was determined to analyze the surface area associated with the number of dimples formed on the surface of the carrier. The surface area of the CS carrier was calculated by the BET equation. The specific surface area determination by the BET equation was dependent on the physical adsorption of the gases on the external and internal surfaces of the porous powder particles. The powder particles were surrounded by and in equilibrium with nitrogen gas at a certain temperature, T and the relative vapor pressure P/P_0 adsorbed physically a certain amount of gas. The adsorption of the gas depended upon its relative vapor pressure and was proportional to the total external and internal surfaces of the powder particles. The surface area of the CS carrier was determined using the Autosorb 1C, Quantachrome analyzer (Florida, USA). About 1 g of the sample was filled into a capillary glass tube and degassed at 120°C for 14 h, and the nitrogen adsorption and desorption was carried out at 77K.

The bulk density ρ_b and tap density ρ_t of the carrier were determined by filling the particles into a 10 mL graduated cylinder and the volume was recorded (bulk volume), then the cylinder was tapped 200 times and the new volume was recorded (Tapped volume). The bulk density and tapped density were calculated as the powder weight divided by the powder bulk volume and the tap volume, respectively. The porosity (P) of the carrier was calculated using equation 2. The angle of repose (α) is the most common method to describe the powder flow properties. In order to calculate the angle of repose, 1 g of CS powder was poured through a 75 mm funnel onto a flat surface and the funnel tip was 3 cm. The angle of repose was then calculated by the following equation 3, where h is the height of the powder cone and D is the diameter of the base of the formed powder pile. A higher α is indicative of a poorer flow property.

$$P = \left(1 - \frac{\rho b}{\rho t}\right) \times 100 \quad (2)$$

$$\text{Tan } \alpha = \frac{2h}{D} \quad (3)$$

3.2.6 Preparation of the EDH formulation by physically mixing EDH with different ratios of CS

Five formulations were prepared by the physical mixing of different ratios of nano-sized EDH and dimple shaped chitosan particles i.e. 1:2, 1:2.5, 1:3.3, 1:5 and 1:10 w/w namely formulation #1 to # 5. The drug dose ratio (2.25 mg) was kept constant but the carrier ratios were varied in each formulation. Specific amount of drug and carrier powder were measured. The drug-carrier mixtures were prepared by mixing in a screw cap tube that was fixed on a V- shaped mixer (Superline, Japan) with tape and operated at 50 rpm for 1 h. The mixing was stopped at 15 min intervals and mixed manually for a further five min.

3.2.7 EDH, CS and EDH formulations imaged by SEM

The morphology of the carrier, drug and drug-carrier mixtures from all formulations were obtained using scanning electron microscopy (Jeol, Japan). A small amount of each sample was scattered on an aluminum stub whose surface was covered with a clear double-sided adhesive tape. In order to obtain uniformly scattered samples the aluminum stub was tapped gently on its edge with a spatula. The particles were then coated with a 15 to 20 nm layer of gold using a sputter coater (SPI supplied, USA) in an argon atmosphere (50 Pa) at 50 mA for 120 s. All micrographs were taken at an acceleration voltage of 20 kV.

3.2.8 Characterization of the EDH, CS, and EDH formulations by DSC

DSC thermograms of the EDH, CS and EDH formulations were recorded with a Perkin Elmer TAC/DX (Massachusetts, USA) instrument by sealing 3 mg samples in aluminium crimp pans (an empty pan was also sealed to act as a reference) and heated from 25-300°C at a scan rate of 10°C /min under a flow of nitrogen at a flow rate of 50 mL/min.

3.2.9 Characterization of the EDH, CS, and EDH formulations by FTIR

The FTIR spectra were recorded over the frequency range of 4000-450 cm^{-1} and 16 scans were obtained at a 4 cm^{-1} resolution. One mg of the drug mixture was carefully mixed with dry KBr (10 mg). The KBr disc was prepared by compressing the powder with a hydraulic press of 10 tons.

3.2.10 Determination of the uniformity of the drug content in each dose of the various formulations

EDH formulations (25 mg) were mixed and weighed. The powder was suspended in 25 mL of distilled water to be dissolved completely by sonication for 15 min to obtain a clear solution. The EDH content in each formulation was analyzed by *high-performance liquid chromatography (HPLC)*. The experiments were performed using a HPLC system consisting of a Spectra System SCM 1000 and Spectra System Pump P2000 with Spectra System AS3000 auto sampler equipped with a Spectra System UV1000 detector (Thermo Scientific, UK). An ODS Hypersil C18 column (Thermo Scientific, USA) (250 x 4.6 mm, 5 μm) was used as a stationary phase. The mobile phase consisted of tetrahydrofuran (250 mL), Milli-Q water (750 mL), sodium 1-heptanesulfonate 2 g and 0.08 g of cupric sulfate (anhydrous). The apparent pH was adjusted to 4.5 with dilute hydrochloric acid. The mobile phase was set at a flow rate of 1 mL/min at ambient temperature, the retention time was 18 min, and the wavelength was set at 260 nm with an injection volume of 20 μL (Jiang et al., 2002).

3.2.11 Determination of the detachment force for the EDH from the carriers by using ultracentrifugation

The separation of drug particles from the dimple shaped CS carrier was performed by an ultracentrifugation method. During centrifugation the drug particles of each formulation were detached from the carrier at different g-forces. The separation of drug with carrier gives an idea about force at which it get separated from carrier inside the respiratory tract and move inside deep into the lungs through various phenomena i.e. impaction, sedimentation and diffusion. The deposition of drug particles in different region of lungs depends upon the size of the drug. If the size of

the drug particle is more than 5 μm then it will not enter inside the alveoli and if its size is less than 1 μm then it will exhale out without depositing inside the alveoli. The centrifugation frequency (f_c) was converted to an angular velocity (ω) according to equation 4.

$$\omega = f_c \left(\frac{\pi}{30} \right) \quad (4)$$

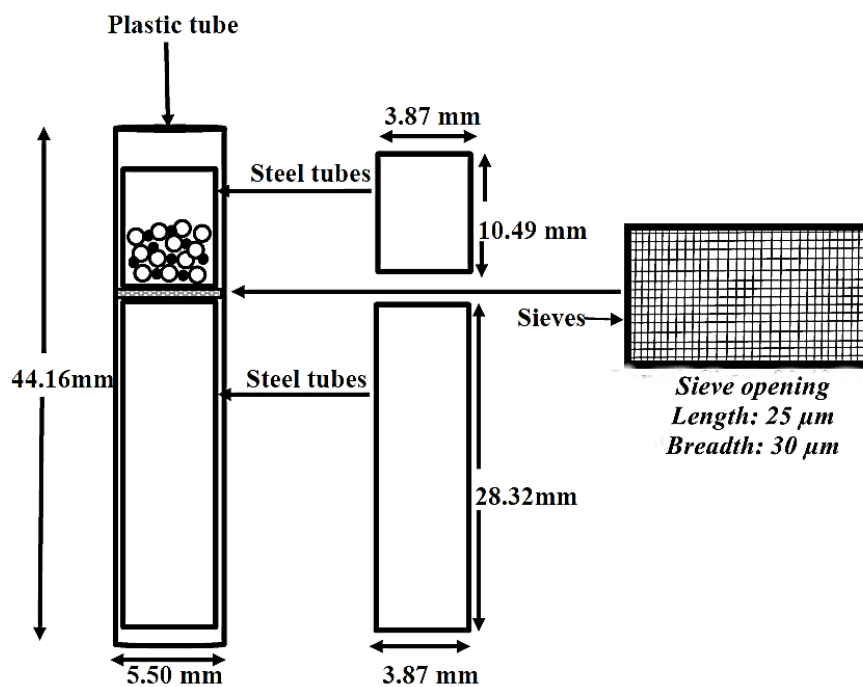
The centrifugal acceleration was then calculated as the product of the centrifugation radius and the square root of its angular momentum as shown in equation 5.

$$a_c = r\omega^2 \quad (5)$$

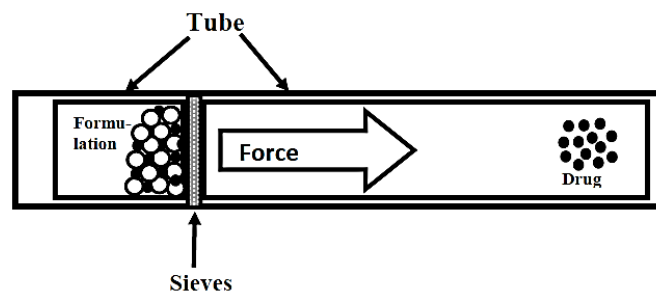
The detachment force F (N) between the drug and carrier was then measured as the product of the drug weight and acceleration as shown in equation 6.

$$F = ma_c \quad (6)$$

Five formulations (#1 to # 5) were used to study the deaggregation of the drug particles at various centrifugal forces (3368 g, 13473 g, 30315 g, 53894 g and 82410 g). The ultracentrifugation was carried out using an in house developed centrifuge tube (length of stainless steel tube: 38.81 mm, diameter: 3.87 mm). The stainless steel tubes were placed in a plastic tube (length: 44.16 mm, diameter: 5.50 mm) with a sieve sandwiched between the two halves of the cut tubes. The sandwiching sieves had a sieve aperture of 25 μm x 30 μm (Figure. 3.1). Twenty-five milligrams of a drug-carrier mixture from each formulation was loaded into the upper portion of the tube.



a) Ultracentrifuge tube at vertical position during drug loading.



b) Ultracentrifuge tube at horizontal position during rotation.

- : Carrier
- : Drug

Figure 3.1 Indigenously prepared Ultracentrifuge tube.

a) The sieves were sandwiched between two stainless steel tubes and kept inside the plastic centrifuge tube which rotates under different rotational centrifugal force (RCF) after loading the dry powder formulation.

b) It showed the position of centrifuge tube under rotation and the separation of drug from the carrier.

The tubes were then put into the ultracentrifuge tube holder and centrifuged in a pre-warmed (25°C) SW60Ti rotor, tube 4.2 mL open top no 328874 using an ultracentrifuge (Optima L100 XP, Beckman Coulter, Palo Alto, California)

at different g-forces at 25 °C for 5 min. After the centrifugation, tubes were carefully removed from the rotor. The EDH that separated from the CS surface was carefully collected from the lower tube by washing it with 5 mL of the mobile phase used for the HPLC and the amount of the drug particles were determined. Graphs were plotted between the percentage of the drug particles detached and the g-forces, the median g-force was determined to calculate the centrifugal force required to remove the drug from the carrier. The median g-force was used to approximate the interactive force between the drug and the carrier (equation 6). The different formulations prepared by physical mixing were further investigated for its deposition in different region of the lung by using Andersen cascade impactor.

3.2.12 *In-vitro* deposition of the EDH formulation in an Andersen Cascade Impactor (ACI)

The ACI studies of various formulations were carried out using a specially designed plastic device (Rojanarat et al., 2011). Twenty-five milligrams of a EDH formulation in capsule size number 3 were loaded into the plastic device and drawn into the ACI (Atlanta, USA) at a flow rate of 60 L/min for 10 s. Each stage of the ACI was then washed with 25 mL of copper sulphate solution. The amount of drug on each stage was evaluated as described in the drug content section. The cumulative percentage of deposition was transformed to a Z-value and plotted against the log cutoff diameter of each stage. The mass median aerodynamic diameter (MMAD) was obtained from the particle diameter at a Z-value of zero. The emitted dose (ED) was the amount of the drug released from the delivery device. The fine particle fraction (FPF) was the fraction of the particles smaller than 4.4 µm. The *in-vitro* deposition gives an idea about the deposition of formulations in different regions of the lung. The formulations were further monitored for its cytotoxicity and bioactivity test on lung cells.

3.3 Cell cultures

3.3.1 Human bronchial epithelial cells (Calu-3)

The Calu-3 cell line (ATCC HTB-55, Maryland, USA) was cultured in Modified Eagles Media (MEM, Gibco, New York, USA) supplemented with 10%

fetal bovine serum (FBS, Gibco, New York, USA), and 50 units/mL penicillin and 50 µg/mL streptomycin (Gibco, New York, USA). The cells were maintained at 37°C in a fully humidified atmosphere at 5% CO₂ in the air and the media were changed every 2-3 days.

3.3.2 Human lung adenocarcinoma cell line (A549)

The A549 cell line (ATCC CCL-185, Maryland, USA) was cultured in Ham's F12K (Gibco, New York, USA) supplemented with 10% FBS, 50 units/mL penicillin and 50µg/mL streptomycin. The cell line was maintained at 37°C in a fully humidified atmosphere at 5% CO₂ in the air and the media were changed every 2-3 days.

3.3.3 Alveolar macrophage cell line (NR8383)

The NR8383 cells (ATCC CRL-2192, Maryland, USA) had been isolated from normal rat lung lavage. The cells were cultured in F-12 Kaighn's cell culture medium supplemented with 15% (v/v) FBS, 50 units/mL penicillin and 50 µg/mL of streptomycin, and then incubated at 37°C, in 5% CO₂ and 95% humidity. The cells were maintained by transferring floating cells to new flasks. Adherent cells could be harvested by scraping. Upon reseeded, about half of the cells re-attached. The medium was replaced with fresh medium two or three times weekly.

3.4 Determination of cytotoxicity of EDH, CS and EDH formulations

The viabilities of Calu-3, A549, and NR8383 cells line were evaluated using the MTT assay to detect functioning mitochondria. Live mitochondria transform MTT to insoluble purple formazan crystals, which were measured with a spectrophotometer. Briefly, 100 µL of 1×10^5 cells/mL was cultured in each well of a 96-well plate and allowed to adhere and grow overnight at 37°C, in a 5% CO₂ and 95% humidity incubator. The following day, the media (100 µL) were replaced with fresh media and 100 µL of EDH, CS, and EDH formulations (2 µg, 4 µg, 8 µg, 16 µg, and 32 µg) were added in culture flask and incubated for 24 h. After incubation, 50 µL of MTT solution (5 mg/mL) in phosphate buffer saline (PBS, Gibco, New York, USA) was added into each well and incubated for 4 h at 37 °C. After that, the

supernatant was carefully removed and the resulting formazan crystals were dissolved by adding 100 μ L of dimethylsulfoxide (DMSO, Seelze, Germany). The absorbance was recorded at 570 nm with the microplate reader (Biohit BP 800, Helsinki, Finland). The proportion of viable cells in the treated well was compared to the untreated well. If the viability is more than 80% then it is considered as non-toxic to the cells. The EDH and chitosan was completely dissolved in media and were used as a solution in the study.

3.5 Determination of cytokine response to EDH formulations

3.5.1 Nitric oxide by the Griess reaction assay

Nitric oxide (NO) released by NR8383 cell after being challenged for 10 min with EDH formulations and LPS. EDH formulations in a concentration range of 2-32 μ g/mL and LPS in 15-1000 ng/mL were detected by the Griess reaction assay. Nitric oxide in the form of nitrite (NO_2), which is one of the two primary, stable, and nonvolatile products of NO, was investigated. This measurement relies on a diazotization reaction of the Griess reagent. Griess reagent was prepared by mixing 1% sulfanilamide, 0.1% N-(1-naphthyl)-ethylenediamine dihydrochloride and 2.5% phosphoric acid in water. Equal volumes of cell supernatant (100 μ L) and Griess reagent (100 μ L) were mixed. After mixing for 10 min, the absorbance was determined using a microplate reader at 450 nm. The NO concentration was calculated from a sodium nitrite standard curve (Huttunen et al., 2000; Punturee et al., 2004).

3.6 Assessments of the anti-mycobacterial activity of EDH formulations

3.6.1 Culture of *M.bovis*

The lyophilized BCG vaccine of *M.bovis* was reconstituted with 1 mL of sterile deionized water for injection. Reconstituted BCG vaccine (200 μ L) was grown in Middlebrook 7H9 broth (M7H9, pH 5.5) containing 0.5% Tween 80 and 10% oleic acid-albumin-dextrose catalase (OADC, Becton Dickinson, Shannon, Ireland) enrichment (Ritelli et al., 2003). The bacilli were incubated at 37 °C and subcultured every 3 weeks. The obtained *M. bovis* suspension at 3 weeks old was used in this experiment.

3.6.2 Determination of MIC against *M. bovis*

MIC was determined by using resazurin method as described by Palomino et al., 2002 with minor modifications. Briefly, 100 μL of the serially diluted EDH, CS, and EDH formulation in a drug concentration range of 64-0.125 $\mu\text{g}/\text{mL}$ were added to each well plate. Inoculum of 3 weeks old were compared with 0.5 McFarland standard which is equivalent to 10^8 CFU/mL, then 10 fold serial dilution were prepared in normal saline to obtain 10^6 CFU/mL. Ten microliters of a suspension of *M. bovis* (10^6 CFU/mL) were added in 100 μL of sample in each well. The final *M. bovis* concentration in each well was 10^5 CFU/mL. M7H9 media was used as a negative control and bacteria inoculum as a growth control in the study. Bacterial growth was assayed by resazurin indicator after incubation of 24 h. After incubation of 24 h, 30 μL of 0.02% resazurin in PBS was added to inoculate well plate and incubate at same condition for next 24 h. A change in color from blue to pink indicates the growth of bacteria and MIC is defined as the lowest concentration of drug that prevents this change in color.

3.7 Determination of cell permeability with EDH formulations

3.7.1 Lipid bilayers

The lipid bilayer is a universal component of cell membrane which gives a structural component and forms a protective layer over cell. When phospholipids are exposed to water, they orient themselves into a bilayer with all the hydrophilic heads face the water at each surface of the bilayer, and the hydrophobic tails are shielded from the water in the interior. There are three major classes of membrane lipid molecules-phospholipids, cholesterol and glycolipids. Bilayers lipid composition is different for inner and outer monolayers, reflects different functions of the two faces of a cell membrane. The head groups of some lipids form docking sites for specific cytosolic proteins. Some extracellular signals that act through membrane receptor proteins activate phospholipases that cleave selected phospholipid molecules in the plasma membrane, thereby generating fragments that act as intracellular signaling molecules.

3.7.2 Preparation of lipid bilayer

Lipid bilayers were prepared by dissolving 67 mole % L- α phosphatidylcholine (0.514 mg/mL) and 33 mole % of cholesterol (127.6 mg/mL) in 35 ml of chloroform in a 100 mL round bottom flask for uniform mixing. The solvent was removed under reduced pressure using a rotary evaporator in 45-50°C till it forms a dried film. The dried film was transferred to a petri dish and further heated at 40°C for 48 h on hot plate to completely remove the solvent from it. The dried mixture of powder was transferred into the round bottom flask with 7 mL of water in it and kept in a water bath (50°C) for 1 h for hydration. The hydrated suspension (500 μ L) was transferred on each transwell and dried at 40°C for 48 h (Figure 3.2). The dried transwell was used in the cell permeability study. The cell permeability test was performed by using chamber (Ostroumova et al., 2012).

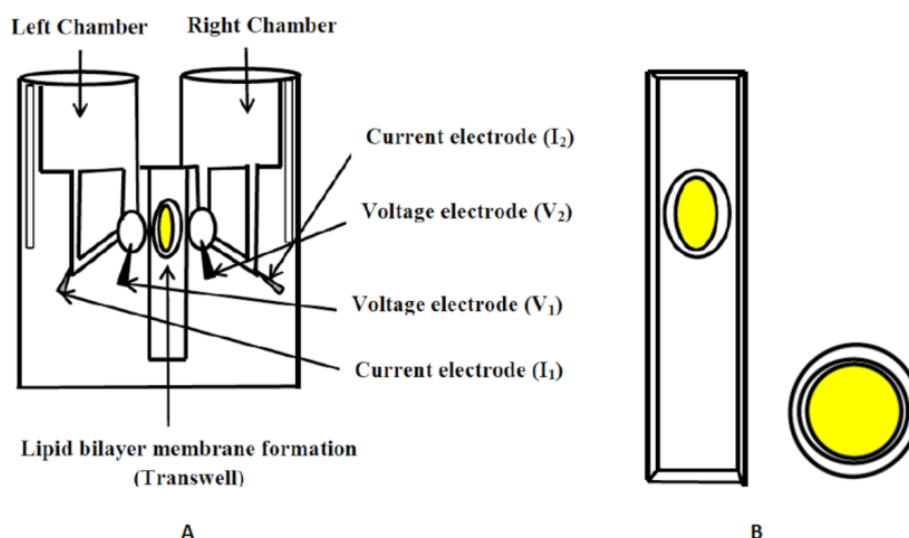


Figure 3.2 Schematic diagram of Ussing chamber fitted with lipid bilayer membrane (A) and transwell (B) (Clarke, 2009).

3.7.3 Preparation of electrodes

Ag/AgCl electrodes with agarose/2 M KCl bridges were used to apply the transmembrane voltage (V) and measure the transmembrane current (I). The electrodes were prepared by dissolving 10 mL of 2 M KCl and (300 mg) 3% Agar in a beaker and kept in a water bath at 100°C for 5 min with continuously stirring it to mix

well and should be free from air bubble trapped. When the solution was completely dissolved and forms a transparent solution, then it was transferred inside electrode (5 mm in length) with the help of the 2 mL syringe from the tip of the electrode and the rest of the space in electrode should be filled with KCl (2 M) solution.

3.7.4 Preparation of transport media

The buffer was prepared by dissolving 0.352 g of sodium dihydrogen phosphate dihydrate ($\text{NaH}_2\text{PO}_4 \cdot 2\text{H}_2\text{O}$) and 1.378 g disodium hydrogen phosphate dihydrate ($\text{Na}_2\text{HPO}_4 \cdot 2\text{H}_2\text{O}$) in 1 L of distilled water. The pH of the buffer was maintained in 7.4 with the help of sodium hydroxide solution.

3.7.5 Sample collections from Ussing chamber

The transwell was fitted into the Ussing chamber and 5 mL of phosphate buffer (10 mM, pH 7.4) was added in both the chamber and left for 1 h to completely hydrate and stabilize the membrane on transwell as a formation of bilayer with phosphate buffer solution. After 1 h, 100 μL of drug solution (concentration of drug 200 $\mu\text{g}/\text{mL}$) was added in left chamber and current were noted at zero interval, then 1 mL of sample were withdrawn for 120 min At each 15 min interval from right chamber and current were noted and volume was compensated with 1 mL of phosphate buffer solution in the right chamber. Sample collected was quantified by the HPLC.

3.7.6 Functioning of Ussing chamber

An Ussing chamber is an equipment which is used to measure the short-circuit current as an indicator of net ion transport taking place across a lipid bilayer membrane/epithelium (Figure 3.2). An Ussing chamber consists of two halves that are clamped together, having the lipid bilayer membrane. The two half chambers are filled with 5 ml of buffer (10 mM) in order to remove any chemical, mechanical and electrical driving forces. In lipid bilayer, there is an ion transport taking place across all sides. This ion transport produces a potential difference (voltage difference) across the lipid bilayer. The voltage difference generated is measured using two

voltage electrodes that are placed nearer to the lipid bilayer. And this voltage is cancelled out by injecting the current using another two current electrodes that are placed away from the lipid bilayer. This amount of current injected is called Short-circuit current (Isc) and is the exact measure of net ion transport taking place across the lipid membrane. The lipid bilayer ion transport is the factor of greatest interest in research involving Ussing chambers. The voltage that is measured as the voltage difference is a result of this ion transport and the voltage difference is easy to measure accurately. The lipid bilayer pumps ions from one side to the other. In order to measure the ion transport, an external current is applied to measure across the bilayer. The resistance between the voltage electrodes external to the lipid bilayer has also to be accounted for in some way. The Isc as measured above is always an underestimate of the ion transport and the error can be as much as 10 times. The error is dependent mostly on the chambers. With the type of chambers correctly suggested by Ussing the error is large. This error is often estimated and compensated for by measuring without the lipid bilayer present. They involve using alternating current in the form of sinus shaped current using several frequencies, square wave pulses, sharp impulses and even random noise.

3.8 Phagocytosis of EDH formulations by macrophage cells

EDH formulation I was reconstituted with distilled water to obtain 10 mg/mL. Quantum dot nanoparticles were employed for particle imaging (Lumidot[®], Sigma-aldrich, St. Louis, USA). Lumidot[®] 640, 20 µg/mL was added to the formulation suspension in a volume ratio of 1:2. The mixture was sonicated for 3 minutes and observed with a fluorescence microscope (Olympus, BX61, Olympus, Tokyo, Japan). One hundred µL of NR8383 cells (1×10^5 cells/ml) were cultured in each well of a 96-well plate and allowed to grow and adhere overnight at 37°C, in a 5% CO₂ and 95% humidity incubator. EDH formulation stained with Lumidot[®] 640 was added. Phagocytosis of this formulation by NR8383 cell was observed with a fluorescence microscope.

3.9 Statistical analysis

Data are presented as a mean \pm standard deviation (SD) from at least three replicates of sample in each experiment. The data were analyzed by one-way analysis of variance (ANOVA) and the Student's *t*-test was used to determine the level of significance of the differences in means. A significant difference was accepted with $p < 0.05$ between data sets. All statistical comparisons were calculated using the SPSS software version 16 (SPSS Inc., Chicago, IL).

CHAPTER 4

Results and discussion

4.1 Optimization of the spray drying process of EDH

The drug with a nano size of 260 nm was produced after nano spray drying at 110°C at an 80% spray rate (Figure 4.1). The size of the drug obtained was dependent on the spray rate and inlet temperature. At a low spray rate with a higher inlet temperature, the drug obtained was of a smaller size than at a low inlet temperature with a low spray rate (Table 3.1).

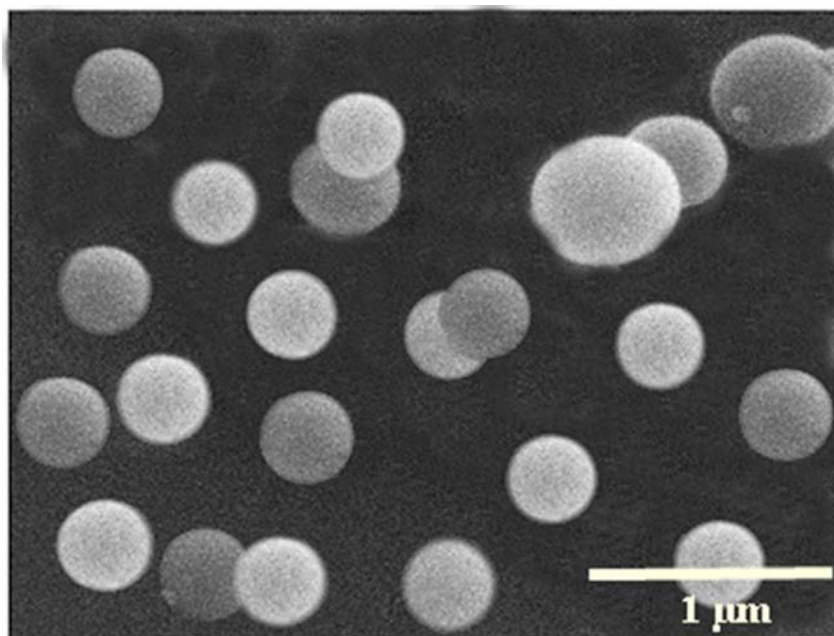


Figure 4.1 The SEM images of EDH at 50,000X after nano spray drying at 80 % spray rate and inlet temperature of 110°C.

The experimental methodology design was employed to systematically evaluate the main effects of various factors and their interactions were calculated. For example, the effects of the spray rate and inlet temperature on the percentage yield of the products. Various processing variables caused a considerable change in the yield of the powder that ranged from 58 to 80%. The R^2 values from polynomial regression analysis were 0.990. The spray rate and inlet temperature were clearly two important factors for the production yield. By polynomial linear regressions, the relationship between the main

factors: the spray rate (X_1) and inlet temperature (X_2) within the yield response have been presented as an equation 7.

$$Y = 546.78 - 9.05X_1 + 0.05X_1^2 - 0.93X_2 + 0.01X_2^2 - 0.005X_1X_2 \quad (7)$$

Where Y is the production yield (%), X_1 is spray rate (%) and X_2 is inlet temperature ($^{\circ}\text{C}$). It was observed that the most important parameter was spray rate and the lesser but also important is inlet temperature; the other coefficients were less effective on the % yield of product. The coefficient of spray rate (X_1) was negative which meant that when the spray rate decreased, there was a high production yield, and as the coefficient of the inlet temperature (X_2) was negative too which helped in increase of product yield (Figure 4.2). Hence the % yield of the powder was dependent on both the inlet temperature and the spray rate. When the formulation was sprayed at a high inlet temperature and low spray rate, the liquid might evaporate from its surface due to the longer duration of stay in the spray chamber that resulted in a smaller size of the powder particles. The prepared drug was used to prepare formulations with carrier and its physicochemical parameters, toxicity, and bioactivity were analyzed.

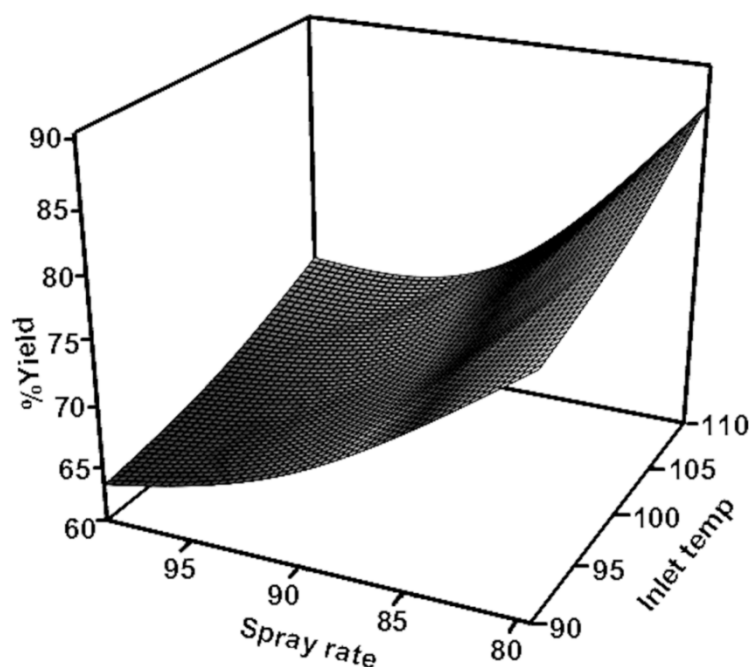


Figure 4.2 Optimization of EDH's % yield at different inlet temperatures (90°C, 100°C and 110°C) and spray rate conditions (80, 90 and 100%).

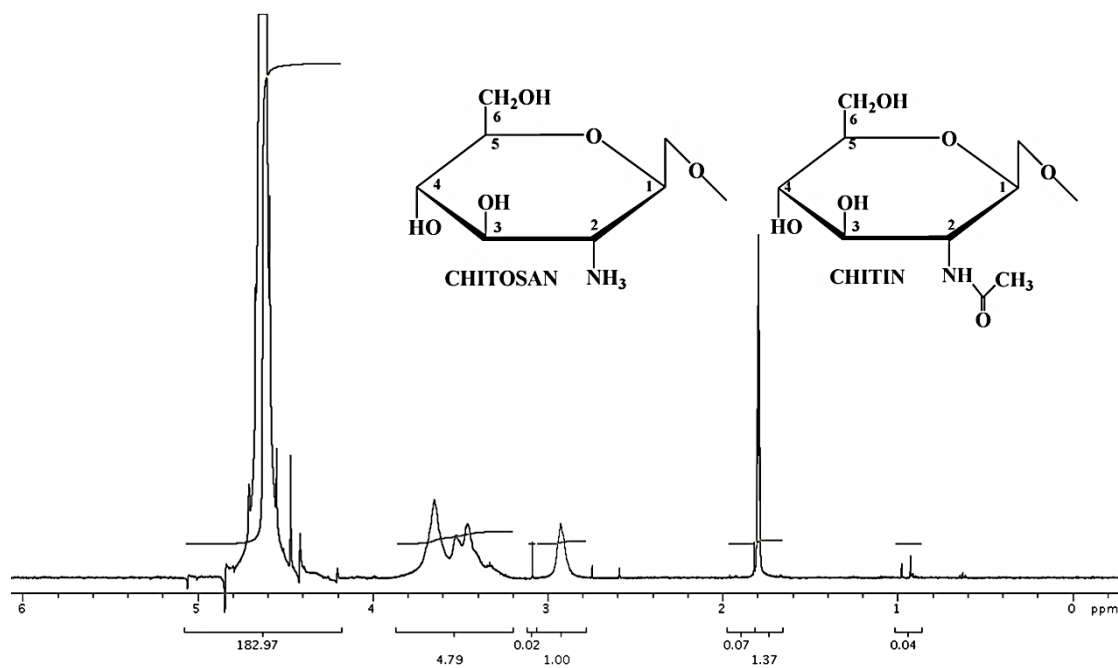
4.2 Physicochemical properties of CS

For CS before spray drying, the solvent (HOD) proton resonated at 4.5-4.8 ppm, the acetyl group resonated at 1.37 ppm and the protons H₂-H₆ showed resonance at 3.2 – 3.8 ppm. After spray drying the solvent (HOD) proton resonated at 4.4 – 4.9 ppm, the acetyl group resonated at 1.08 ppm and the protons H₂-H₆ showed resonance at 3.3 – 4 ppm. CS before spray drying had a 56% DD and after spray drying this value was 58% (Figure 4.3). There was no any significant change in the DD of CS before and after spray drying. The molecular weight of the CS solution was 3.2 kDa at any time point. There were no differences found in the CS molecular weights. The surface areas of the CS carrier increased from a low CS (0.1%) to a high CS concentration (0.4%). The surface area decreased significantly in the 1% CS due to the increase in the CS carrier size. The carrier of 0.1 % had a size of 942 nm with a surface area of 11.2 m²/g, while the carrier of 1% had a size of 1226 nm with a surface area of 6.21 m²/g (Table 4.2). When the solution was sprayed at a high inlet temperature (150°C) with a low feed rate, the particles emitted through the nozzles showed shrinkage on their surfaces. This may be due to water evaporation at a high

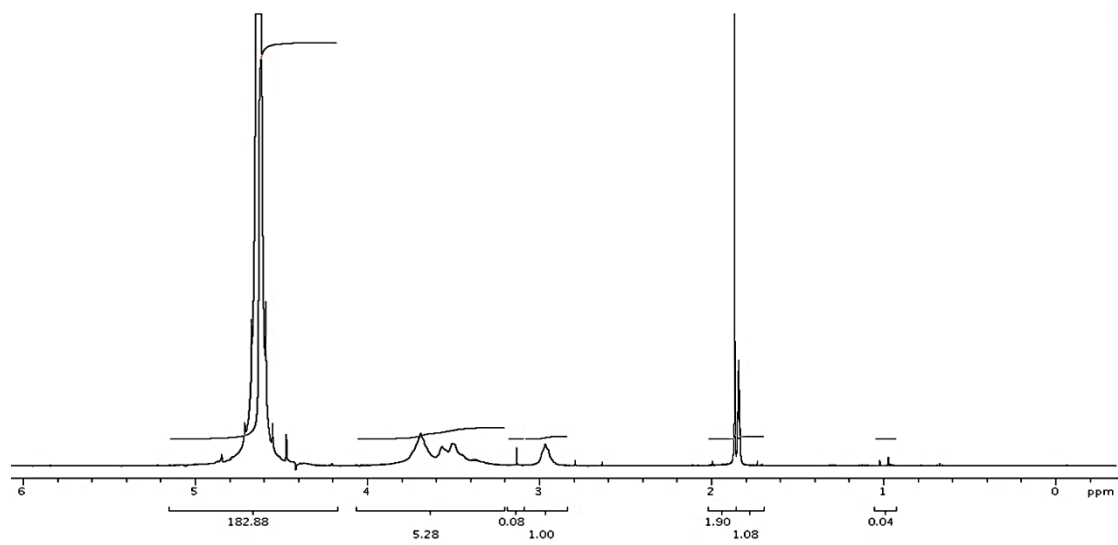
inlet temperature that resulted in the formation of dimples on the particle surface (He et al., 1999) (Figure 4.4). The carrier particles obtained upon spray drying were positively charged spherical microparticles with dimples over their surface. The chitosan carrier obtained was dry, non-cohesive with good powder particle flowability. The 1% CS obtained after spray drying had a porosity of 40% and an angle of repose of 28.8°, and this indicated a good flowability. Generally, powder particles having an angle of repose below 30° are considered to have good flowability (Geldart et al, 2006). The SEM micrograph of the carrier showed a gradual increase in the number of dimples on its surface with increasing chitosan concentrations (0.1-1%).

Table 4.2 Particle size and surface area of CS powders obtained from the spray drying process of a CS solutions (mean \pm SD) (n=3)

Chitosan (%)	Particle size (nm)	Specific surface area (m ² /g)	Porosity (%)	Angle of repose (α)
0.1	943 \pm 156	11.0	26 \pm 1.2	31° \pm 3
0.2	1015 \pm 84	11.7	28 \pm 1	27° \pm 2
0.3	686 \pm 49	12.5	31 \pm 1	25° \pm 1
0.4	837 \pm 22	15.4	27 \pm 1	29° \pm 1
0.5	808 \pm 88	12.8	34 \pm 1	28° \pm 2
1	1223 \pm 115	6.2	40 \pm 1.5	29° \pm 1



(a)



(b)

Figure 4.3 NMR spectra of CS (a) before spray drying and (b) after spray drying.

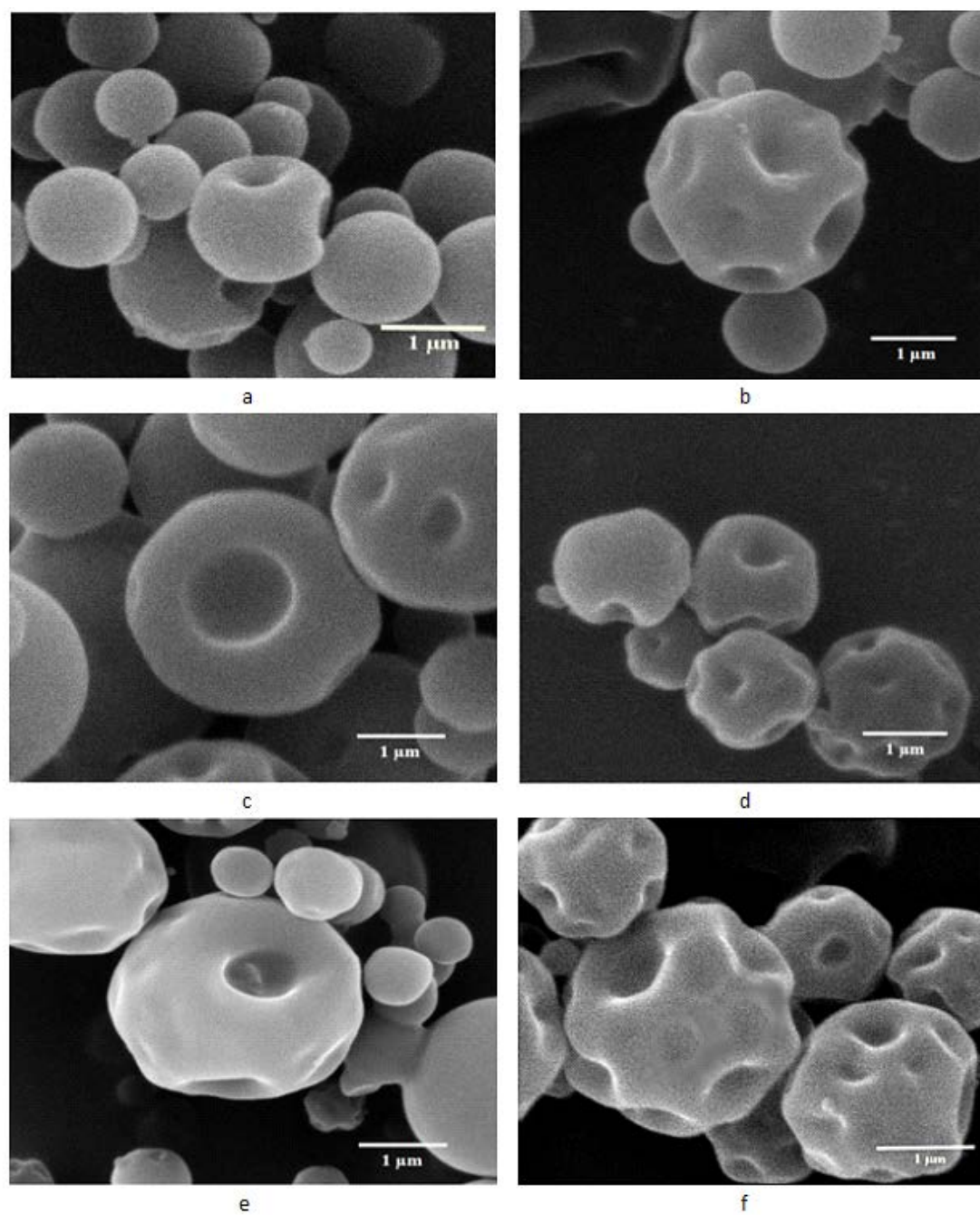


Figure 4.4 The SEM images of CS particle which was taken at 50,000X (1-6) from spraying of 0.1% (Control/sphere) at 80°C (a), 0.2% (b), 0.3% (c), 0.4% (d), 0.5% (e) and 1% (f) CS solution at 150°C with feeding rate of 3 mL/min.

4.3 Physicochemical properties of EDH formulations

The formulated mixtures of ethambutol and chitosan were free flowing and non-hygroscopic in nature. The SEM micrographs of the formulations (#1 to #5) showed the binding of the drug on the carrier dimples (Figure 4.5). The drug was bound to the whole surface of the chitosan as well as on the grooves of the dimple. As the concentration of carrier increased the binding of the drug with chitosan became mostly restricted to the dimples of the chitosan body. When the ratio of carrier was 1:2 to 1:2.5 in the formulations #1 and #2, the drug was bound over the entire surface of the carrier as well as forming clumps. The drug-carrier binding was relatively better in the formulation #3, in which the drug binding was restricted to the grooves in the formulations #4 and #5. The DSC thermograms clearly indicated that the drug was crystalline in nature with a melting point at about 203 °C (Figure 4.6). The CS carrier after spray drying had an amorphous property. The formulations showed small peaks of crystallinity between 45-49 °C but later became amorphous. The FT-IR spectra of the EDH showed O-H stretching at 3435.05 cm^{-1} , N-H stretching at 2345.77 cm^{-1} and C-N stretching at 1260.33 cm^{-1} (Figure 4.7). The spectra of CS showed N-H stretching (1° amine) at 3400.41 cm^{-1} and C=O stretching at 1638.93 cm^{-1} while the spectra of the formulation 1:2 retained the N-H stretching of chitosan at 3400.41 cm^{-1} but had a C=O stretching at 1631.35 cm^{-1} .

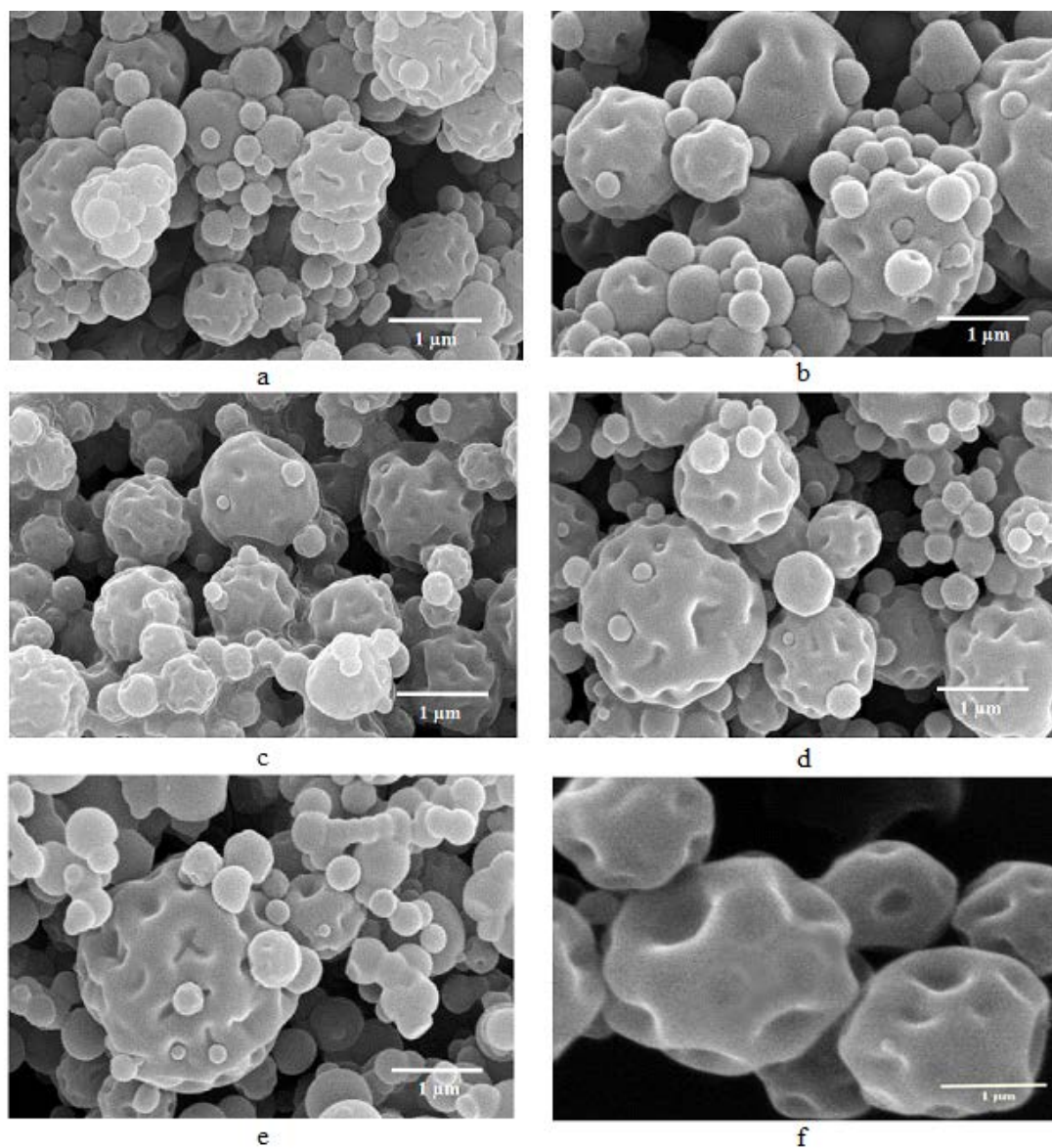


Figure 4.5 The SEM images of CS and EDH formulations of 1:2 (a), 1:2.5 (b), 1:3.3 (c), 1: 5 (d) and 1:10 (e) and plain CS (f).

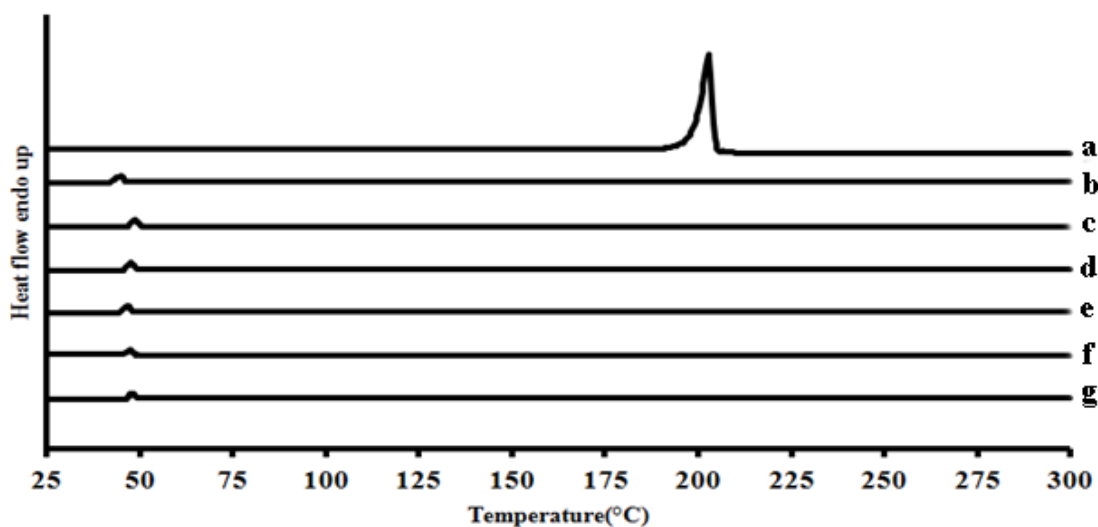


Figure 4.6 The DSC thermograms of EDH, CS, and EDH formulations at different ratios. EDH (a), CS (b), and EDH formulations at various ratios of 1:2 (c), 1:2.5 (d), 1:3.3 (e), 1:5 (f) and 1:10 (g).

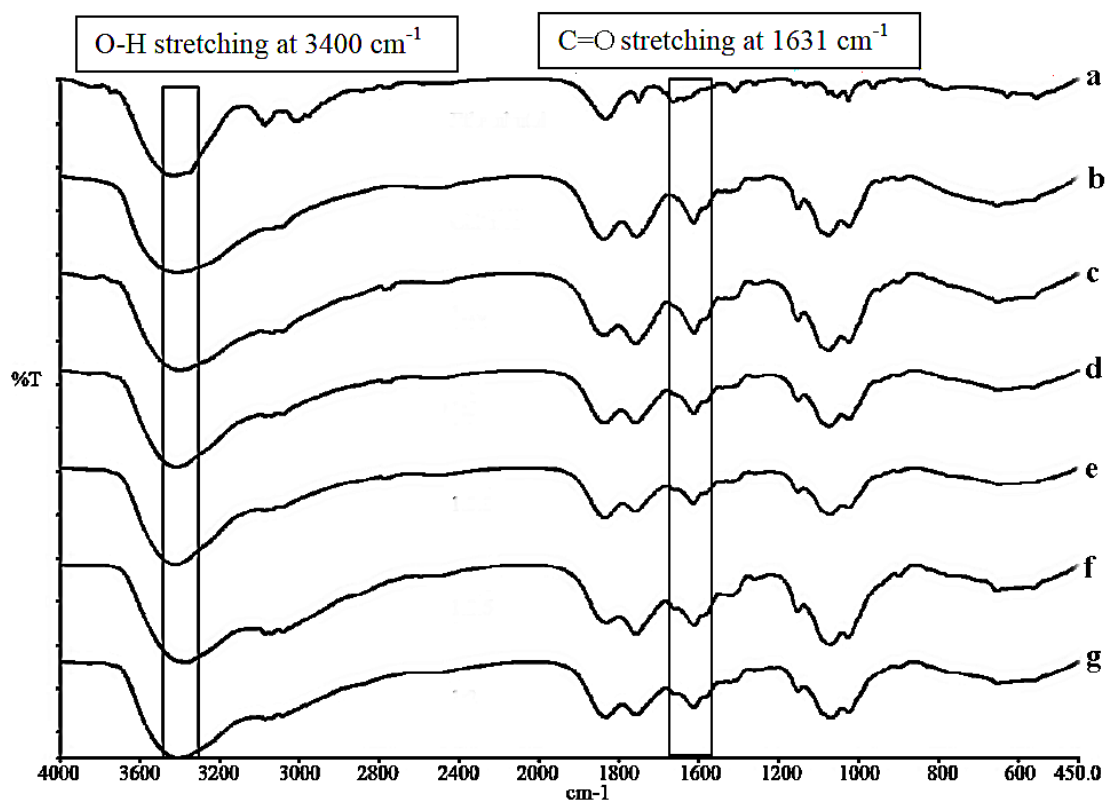


Figure 4.7 The FT-IR spectra of EDH (a), CS, (b) and EDH formulation mixtures at various ratios of 1:2 (c), 1:2.5 (d), 1:3.3 (e), 1:5, (f) and 1:10 (g).

4.4 Content uniformity of EDH formulations

Formulations (#1 to #4) showed a uniform drug content within the acceptable range (%RSD less than 2, USP 30, and NF 25; USP-NF, 2007). The drug contents of these four formulations were between 99-107% (Table 4.3) of their labeled amount. The formulation #5 did not have a uniform content. This might be due partly to the drug binding strongly to the CS solution.

Validation for EDH was also performed to determine the precision and reliability of the method. It was observed that standard curves were linear over the investigated range (20-100 $\mu\text{g/ml}$) for EDH with the correlation coefficient (r^2) over 0.9995. Therefore, these ranges of concentration were suitable for preparing the standard solution and sample for analysis. The results of accuracy and system precision tests performed on each concentration of EDH are shown in Table 4.4. For accuracy, both intra- and inter-day run gave the values of % recovery varied between 99-100% which was lined in the acceptable range. The system precision was considered to be satisfactory since the % RSD values were not more than 2.74 % for both intra- and inter-day run (ICH, 2005). The limit of detection of EDH was found to be 1.6 $\mu\text{g/mL}$ and the limit of quantitation was determined to be 4.9 $\mu\text{g/mL}$ respectively.

Table 4.3 Physicochemical properties of EDH formulations (mean \pm SD, n=3).

Formulation (#)	EDH: Chitosan	Drug content (%)	MMAD (μm)	ED (%)	FPF (%)
1	1:2	101.6 \pm 1.0	2.3 \pm 0.1	84 \pm 1	42 \pm 1
2	1:2.5	107.2 \pm 1.0	2.4 \pm 0.1	83 \pm 1	36 \pm 2
3	1:3.3	105.1 \pm 0.7	2.5 \pm 0.1	80 \pm 1	34 \pm 0
4	1:5	99.2 \pm 0.8	2.7 \pm 0.1	83 \pm 1	32 \pm 0
5	1:10	61.0 \pm 1.0	2.9 \pm 0.0	85 \pm 1	31 \pm 0

Table 4.4 Percent recovery and RSD for accuracy and precision of EDH (mean \pm SD, n=5)

Concentration ($\mu\text{g/mL}$)	Accuracy (% Recovery \pm SD)		Precision (% RSD)	
	Intra-day	Inter-day	Intra-day	Inter-day
20	103.30 \pm 0.297	100.94 \pm 2.75	0.28	2.74
40	100.07 \pm 1.743	99.50 \pm 1.62	1.74	1.63
60	99.22 \pm 2.46	101.73 \pm 1.26	2.46	1.24
80	99.32 \pm 2.47	99.24 \pm 0.87	2.49	0.88
100	100.73 \pm 0.69	99.23 \pm 2.56	0.69	2.58

4.5 Drug-carrier deaggregation by ultracentrifugation

Separation of the drug from the carrier was carried out by the ultracentrifugation technique. Separation of the drug from the carrier showed a sigmoidal curve for each formulation (Figure 4.8). Formulation #1 and #2 showed 50% detachment at 20000 and 30000 g force while the formulations: #3, #4 and #5 showed 50% detachment at 45000, 65000, 80000 g force, respectively. The centrifugal force ($F_{\text{centrifugal}}$) of formulation #1 at 50% detachment was calculated by using equation 8, to be 122 μN (Table 4.5). Formulation #2 and #3 had an $F_{\text{centrifugal}}$ at 50% detachment force of 138 μN and 161 μN while formulation #4 and #5 had values of 657 μN and 993 μN respectively.

$$\text{Adhesion force at 50\% detachment} = \frac{50 \times \omega^2 \times r}{1000000000} \quad (8)$$

Where, ω = Angular velocity

r = centrifugation radius

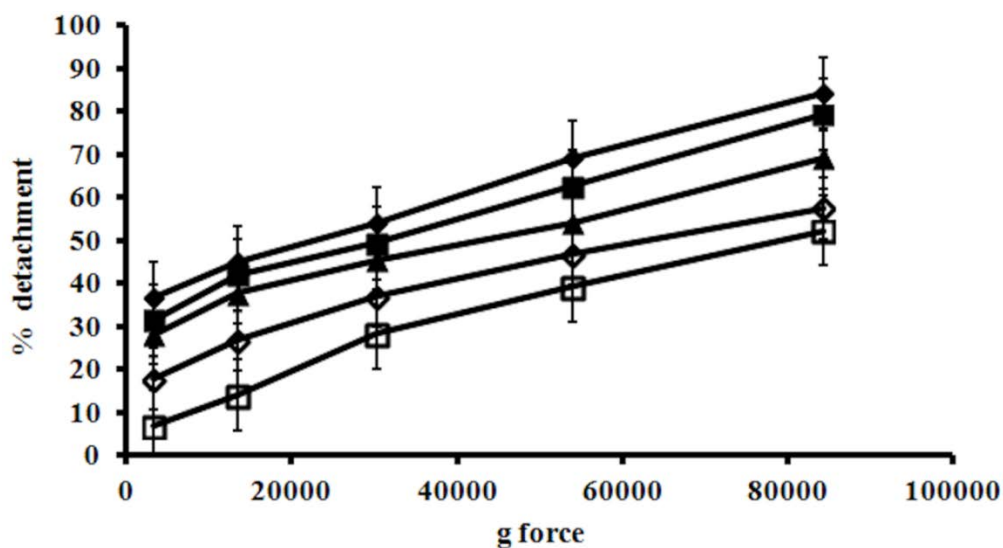


Figure 4.8 The % detachment of EDH formulations at various centrifugal forces, 1:2 (◆), 1:2.5 (■), 1:3.3 (▲), 1:5 (◇) and 1:10 (□).

Table 4.5 Adhesion forces at 50% drug detachment for different formulations

Formulation (#)	Drug: carrier EDH: Chitosan	Adhesion force for 50% Drug detachment (μN)
1	1:2	122
2	1:2.5	138
3	1:3.3	161
4	1:5	657
5	1:10	993

4.6 ACI evaluation of differebtEDH formulations

ACI studies of the formulations (#1 to #5) were carried out to evaluate MMAD, FPF, and ED. The MMAD values of the formulations #1 to #5 correlated to their FPF (the fraction of particles smaller than $4.4 \mu\text{m}$) in the range of 34-42%. The ED of all formulations from the especially designed plastic device was more than 80%. To deliver the dry powder from the inhaler to the lower part of the respiratory tract, the MMAD of the formulation should be less than $5 \mu\text{m}$. The formulation #1 had an MMAD of $2.3 \mu\text{m}$ with a FPF value of 42% and an ED of 84%, formulation #2 had a MMAD of $2.4 \mu\text{m}$ with an ED of 83% and a FPF value of 36%, formulation #3 had a MMAD of $2.5 \mu\text{m}$ with a FPF of 34%, an ED of 80% while formulation #4 had

a MMAD of 2.7 with a FPF of 32% and an ED of 83 % and formulation #5 had a MMAD of 2.9 μm with a FPF value of 31% and an ED dose of 85 % (Table 4.3).

4.7 Cytotoxicity of EDH, CS and different EDH formulations

Five formulations were developed by mixing EDH and CS in different w/w ratios. These developed EDH formulations were tested on A549, Calu-3 and NR8383 cell cultures for their *in vitro* compatibility. The cell viability of A549 after exposing them to different concentrations at 2, 4, 8, 16, and 32 $\mu\text{g/mL}$ of the EDH was 79.2 % \pm 1.4, 78.70 % \pm 0.73, 79.15 % \pm 0.82, 78.14 % \pm 0.22 and 77.70 % \pm 1.12 while the CS at concentration 2, 4, 8, 16, and 32 $\mu\text{g/mL}$ showed cell viability of 98.5 % \pm 1.73, 99.3 % \pm 6.6, 99.8 % \pm 4.92 and 98.2 % \pm 5.24. The formulation 1:2, 1:2.5, 1:3.3, 1:5 and 1:10 ratio showed viabilities of 96.3 \pm 17.2, 102 \pm 13.6, 97.5 \pm 10, 98.1 \pm 14.3, 92.9 \pm 2.6, respectively (Figure 4.9 A). The viability of the Calu-3 cells treated with EDH was 79.5 % \pm 1.0, CS showed 104.7 % \pm 2.6 and the formulations 1:2, 1:2.5, 1:3.3, 1:5, and 1:10 showed viability 99.1 % \pm 10.5, 102 % \pm 9.2, 98.3 % \pm 2.7, 96.2 % \pm 5.3 and 98.4 % \pm 5.5, respectively (Figure 4.9 B). The viability of the NR8383 cells treated with EDH was 74.5 % \pm 7.3 for the CS was 100.3 % \pm 6.1 and for the formulations 1:2, 1:2.5, 1:3.3, 1:5 and 1:10 showed viabilities of 90.4 % \pm 5.4, 99 % \pm 3.8, 94.4 % \pm 5.4, 99.6 % \pm 12.1, 101.2 % \pm 9.3, respectively (Figure 4.9 C). The pure EDH showed slight toxicity in our study while the CS (Mw: 3.2 kDa and DD: 58%) showed viability of 100.3% \pm 6.1 to the lung cells (A549, Calu-3 and NR8383) while all five formulations (1:2, 1:2.5, 1:3.3, 1:5, and 1:10) showed viabilities between 80-99%, which is non-toxic to the lung cells.

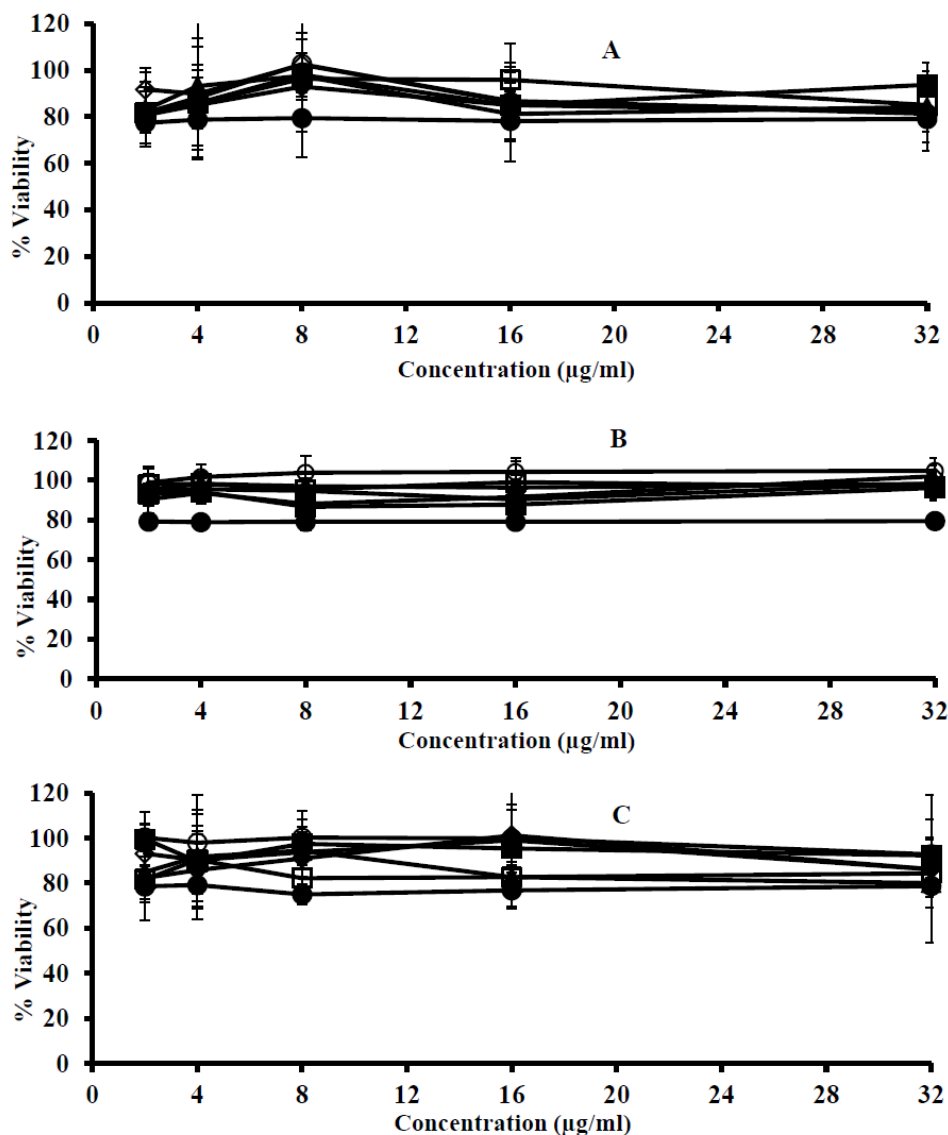


Figure 4.9 % Cell viability of A549 (A), Calu 3 (B), NR8383 cell (C) after exposing with different concentration of EDH (●), CS (○) and EDH formulations 1:10 (◆), 1:5 (■), 1:3.3 (▲), 1:2.5 (◇), 1:2 (□).

4.8 NO release by AM on interaction with EDH formulations

The alveolar macrophage (NR8383 cells) produced inflammatory mediators such as NO after being stimulated. NO produced by NR8383 on stimulation by LPS at 15.63 and 1000 ng/mL was 25.19 ± 4.6 to 34.85 ± 13.4 μM , respectively. NO generated from the NR8383 cells responding to EDH, CS and the EDH formulations 1:2, 1:2.5, 1:3.3, 1:5 and 1:10 was in the range of 2-32 $\mu\text{g/mL}$ (Figure 4.10). For the EDH itself the NO was not more than 25 μM .

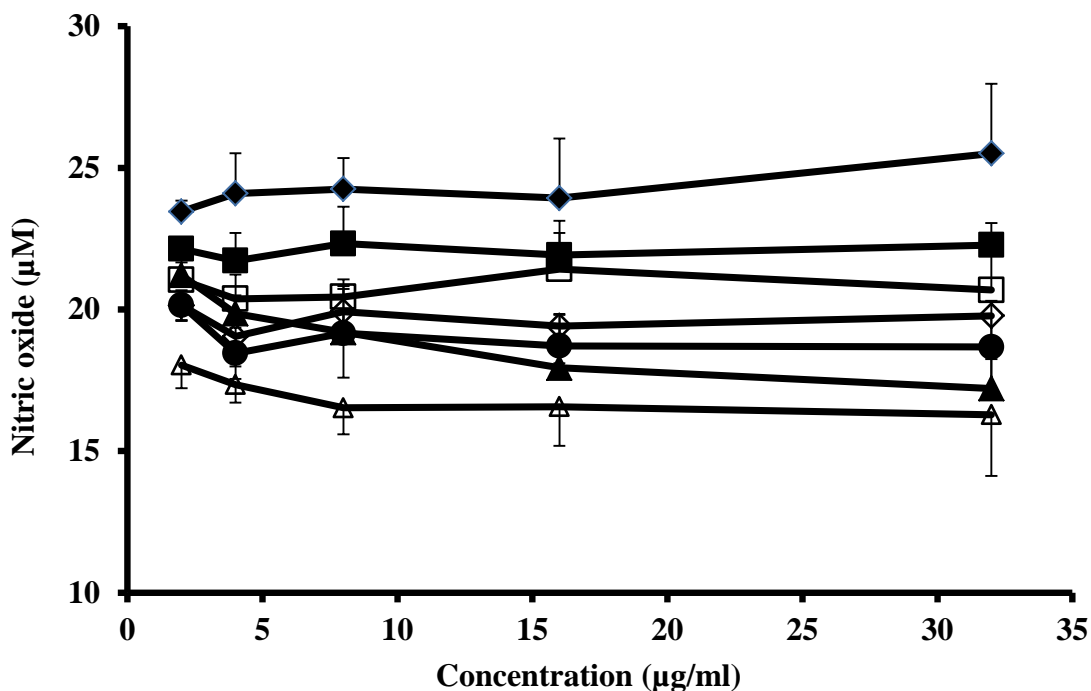


Figure 4.10 Nitric oxide (NO) production by macrophage cell (NR8383) after incubating it with EDH (◆), CS (■) and EDH formulations of 1:10 (▲), 1:5 (●), 1:3.3 (◇), 1:2.5 (□), 1:2 (Δ)

4.9 MIC determination of EDH, CS, and EDH formulations on *M. bovis*.

The MIC of EDH, chitosan and EDH formulations were determined by resazurin method on *M. bovis*. The EDH and chitosan had shown the MIC of 2 and 4 µg/mL, respectively. The formulation of EDH (1:3.3, 1:2.5 and 1:2.5) had shown that MIC at 2 µg/mL. While EDH formulations of 1:5 and 1:10 had shown MIC at 1 µg/mL (Table 4.6).

Table 4.6 MIC values of EDH, CS and EDH formulations (n=3).

Formulations	MIC ($\mu\text{g/mL}$)
EDH	2
CS	4
EDH: CS (1:10)	1
EDH: CS (1:5)	1
EDH: CS (1:3.3)	2
EDH: CS (1:2.5)	2
EDH: CS (1:2)	2

4.10 Determination of cell permeability through lipid bilayers

EDH at 100 $\mu\text{g/mL}$ showed a % drug permeation through a lipid bilayer membrane over a period of 2h of 48.7 ± 2.1 ($15.8 \mu\text{g/cm}^2$) while the formulation 1:2, 1:2.5, 1:3.3, 1:5 and 1:10 showed the % drug permeability of 56.4 ± 2.5 , 58.6 ± 2.7 , 62.3 ± 2.9 , 66.4 ± 2.7 and 71 ± 2.6 , respectively. During this study current were also measured to check the flow of ions from left to right chamber of lipid bilayer membrane. At zero time when the 100 $\mu\text{g/mL}$ EDH was added to the left chamber, showed the current of 0.5 μA and at the end of 2 h showed the current of 1.1 μA . The variations in current were also observed in different EDH formulations at zero time 0.8 to 2.1 μA at 2 h. This fluctuation in current from left to right chamber across the lipid bilayer indicates the flow of ions through the membrane (Figure 4.11).

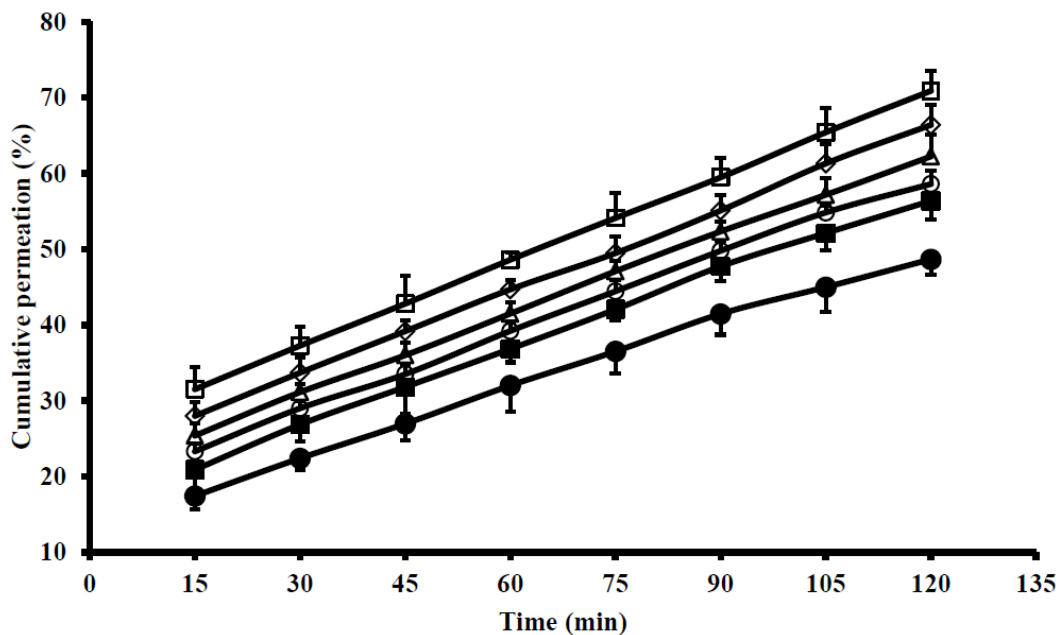


Figure 4.11 %Cumulative transport showing permeability of EDH (●), and EDH formulations: 1:10(□), 1:5(◇), 1:3.3(Δ), 1:2.5 (○) and 1:2(■) across the lipid bilayer.

4.11 Phagocytosis of EDH formulation by macrophage cells

NR8383 cell was slight green when photographed in bright field mode (Figure 4.12). To observe the phagocytosis, EDH formulation 1:2 was reconstituted in distilled water and stained with Lumidot® 640 for better picture intensity in florescent mode. Figure 4.13 showed phagocytosis of NR8383 cells taken in florescent mode. The phagocytosis started within 2 min and continued for 30 min, cell showed changes in morphology by getting enlarge at around 30 min. It indicated that NR8383 could phagocytose the particles stained with Lumidot® 640. These results also correlated with the size measurement after the reconstitution study. In our formulation the drug had the size of 260 nm. Kanchan and Panda (2007) reported that nanoparticles of 200–600 nm in size were efficiently phagocytosed. This indicated that infected NR8383 cells could take up reconstituted EDH formulation 1:2 stained with Lumidot® 640. The observation of florescent mode images of formulation 1:2 indicates phagocytation by NR8383 cells.

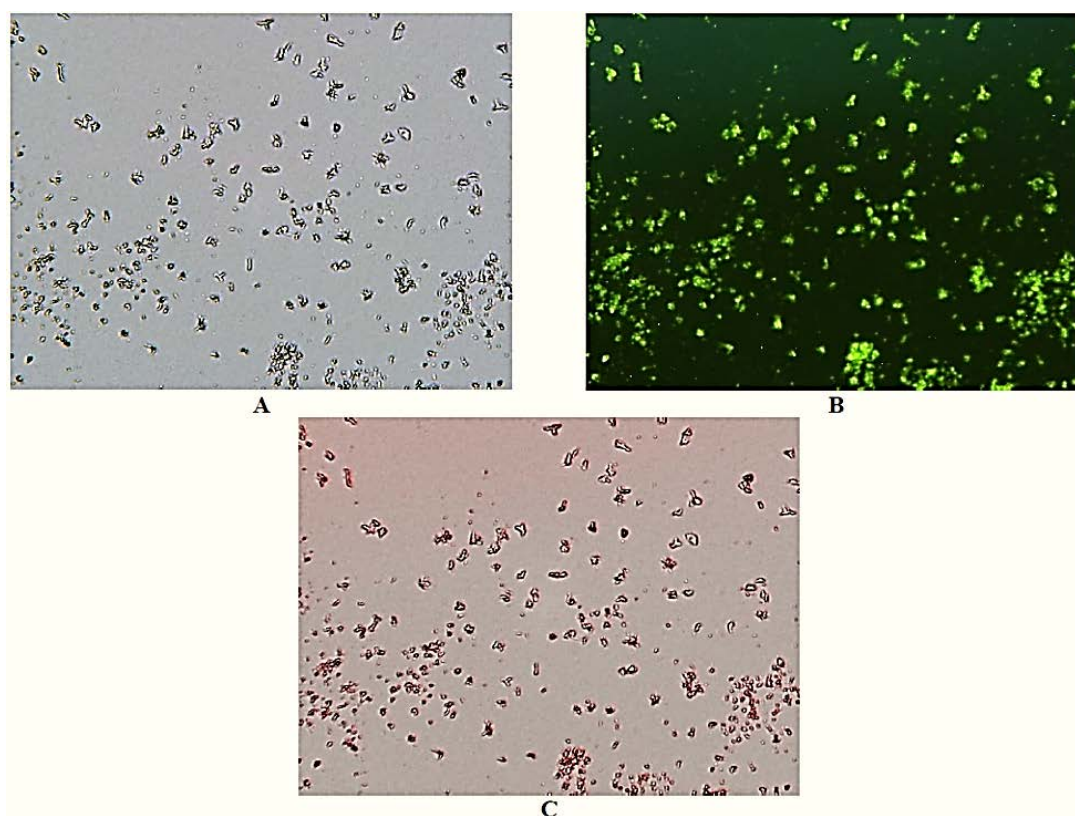


Figure 4.12 Formulation 1:2 treated with Lumidot® 640 bright (A), florescent (B) and overlay mode (C).

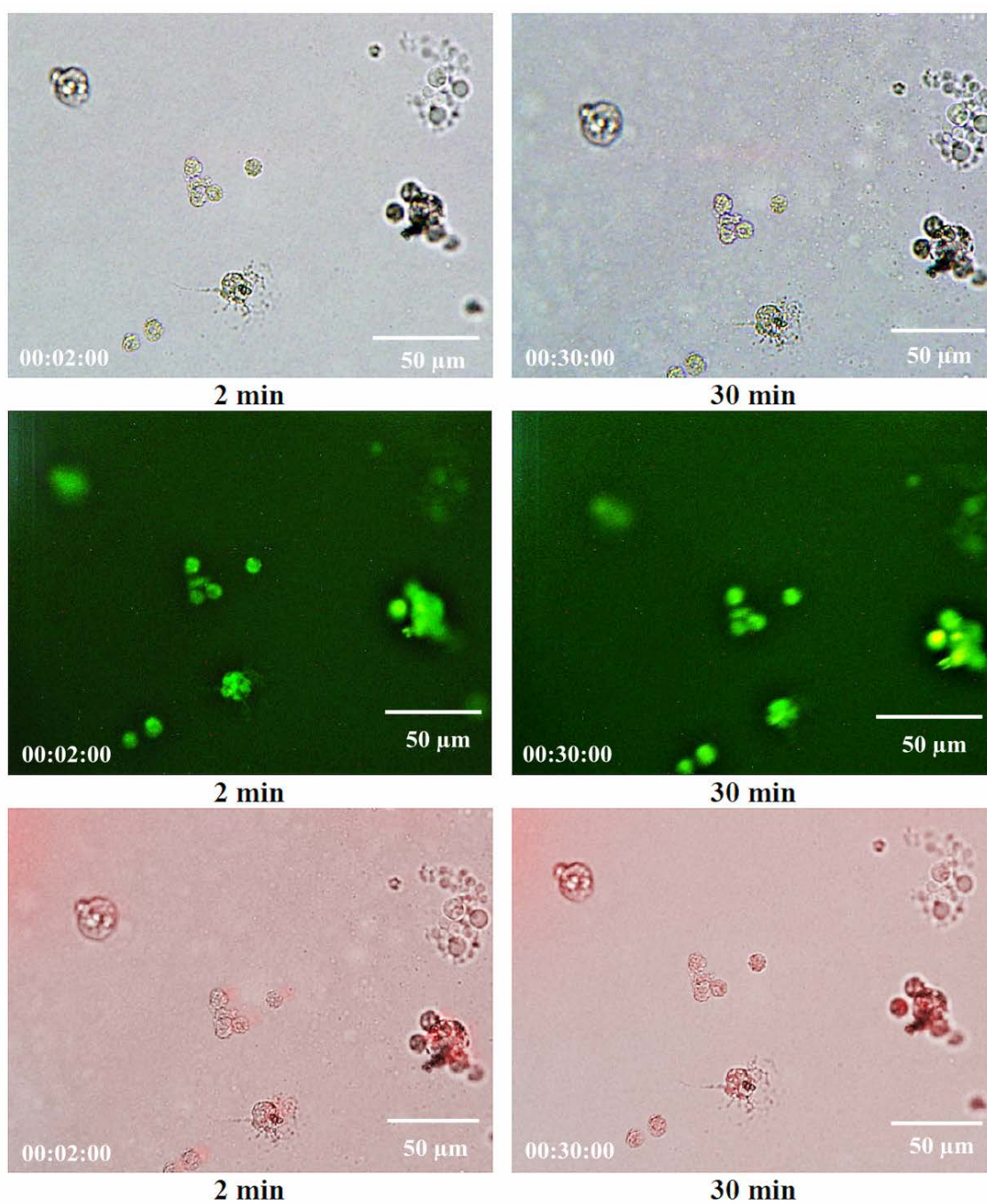


Figure 4.13 Phagocytosis of formulation 1:2 treated with Lumidot® 640 to a macrophage in florescent mode at 2 min and 30 min in bright, florescent and overlay mode.

4.12 Discussion

4.12.1 Optimization of nano spray drying of EDH

The EDH particles formed after the nano spray drying were spherical and smooth in nature (Figure 4.1) with % yield of more than 80%, had an appropriate size that allowed them to attach to the carrier. Pulmonary route is the most favorable route to target lungs with anti-tuberculosis drugs. Inhalable nano size drug has a better chance of mucosal adherence, particle(s) delivery, and hence net drug delivery to the lungs (Pandey et al., 2011). In addition, nanoparticles are efficiently taken up by phagocytic cells and subsequently release their payload (Pandey et al., 2011). When the drug was sprayed at a higher temperature (110°C) with a lower spray rate (85%) a non-cohesive free flowing powder particle was obtained. At a lower temperature (90°C) and a high spray rate (100%) the powder particles retained some moisture and stuck to the side walls of the glass chamber that led to a reduction in the amount of powder particles. At a high temperature of 110°C and a low spray rate of 85%, powder particles were deposited on the wall of the collecting drum from which the drug was separated by scraping. The electrical charge on the powder particle derives generally from the application of an external electrical field. The electrical charge applications play an important role in producing the nano sized powder particles. The negatively charged powder particles when sprayed within an electrical field, become attached to the positively charged collecting drum wall (Burki et al., 2011), then later the powder particles were obtained by scraping from the collecting drum.

4.12.2 Physicochemical characterization of CS

Five different concentrations of chitosan were sprayed to obtain dimple shaped carrier particles. The particles were first sprayed at 80°C, and had a spherical shape, while slight distortions in the shape of the CS surface were observed at 120-130°C. CS showed the best dimple formations on its surface using a 1% concentration at 150°C. The dimples that appeared on the surface of the CS were highly dependent on the inlet temperature, the concentration of the CS solution and the feeding rate for the spray drying. When the solution was sprayed at a low temperature of 110°C with a

feed rate of 10 mL, the particles produced were spherical in shape but at a higher inlet temperature of 150°C and a lower feed rate of 3 mL, the particles showed shrinkages at the particle surface. This may be due to evaporation of water from the matrix of the CS at such a high inlet temperature that it resulted in the formation of the dimples on the particle surface (He et al., 1999). The dimple formation on the carrier surface became more prominent as the concentration of the carrier increased. The number of dimples on the carrier surface also increased with an increasing concentration of carrier. These dimple surfaces provided more space for the drug to adhere. These dimple surfaces allows maximum deaggregation of the drug particle inside the lung as the dimple/rough surface reduces the van der Waals force between drug and carrier increases its aerosolization property (Minne et al., 2008).

The CS molecular weight also plays an important role as a carrier for enhancing the aerosolization property of the drug. Low molecular weight CS has a better aerosolization property than a high molecular weight CS (Learoyd et al., 2009). A molecular weight of 3.2 kDa was unchanged at all the time intervals used before and after the spray drying.

Determination of the surface area of the carrier was an important parameter as it provided information on the number of dimples formed on the carrier's surface on which the drug binds and deaggregates. The carrier particle surface area decreased with increasing carrier size i.e. the carrier particle with less than 1% concentration had shown poor flowability, high surface area, and variation in particle size which would have formed unstable formulation. The 1% CS solution had shown size in range good enough to target the alveoli, low specific surface area, high porosity, and low angle of repose as compared to other tested concentrations of CS (0.1%, 0.2%, 0.3%, 0.4%, and 0.5%). The dimple surface with a lower surface area (1% chitosan) provided weak van der Waals force for the drug to bind to the carrier surface and would lead to a better drug deaggregation (Tang et al., 2004) in the lungs. The porosity and angle of repose also increased with increase in the size of the carrier particle i.e. 0.1 %- 1% which helps in increasing the flowability of carrier particle.

4.12.3 Physicochemical characterization of EDH formulations

The five formulations were prepared by physical mixing in a fixed ratio between the drug and carrier. Van der Waals forces play an important role in the adhesion of EDH with the chitosan in a complex formation by physical mixing (Harjunen et al, 2002). The drug binding depends on the position of drug and the amount of carrier available in the formulations.

The DSC thermograph showed that the drug was crystalline in nature and had a sharp melting point at 203 °C. The carrier was amorphous in nature and when EDH was mixed with the CS; the powder mixtures became nearly amorphous. At a high temperature of 203 °C the carrier melting occurred and acted as a solvent for the drug to dissolve. Hence the drug finally transformed to becoming amorphous. Hence, all the formulations were highly amorphous in nature. The amorphous material showed a higher solubility, a faster dissolution rate and a better bioavailability of the pharmaceutical drug (Marsac et al., 2006).

The FTIR spectrum of EDH showed a strong hydrogen bonding (O-H) due to its crystalline nature. The CS spectrum showed a wide C=O peak due to its amorphous nature. The spectrum of the formulations from #1 to #5 had shown the C=O bond shifted to a lower value which indicate the interaction between carrier and drug. The increase in weight ratio of carrier in the formulation showed larger shift which indicated stronger interaction and this is in agreement with their adhesion force.

The drug content uniformity is an important parameter in the DPI formulations, the change in content uniformity will lead to change in the dose administered (Islam et al, 2012). The drug delivery from formulation #1- #4 was in an acceptable range (USP 30). There was a 101.6 % drug release from formulation #1, while formulation #3 released 105.1 % of the drug content. Formulations #1- #4 had a uniform content that was within the acceptable range as each formulation was developed by physical mixing and the drug was released easily in a solution. The formulation #5 did not have a uniform content within the acceptable range. Since the ratio of the carrier with the drug was 10 times higher in formulation #5 so there might

be a possibility that the drug became trapped in the chitosan polymer that inhibited its release into solution.

In EDH formulation, two main forces are involved in deagglomeration of drug particles from the carrier surfaces; aerodynamic lifting and dragging. During inhalation the entrainment of powder particle took place by sudden change in velocity and impaction in the respiratory region (Voss et al., 2002; Milenkovic et al., 2014). In formulation #1, #2 and #3, the drug was bound to carrier grooves as well as over its entire surface which allowed formulations #1, #2, and #3 to separate easily. The formulations #4 and #5 required a much higher g-force to produce a 50% detachment due to the higher concentration of carrier on which the drug was tightly bound onto the grooves. The drug entrapped on the carrier surface dimple requires a higher rotational centrifugal force to separate it from the carrier (Iida et al., 2003; Tena et al., 2012). The detachment force required to remove drug particles from formulation #1 to #5 increased considerably at the 50% detachment force. This shows that the centrifugal force required to separate the drug from carrier depended on the drug-carrier ratio in the formulation. The formulation # 1 had less amount of carrier and drug bound all over its surface and grooves so it was easy for the drug to separate from the carrier surface but as the amount of carrier increased i.e. #2, #3, #4 and #5 the drug was restricted to the grooves of the carrier dimples and hence the centrifugal force required to separate the drug from carrier was higher. Formulation #1 gave an FPF value of 42 % with the highest ED value of 84 %. To deliver the dry powder inhaler to the lower part of the respiratory tract, the MMAD of the formulation should be less than 5 μ m and the prepared formulations (#1, #2, #3 and #4) met this requirement.

4.12.4 Cytotoxicity and bioactivity of EDH, CS and EDH formulations

CS is a biocompatible, biodegradable, permeation enhancer and mucoadhesive polysaccharide which exhibits low toxicity (Grenha et al., 2007, 2008, Vinsova & Vavrikova, 2008). It is widely accepted that the toxicity of chitosan in cell culture is dependent upon numerous factors such as DD, MW and pH (Kudsiova and Lawrence, 2008). CS exhibits a pH- or ionization level-dependent toxicity (higher toxicity in more acidic environments). Hence the pharmacokinetic and biodistribution

profiles of formulations containing CS get changed. Charge interaction of CS plays an important role in cellular uptake kinetics. The balancing or reduction of positive charges on the CS molecule has effects on its interaction with cells and the microenvironment, often leading to decreased uptake and a decrease in toxicity (Kean and Thanou, 2010). It has been reported in studies that CS (having MW and DD; <5 kDa, 65.4%) were found to display very low cytotoxicity against human lung cells (Richardson et al, 1999; Yang et al., 2014). The EDH has shown slight toxicity in our study while the CS (Mw: 3.2 kDa and DD: 58%) has not shown any toxicity to the lung cells (A549, Calu-3 and NR8383). The five formulations (1:2, 1:2.5, 1:3.3, 1:5, and 1:10) have shown viability between 80-99%. The decrease in formulation toxicity might be due to the presence of chitosan in formulation. CS might have decreased the toxicity due to its low molecular weight (3.2 kDa) or by NH_3^+ charge interaction with the lung cells (Kumirska et al., 2011).

It has been reported in several studies that CS is a natural permeation enhancer; it enhances the permeation by opening the tight junction of cells. The paracellular space containing the tight junction complex is hydrated and contains fixed negative sites. The NH_3^+ of CS causes change in the ionic concentration in these pores, which result in alteration of the tight junction structures leading to their “opening” for larger solutes to pass through it (Benediktsdottir et al., 2014). Antimicrobial activity generally increases as the ratio of CS increases in the formulation. As the ratio of CS increases, more amount of EDH passes into the cell and decrease MIC of formulations. From the MIC values observation, it showed that the MIC values decreased with increasing ratios of CS in formulation which made it more lethal for the bacteria and enhance the potency of formulations (Benediktsdottir et al., 2014).

4.12.5 Cumulative permeation of EDH and EDH formulations through lipid bilayers.

The % drug permeation has increased with increase in the ratio of CS in the formulation. This ability of chitosan to increase the permeation can be explained by the possible interactions of its positive surface charge with the anionic components of the lipid bilayer to increase the permeability of drugs. It has been

reported that the electrostatic interaction between the protonated NH_3^+ groups of CS and the negatively charged surface of the lipid bilayer play an important role (Sadeghi et al., 2008). The presence of N-acetyl group on the chitosan backbone and the hydrophobic core of the lipid bilayer formed a hydrophobic interaction and cause elasticity, expansion and permeation enhancement in lipid bilayer membrane (Yang et al., 2014). The cell permeability study was based on the concentration gradient through a lipid bilayer in Ussing chamber. The drug particles were diffused from region of high concentration (left chamber) to low (right chamber). The lipid bilayers were prepared on the transwells and suspended in the Ussing chamber, once the transwell came in contact with the buffer the lipid bilayer formed by swelling and volume get increase in aqueous condition. At the beginning the permeation of the drug was dependent on the concentration gradient only. In case of formulation, the permeation was enhanced due to the concentration gradient and permeation enhancement by chitosan through lipid bilayer (Benediktsdottir et al., 2014). As the ratio of CS increased in the formulation the % drug permeation get enhanced considerably. So, there was consistent enhancement in the % drug permeation in the DPI formulations (1:2 to 1:10).

CHAPTER 5

CONCLUSION

Nano sized drugs with a smooth and spherical surface were successfully prepared by nano spray drying. The chitosan carrier particles with dimples were prepared by spray drying. The prepared carriers had good flow ability and all its physico-chemical parameters were shown to be within the appropriate range. Five formulations were developed by mixing the drug in a fixed ratio with a varied ratio of the carrier. The SEM images of carriers clearly showed the presence of dimples on its surface and the SEM images of different formulations clearly showed the attachment of the drug to the dimples of the carrier surface. The DSC thermograms of the formulation showed the conversion of a crystalline drug into an amorphous state. The FTIR spectra showed the interactions between the drug and the carrier in different ratios. The uniformity of the drug content of the four formulations was found to be within the acceptable range of the USP. The ultracentrifugation for all the formulations showed that the detachment of the drug required different centrifugal forces that allowed deaggregation of the drug from the carrier. The MMAD of the drug was less than 5 μm so they would be expected to be transported into the lower regions of the lung. The EDH DPI on interaction with respiratory cell lines has shown low toxicity as compared to the pure drug. The NO production after treatment with the formulation has produced low NO than pure drug. The prepared EDH DPI formulations were more potent than the pure drug. The EDH DPI has shown much higher % drug permeability through lipid bilayer membrane than by the pure drug. It can be concluded that EDH DPI formulation prepared were suitable to target the lungs for controlling resistance in tuberculosis.

BIBLIOGRAPHY

- Acerbi, D., Brambilla, G., Kottakis, I. 2007. Advances in asthma and COPD management: Delivering CFC-free inhaled therapy using Modulite (R) technology. *Pulm Pharmacol Ther* 20(3):290-303.
- Adjei, A.L., Gupta, P.K. 1997. Inhalation delivery of therapeutic peptides and proteins. New York. Marcel Dekker.
- Andersen, P., Woodworth, J.S. 2014. Tuberculosis vaccines – rethinking the current paradigm. *Trends in Immunology*. 35 (8):387-395.
- Azarmi, S., Roa, W.H., Lobenberg, R. 2008. Targeted delivery of nanoparticles for the treatment of lung diseases. *Adv Drug Deliv Rev*. 60:863–875.
- Benediktsdóttir, B.E., Baldursson, O., Másson, M. 2014. Challenges in evaluation of chitosan and trimethylated chitosan (TMC) as mucosal permeation enhancers: From synthesis to in vitro application. *J Control Release*. 173: 18-31.
- Borgstrom, L., Derom, E., Stahl, E., WahlinBoll, E., Pauwels, R. 1996. The inhalation device influences lung deposition and bronchodilating effect of terbutaline. *Am J Respir Crit Care Med*. 153(5):1636-1640.
- Bryskier, A., Grosset, J. 2005. Antimicrobial agents: Antibacterials and antifungals. ASM Press, American Society of Microbiology, Washington.1088-1124.
- Chan, J.G.Y., Chan, H-K., Prestidge, C.A., Denman, J.A., Young, P.M., Traini, D. 2013. A novel dry powder inhalable formulation incorporating three first-line anti-tubercular antibiotics. *Eur J Pharm Biopharm*. 83:285–292.
- Chernyaeva, E., Fedorova, E., Zhemkova, G., Korneev, Y., Kozlov, A. 2013. Characterization of multiple and extensively drug resistant

- Mycobacterium tuberculosis* isolates with different ofloxacin-resistance levels. *Tuberculosis*. 93:291-295.
- Chew, N.Y.K., Tang, P., Chan, H.K., Raper, J.A. 2005. How much particle surface corrugation is sufficient to improve aerosol performance of powders? *Pharm Res*. 22:148–52.
- Chung, Y.C., Chen, C.Y. 2007. Antibacterial characteristics and activity of acid- soluble chitosan. *Bioresource Technol*. 99 (2008):2806–2814.
- Clarke, L.L. 2009. A guide to Ussing chamber studies of mouse intestine. *Am J Physiol Gastrointest Liver Physiol*. 296: 1151–1166.
- De Backer, A.I., Mortele, K.J., De Keulenaer, D.I., Parizel, P.M. 2006. Tuberculosis: epidemiology, manifestations, and the value of medical imaging in diagnosis. *JBR–BTR*. 89: 243-250.
- Demoly, P., Hagedoorn, P., De Boer, A.H., Frijlink, H.W. 2014. The clinical relevance of dry powder inhaler performance for drug delivery. *Respir Med*. 108:1195-1203.
- Dube, D., Gupta, M., Agrawal, U., Vyas, S.P. 2014. Animal models of tuberculosis. *Animal biotechnol*. 2:21-37.
- Ernst, J.D. 2012. The immunological life cycle of tuberculosis. *Nat Rev Immunol*. 12: 581–591.
- Ferguson, J.S., Weis, J.J., Martin, J.L., Schlesinger, L.S. 2004. Complement protein C3 binding to *Mycobacterium tuberculosis* is initiated by the classical pathway in human bronchoalveolar lavage fluid. *Infect Immun*. 72: 2564-2573.
- Frieden, T.R., Sterling, T.R., Munsiff, S.S., Watt, C.J., Dye, C. 2003. Tuberculosis. *Lancet*. 362:887-899.

- Fröhlich, E., Salar-Behzadi, S. 2014. Toxicological Assessment of Inhaled Nanoparticles: Role of *in Vivo*, *ex Vivo*, *in Vitro*, and *in Silico* Studies. *Int J Mol Sci.* 15:4795-4822.
- Getahun, H., Mark, H., Rick, O'Brien., Paul, Nunn. 2007. Diagnosis of smear-negative pulmonary tuberculosis in people with HIV infection or AIDS in resource-constrained settings: informing urgent policy changes. *Lancet.* 369:2042–2049.
- Ghebreyesus, T.A., Kazatchkine. M., Sidibe, M., Nakatani, H., 2010. Tuberculosis and HIV: time for an intensified response. *Lancet.* 375: 1757–1758.
- Gradon, L., Sosnowski, T.R. 2013. Formation of particles for dry powder inhalers. *Adv Powder Technol.* 25:43–55
- Grange, J.M., Zumla, A. 2002. Chapter 57: Tuberculosis. In section 1 Underlying factor in tropical medicine. S.I. 1-59.
- Grenfell, P., Leite, B.R., Garfeinc, R., Lussigny, S., Platt, L., Rhodes, T. 2013. Tuberculosis, injecting drug use and integrated HIV-TB care: A review of the literature. *Drug Alcohol Depend.* 129:180–209.
- Grenha, A., Graingerb, C.I., Dailey, L.A. 2007. Chitosan nanoparticles are compatible with respiratory epithelial cells in vitro. *Eur J Pharm Sci.* 31:73–84.
- Grenha, A., Seijo, B., Remunan-Lopez, C. 2005. Microencapsulated chitosan nanoparticles for lung protein delivery. *Eur J Pharm Sci.* 25: 427–37.
- Hall, R.G., Swancutt, M.A., Meek, C., Leff, R.D., Gumbo, T. 2011. Ethambutol pharmacokinetic variability is linked to body mass in overweight, obese, and extremely obese people. *Antimicrob Agents Chemother.* 56(3):1502–1507.
- Harris, R., Acosta, N., Heras, A. 2013. Chitosan and inhalers: a bioadhesive polymer for pulmonary drug delivery. *Inhaler Devices.* 6:77-93.

- Hasenbosch, R.E., Alffenaar, J.W.C., Koopmans, S.A. 2008. Ethambutol induced optical neuropathy. *Int J Tuberc Lung Dis.* 12(8):967–971.
- He, P., Davis, S.S., Illum, L. 1999. Chitosan microspheres prepared by spray drying. *Int J Pharm.* 187:53–65.
- Healy, A.M., Amaro, M.I., Paluch, K.J., Tajber, L. 2014. Dry powders for oral inhalation free of lactose carrier particles. *Adv Drug Del Rev.* 75:32-52.
- Hejazi, R., Amiji, M. 2003. Chitosan based gastrointestinal delivery systems. *J Control Rel.* 89:151–165.
- Hendeles, L., Colice, G.L., Meyer, R.J. 2007. Current concepts withdrawal of albuterol inhalers containing chlorofluorocarbon propellants. *N. Engl. J. Med.* 356(13):1344-1351.
- Heyder, J., Gebhart, J., Scheuch G. 1998. Influence of human lung morphology on particle deposition. *J Aerosol Med.* 1(2): 81-88.
- Hirai A., Odani H., Nakajima A.1991. Determination of degree of deacetylation of chitosan by ¹H NMR spectroscopy. *Polym Bull.* 26:87–94.
- Hoppentocht, M., Hagedoorn, P., Frijlink, H.W., De Boer, A.H. 2014. Technological and practical challenges of dry powder inhalers and formulations. *Adv Drug Deliv Rev.* 1-14.
- Hunter, R.L. 2011 Pathology of post primary tuberculosis of the lung: An illustrated critical review. *Tuberculosis.* 91:497-509
- Islam, N., Cleary, M.J. 2011. Developing an efficient and reliable dry powder inhaler for pulmonary drug delivery – A review for multidisciplinary researchers. *Med Eng & Phy.* 34:409–427.
- Islam, N., Gladki, E. 2008. Dry powder inhalers (DPIs)—A review of device reliability and innovation. *Int J Pharm.* 360:1-11.

- Joe, M., Bai, Y., Nacario, R.C., Lowary, T.L. 2007. Synthesis of the docosanasaccharide arabinan domain of mycobacterial arabinogalactan and a proposed octadecasaccharide biosynthetic precursor. *J Am Chem Soc.* 129 (32):9885-9901.
- Kaialy, W., Martin, G.P., Larhrib, H. 2012. The influence of physical properties and morphology of crystallised lactose on delivery of salbutamol sulphate from dry powder inhalers. *Colloids Surf B.* 89:29–39.
- Karner, S., Littringer, E.V., Urbanetz, N.A. 2014. Triboelectrics: The influence of particle surface roughness and shape on charge acquisition during aerosolization and the DPI performance. *Powder Technol.* 262:22–29.
- Khuller, G. K., Manisha. K., Sadhna, S. 2004. Liposome technology for drug delivery against mycobacterial infections. [*Curr Pharm Des.* 10:3263-3274.](#)
- Kim, K.M., Son, J.H., Kim, S-K., Weller, C.L., Hanna, M.A. 2006. Properties of chitosan films as a function of pH and solvent type. *J Food Sci.* 71:E119–24.
- Kim, Se-Kwon., Rajpakse, N. 2005. Enzymatic production and biological activities of chitosan oligosaccharides (COS): a review. *Carbohydr Polym* 62(4): 357-368.
- Kumar, M.N.V.R. 2000. A review of chitin and chitosan applications. *React Funct Polym.* 46:1-27.
- Kumirska, J., Weinhold, M.X., Thöming, J., Stepnowski, P. 2011. Biomedical Activity of Chitin/Chitosan Based Materials-Influence of Physicochemical Properties Apart from Molecular Weight and Degree of N-Acetylation. *Polymer.* 3:1875-1901.
- Kwan, C.K., Ernst, J.D. 2011. HIV and tuberculosis: a deadly human syndemic. *Clin Microbiol Rev.* 24(2):351–376.

- Labiris, N.R., Dolovich, M.B. 2003. Pulmonary drug delivery. Part I: Physiological factors affecting therapeutic effectiveness of aerosolized medications. *Br J Clin Pharmacol.* 56(6):588-599.
- Larhrib, H., Martina, G.P., Marriotta, C., Prime, D. 2010. The influence of carrier and drug morphology on drug delivery from dry powder formulations. *Int J Pharm* 257:283–296.
- Lawn, S.D., Brook, S.V., Kranzor, K., Nicol, M.P., Whitelaw, A., Vogt, M., Bekker, L.G., Wood, R. 2011. Screening for HIV-associated tuberculosis and rifampicin resistance before antiretroviral therapy using the Xpert MTB/RIF assay: A prospective study. *PLOS Medicine.* 8(7):1-11.
- Learoyd, T.P., Burrows, J.L., French, E., Seville, P.C. 2009. Chitosan-based spray-dried respirable powders for sustained delivery of terbutaline sulfate. *Eur J Pharm Biopharm.* 68:224–234.
- Lee, R.B., Li, W., Chatterjee, D., Lee, R.E. 2005. Rapid structural characterization of the arabinogalactan and lipoarabinomannan in live mycobacterial cells using 2D and 3D HR-MAS NMR: structural changes in the arabinan due to ethambutol treatment and gene mutation are observed. *Glycobiology.* 15(2):139-151.
- Li, Y., Petrofsky, M., Bermudez, L.E. 2002. Mycobacterium tuberculosis uptake by recipient host macrophages is influenced by environmental conditions in the granuloma of the infectious individual and is associated with impaired production of interleukin-12 and tumor necrosis factor alpha. *Infect Immun.* 70:6223-6230.
- Luca, R. 2006. An update on the diagnosis of tuberculosis infection. *Am J Respir Crit Care Med.* 174:736–742.
- Maretti, E., Rossi, T., Bondi, M., Crocea, M.A., Hanuskova, M., Leoa, E., Sacchetti, F., Iannuccelli, V. 2014. Inhaled solid lipid microparticles to target alveolar macrophages for tuberculosis. *Int J Pharm.* 462:74–82.

- Marsac, J.P., Konno, H., Taylor, L.S. 2006. A comparison of the physical stability of amorphous felodipine and nifedipine systems. *Pharm Res.* 23:2306–16
- Martin, A., Camacho, M., Portaels, F., Palomino, J.C. 2003. Resazurin microtiter assay plate testing of *Mycobacterium tuberculosis* susceptibilities to second-line drugs: rapid, simple, and inexpensive method. *Antimicrob Agents Chemother.* 47(11):3616–3619.
- Martindale: The Complete Drug Reference. Pharmaceutical press. London. 2009. 36:274-275.
- Medcalf, A., Altink, H., Saavedra, M., Bhattacharya, S. 2013. Tuberculosis- a short history, centre for chronic diseases and disorders, centre for global health histories, humanities research center, orient blackswan private limited. Chapter 1, 1-2.
- Mehanna, M.M., Mohyeldin, S.M., Elgindy, N.A. 2014. Respirable nanocarriers as a promising strategy for antitubercular drug delivery. *J Control Release.* 187:183–197.
- Milenkovic, J., Alexopoulos, A.H., Kiparissides, C. 2014. Deposition and fine particle production during dynamic flow in a dry powder inhaler: A CFD approach. *Int J Pharm.* 461:129–136.
- Minne, A., Boireau, H., Horta, M.J., Vanbever, R. 2008. Optimization of the aerosolization properties of an inhalation dry powder based on selection of excipients. *Eur J Pharm Biopharm.* 70:839–844.
- Misra, A., Hickey, A.J., Rossi, C., Borchard, G., Terada, H., Makino, K., Fourie, P.B., Colombo, P. 2011. Inhaled drug therapy for treatment of tuberculosis. *Tuberculosis.* 91:71-81.
- Muzzarelli, R.A.A. 1990. Modified chitosans and their chemical behavior. *Polym Prep (Am Chem Soc Div Polym Chem).* 31:626.

- Nair, V., 2002. HIV integrase as a target for antiviral chemotherapy. *Rev Med Virol.* 12: 179–193.
- Nancy, A., Knechel, R.N. 2009. Tuberculosis: pathophysiology, clinical features, and diagnosis. *Crit Care Nurse.* 29(2): 34-43.
- Newhouse, M., Hirst, P., Duddu, S., Walter, Y., Tarara, T., Clark, A., Weers, J. 2003. Inhalation of a dry powder tobramycin pulmosphere formulation in healthy volunteers. *Chest.* 124:360–366.
- Nicod, L.P., 2007. Immunology of tuberculosis. *Swiss Med Wkly.* 137:357-362.
- Orme, I.M. 2014. A new unifying theory of the pathogenesis of tuberculosis. *Tuberculosis.* 94:8-14.
- Ostroumova, O.S., Efimova, S.S., Chulkov, E.G., Schagina, L.V. 2012. The interaction of dipole modifiers with polyene-sterol complexes. *Plos one.* 7(9): 1-7.
- Palomino, J-C., Martin, A., Camacho, M., Guerra, H., Swings, J., Portaels, F. 2002. Resazurin microtiter assay plate: simple and inexpensive method for detection of drug resistance in *Mycobacterium tuberculosis*. *Antimicrob Agents Chemother.* 46(8):2720–2722.
- Pandey, R., Ahmad, Z. 2011. Nanomedicine and experimental tuberculosis: facts, flaws, and future. *Nanomed Nanotech Biol Med.* 7:259–272.
- Pandey, R., Khuller, G. K. 2005b. Antitubercular inhaled therapy: opportunities, progress and challenges, *J Anti Chem.* 55:430–435.
- Paranjpe, M., Müller-Goymann, C.C. 2014. Nanoparticle-mediated pulmonary drug delivery: A review. *Int J Mol Sci* 15:5852-5873.
- Parikh, R., Dalwadi, S., Aboti, P., Patel, L. 2014. Inhaled microparticles of antitubercular antibiotic for in vitro and in vivo alveolar macrophage targeting and activation of phagocytosis. *J Antibiot.* 67:387-394.

- Patil-Gadhe, A., Pokharkar, V. 2014. Single step spray drying method to develop proliposomes for inhalation: A systematic study based on quality by design approach. *Pulm Pharmacol Ther.* 27:197-207.
- Pereda, M., Amica, G., Marcovich, N.E. 2012. Development and characterization of edible chitosan/olive oil emulsion films. *Carbohydr Polym.* 87:1318–1325.
- Pilcer, G., Amighi, K. 2010. Formulation strategy and use of excipients in pulmonary drug delivery. *Int J Pharm.* 392:1–19.
- Pilcer, G., Vanderbist, F., Amighi, K. 2009. Preparation and characterization of spray-dried tobramycin powders containing nanoparticles for pulmonary delivery. *Int J Pharm.* 365:162–169.
- Pillai, C.S.K., Paul, W., Sharma, C.P. 2009. Chitin and chitosan polymers: Chemistry, solubility and fiber formation. *Prog Polym Sci.* 34:641–678.
- Podczek, F. 1999. The influence of particle size distribution and surface roughness of carrier particles on the in-vitro properties of dry powder inhalations. *Aerosol Sci Technol.* 31:301–21.
- Pourshahab, P.S., Gilani, K., Moazeni, A. 2011. Preparation and characterization of spray dried inhalable powders containing chitosan nanoparticles for pulmonary delivery of isoniazid. *J Microencapsul.* 28:605–13.
- Rahimpour, Y., Kouhsoltani, M., Hamishehkar, H. 2014. Alternative carriers in dry powder inhaler formulations. *Drug Discovery Today.* 19:618-626.
- Richardson, S.C., Kolbe, H.V., Duncan, R. 1999. Potential of low molecular mass chitosan as a DNA delivery system: biocompatibility, body distribution and ability to complex and protect DNA. *Int J Pharm.* 178:231–243.
- Rinaudo, M. 2008. Main properties and current applications of some polysaccharides as biomaterials. *Polym Int.* 57:397–430.

- Roa, W.H., Azarmi, S., Al-Hallak, M.H.D.K., Finlay, W.H., Magliocco, A.M., Lobenberg, R. 2011. Inhalable nanoparticles, a non-invasive approach to treat lung cancer in a mouse model. *J Control Release*. 150:49–55.
- Robert, L., Wani, S. 2013. Clinical manifestations of pulmonary and extra-pulmonary tuberculosis, *South Sudan Medical Journal*. 6 (3): 52-56.
- Rojanarat, W., Changsan, N., Tawithong, E., Pinsuwan, S., Chan, H-K., Srichana, T. 2012, Isoniazid proliposome powders for inhalation—preparation, characterization and cell culture studies. *Int J Mol Sci*. 12:4414-4434.
- Sadeghi, A.M.M., Dorkoosh, F.A., Avadi, M.R., Weinhold, M., Bayat, A., Delie, F., Gurnu, R., Larijani, A., Rafiee-Tehrani, A., Junginger, H.E. 2008. Permeation enhancer effect of chitosan and chitosan derivatives: Comparison of formulations as soluble polymers and nanoparticulate systems on insulin absorption in Caco-2 cells.
- Shepherd, R.G., Baughn, C., Cantral, M.L., Goodstein, B., Thomas, J.P., Wilkinson, R.G. 1966. Structure-activity studies leading to ethambutol, a new type of antituberculous compound. *Annals of the New York Academy of Sciences*. New antituberculosis agents: laboratory and clinical studies. 135:686–710.
- Singh, S., Tuberculosis, current anesthetic and critical care, 2004, 15, 165-171.
- Sinha, V.R., Singla, A.K., Wadhawan, S., Kaushik, R., Kumria, R., Bansal, K., Dhawan, S. 2004. Chitosan microspheres as a potential carrier for drugs. *Int J Pharm* 274:1–33.
- Smith, I.J., Parry-Billings, M. 2003. The inhalers of the future? A review of dry powder devices on the market today. *Pulm Pharmacol Ther*. 16(2):79-95.
- Smyth, H.D.C., Hickey, A.J. 2005. Carriers in Drug Powder Delivery: Implications for Inhalation System Design. *Am J Drug Deliv*. 3:117-132.

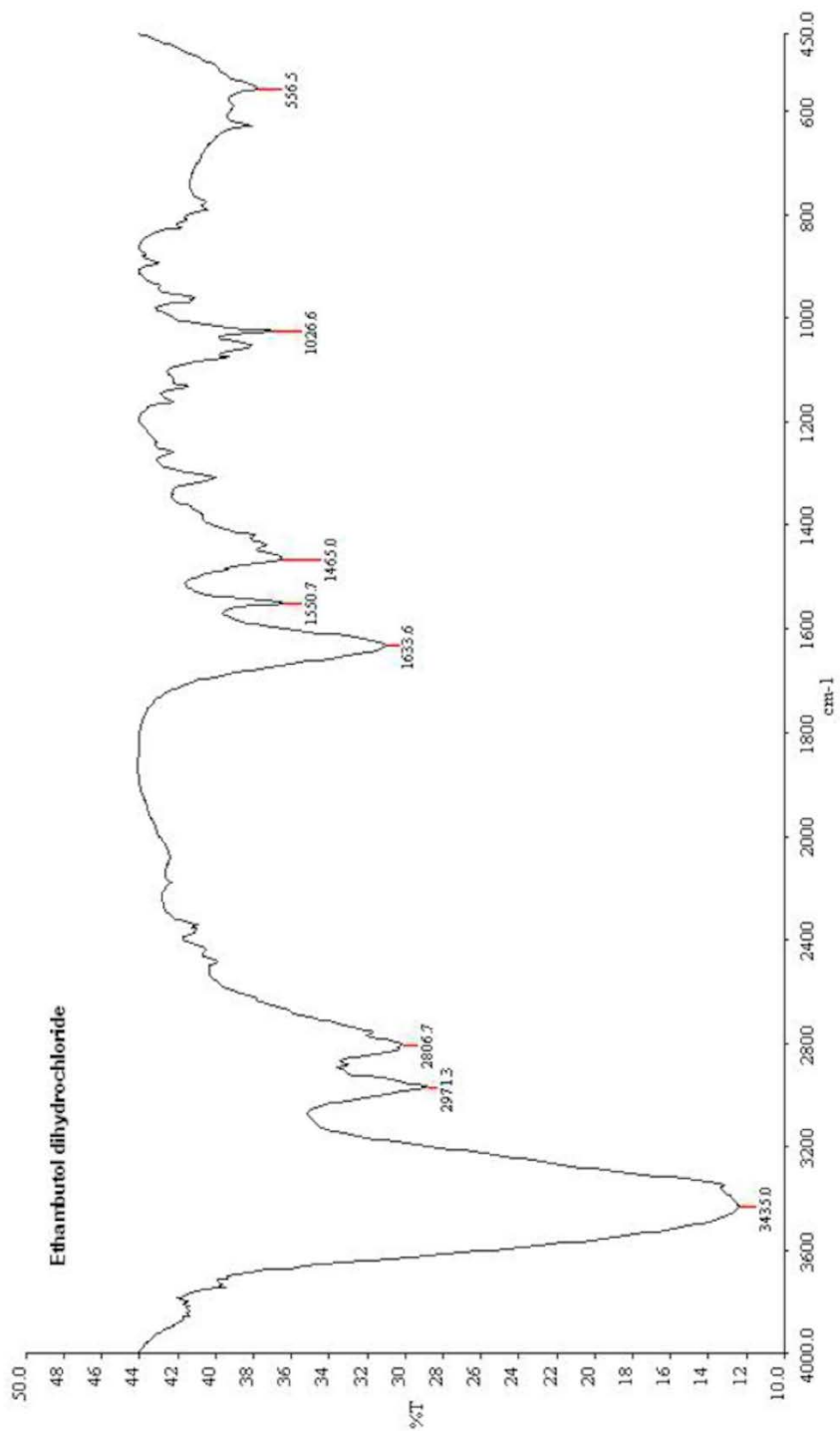
- Steckel, H., Brandes, H.G. 2004. A novel spray-drying technique to produce low density particles for pulmonary delivery. *Int J Pharm.* 278: 187–95.
- Steenwinkel, J.E.M., Vianen, W.V., Kate, M.T., Verbrugh, H.A., Agtmael, M.A., Schiffelers, R.M., Bakker-Woudenberg, I.A.J.M. 2007. Targeted drug delivery to enhance efficacy and shorten treatment duration in disseminated *Mycobacterium avium* infection in mice. *J Antimicrob Chemother.* 60:1064–1073.
- Tang, P., Chew, N., Chan, H.K., Raper, P. 2003. Limitation of determination of surface fractal dimension using N₂ absorption isotherms and modified Frenkel–Halsey–Hill theory. *Langmuir.* 19:2632–8.
- Tappenden, P., Harnan, S., Uttley, L., Mildred, M., Carroll, C., Cantrell, A. 2013. Colistimethate sodium powder and tobramycin powder for inhalation for the treatment of chronic *Pseudomonas aeruginosa* lung infection in cystic fibrosis: systematic review and economic model. *Health Technol Assess.* 17:1–182.
- Tee, S.K., Marriott, C., Zeng, X.M., Martin, G.P. 2000. The use of different sugars as fine and coarse carriers for aerosolised salbutamol sulphate. *Int J Pharm.* 208:111–123.
- Telko, M.J., Hickey, A.J. 2005. Dry powder formulation. *Respir care.* 50(9):1209–1227.
- Tena, A.F., Clara, P.C. 2012. Deposition of inhaled particles in the lungs. *Arch Bronconeumol.* 48(7):240–246.
- Tsaih, M.L., Chen, R.H. 2003. The effect of reaction time and temperature during heterogenous alkali deacetylation on degree of deacetylation and molecular weight of resulting chitosan. *J Appl Polym Sci.* 88:2917–2923.

- Van Crevel, R., Ottenhoff, T.H.M., Van der Meer, J.W.M. 2002 Innate immunity to *Mycobacterium tuberculosis*. *Clin Microbiol Rev.* 15: 294-309.
- Vllasaliu, D., Casettari, L., Fowler, R., Exposito-Harris R, Garnett M, Illuma L, Stolnik S. 2012. Absorption-promoting effects of chitosan in airway and intestinal cell lines: A comparative study. *Int J Pharm.* 430:151–160.
- Wanakule, P., Liu, G.W., Fleury, A.T., Roy, K. 2012. Nano-inside-micro: Disease-responsive microgels with encapsulated nanoparticles for intracellular drug delivery to the deep lung. *J Control Release.* 162:429–437.
- Weibel, E.R. 1963. Morphometry of the Human Lung. Berlin. Springer Verlag. 151.
- Westerman, E.M., De Boer, A.H., Le Brun, P.P.H., Touw, D.J., Roldaan, A.C., Frijlink, H.W., Heijerman, H.G.M. 2007. Dry powder inhalation of colistin in cystic fibrosis patients: a single dose pilot study, *J Cyst Fibros.* 6:284–292.
- WHO. Global tuberculosis control. 2011 WHO. 2: 9-27.
- Wilkinson, R.G., Shepherd, R.G., Thomas, J.P., Baughn, C. 1961. Stereo specificity in a new type of synthetic antituberculous agent. *J Am Chem Soc.* 83(9):2212–2213.
- Wydro, P., Krajewska, B., Wydro, H.K. 2007. Chitosan as a lipid binder: A langmuir monolayer study of chitosan-lipid interactions, *Biomacromolecules.* 8:2611-2617.
- Yang, Y., Wang, S., Wang, Y., Wang, X., Wang, Q., Chen, M. 2014. Advances in self-assembled chitosan nanomaterials for drug delivery. *Biotechnol Adv.* 1-16.
- Yi, H., Wu, L-Q., Bentley, W.E., Ghodssi, R., Rubloff, G.W., Culver, J.N. 2005. Biofabrication with chitosan. *Biomacromolecules.* 6:2881–94.

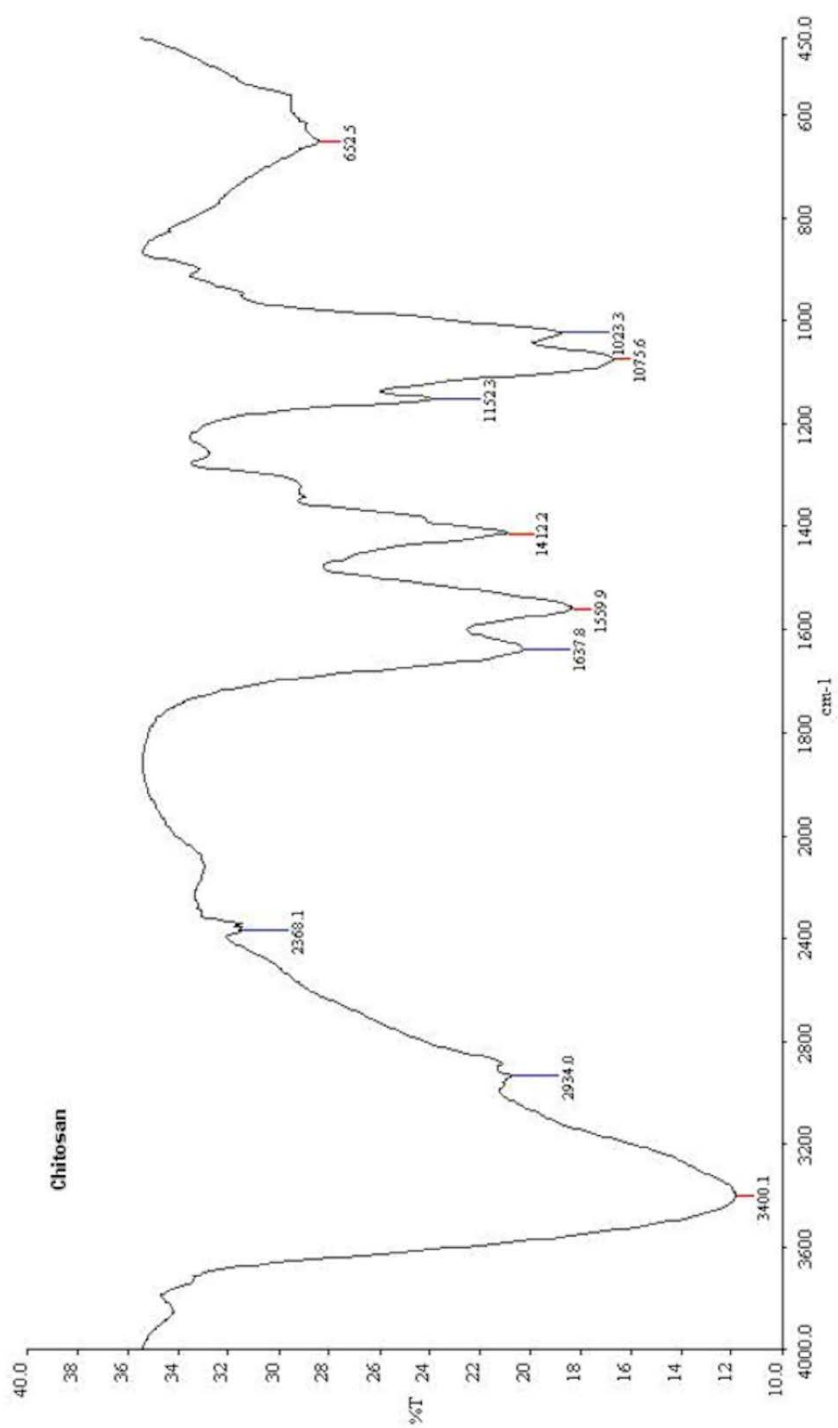
- Yoshida, S., Tanakab, T., Kitab, Y., Kuwayama, S., Kanamaru, N., Murakib, Y., Hashimotob, S., Inoueb, Y., Sakatanib, M., Kobayashi, E., Kanedad, Y., Okada M. 2006. DNA vaccine using hemagglutinating virus of Japan-liposome encapsulating combination encoding mycobacterial heat shock protein 65 and interleukin-12 confers protection against *Mycobacterium tuberculosis* by T cell activation. *Vaccine*. 24:1191–1204.
- Zahoor, A., Sadhna, S., Khuller, G.K. 2005. Inhalable alginate nanoparticles as antitubercular drug carriers against experimental tuberculosis. *Int J Antimicrob Ag*. 26:298–303.
- Zeng, X.M., Martin, G.P., Marriott, C., Pritchard, J. 2000. The influence of carrier morphology on drug delivery by dry powder inhalers. *Int J Pharm*. 200:93–106.
- Zhang, J., Khoo, K.H., Wu, S.W., Chatterjee, D. 2007. Characterization of a distinct arabinofuranosyl transferase in *Mycobacterium smegmatis*. *J Am Chem Soc*. 129:9650.

Appendices

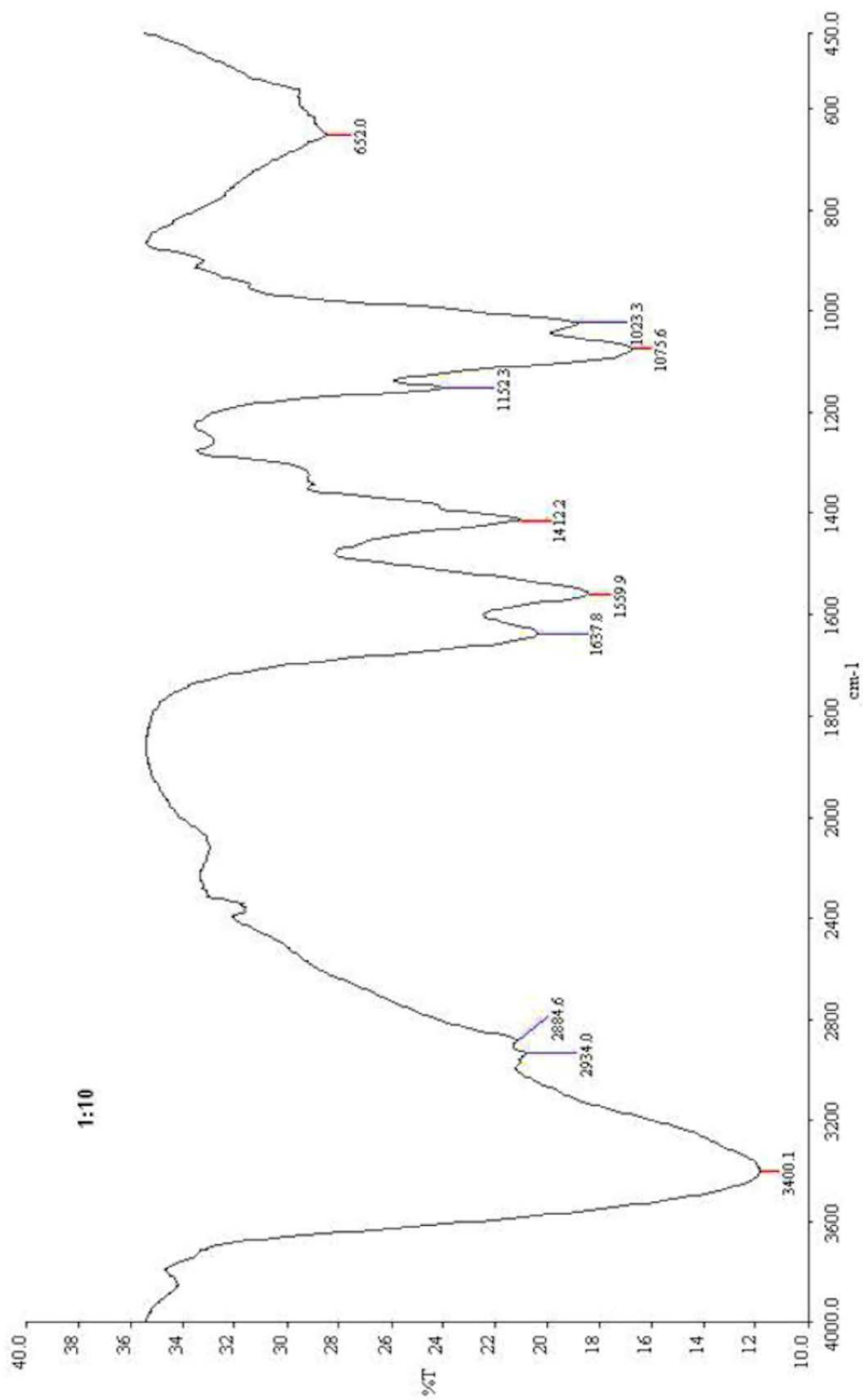
FTIR spectra of EDH, Chitosan and its formulations



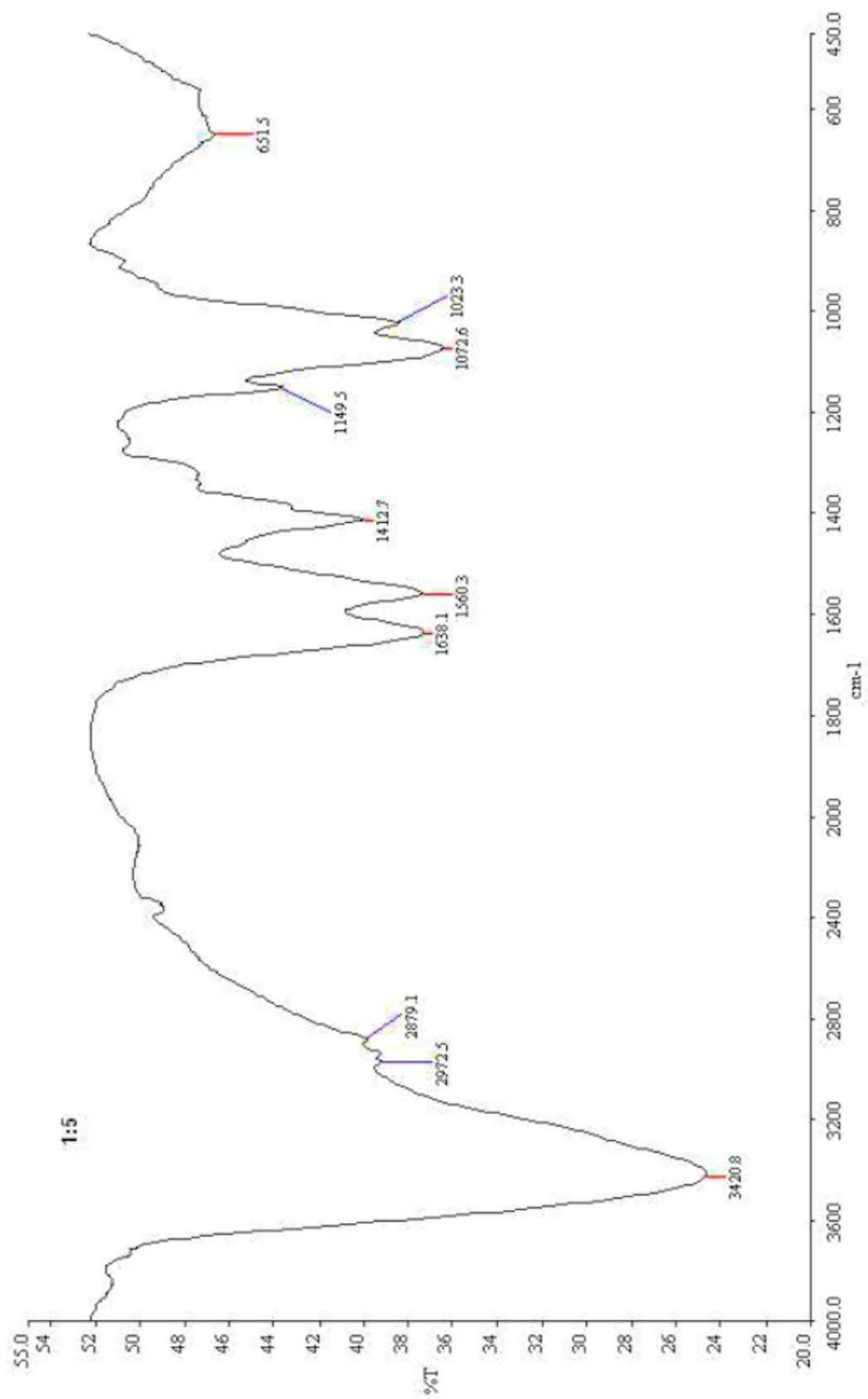
FTIR spectra of ethambutol dihydrochloride



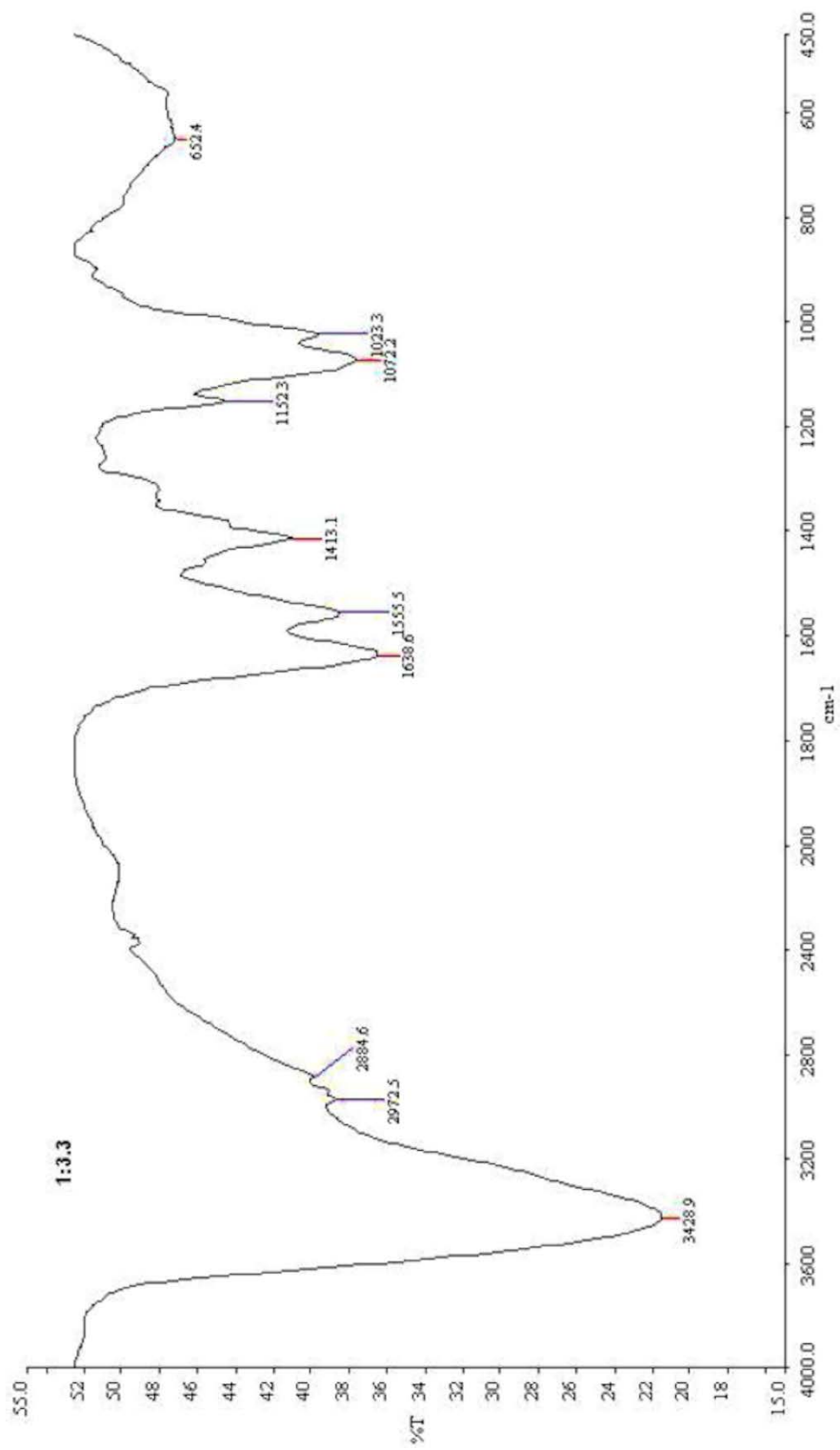
FTIR spectra of chitosan



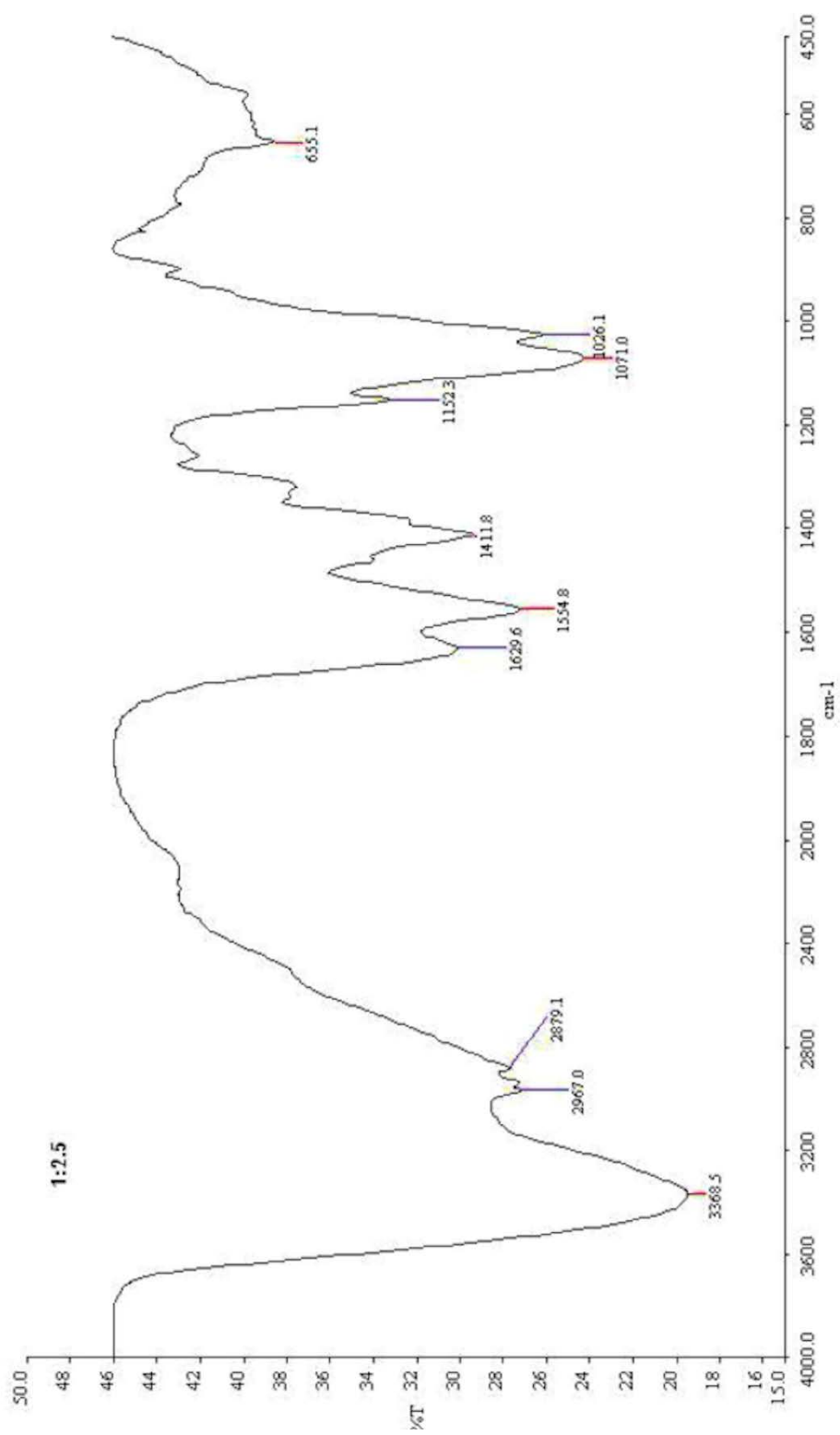
FTIR spectra of EDH:Chitosan (1:10)



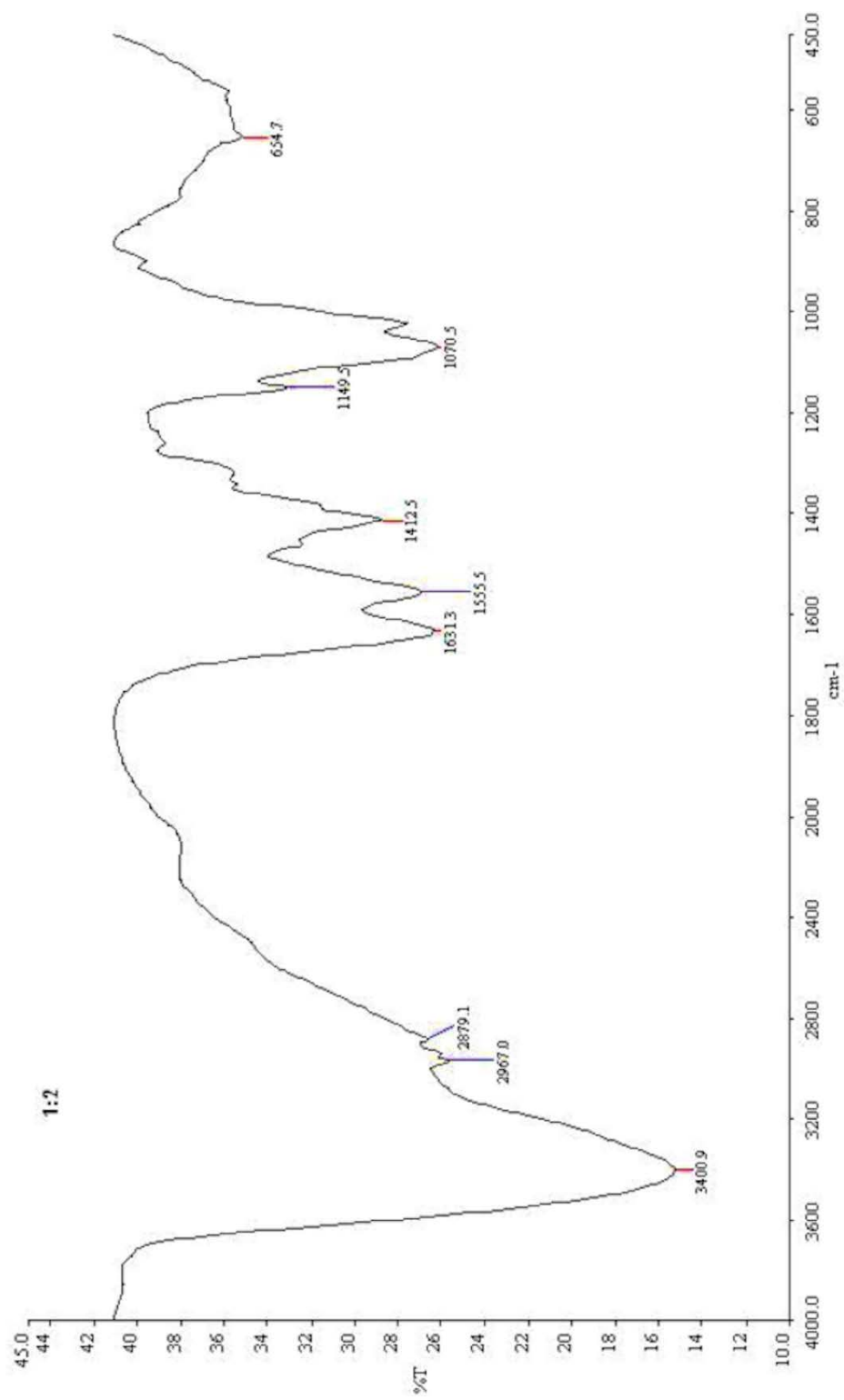
FTIR spectra of EDH:Chitosan (1:5)



FTIR spectra of EDH:Chitosan (1:3.3)



FTIR spectra of EDH:Chitosan (1:2.5)



FTIR spectra of EDH:Chitosan (1:2)

VITAE

Name: Md Iftekhar Ahmad **National:** India

Student ID: 5310730012

Educational Attainment

Degree	Name of Institution	Year of Graduation
M. Pharm	Manipal University, Karnataka, India	2005
B. Pharm	Jamia Hamdard, New Delhi, India	2003

Scholarship Awards during Enrolment

1. Thesis Grant, Educational fee and salary
The Graduate School, Prince of Songkla University
2. Thesis Grant
The Nanotec-PSU Excellence center on Drug Delivery System, Faculty of Pharmaceutical Sciences, Prince of Songkla University.
3. Conference Scholarship
Faculty of Pharmaceutical Sciences, Prince of Songkla University.

List of Publication and Proceeding

Publications

Ahmad MI, Ungphaiboon S, Srichana T, 2014. The development of dimple-shaped chitosan carrier for ethambutol dihydrochloride dry powder inhaler. *Drug Dev Ind Pharm*. Early online: 1-10.

Ahmad MI, Nakpheng T, Srichana T, 2014. The safety of ethambutol dihydrochloride dry powder formulations containing chitosan for the possibility of treating lung tuberculosis. *Inhal Toxicol* (Accepted).

Proceedings

1. Presented oral presentation on the “Determination of cell toxicity and bioactivity of ethambutol dihydrochloride as a dry powder inhaler formulation,” CDD 2014, Krabi, Thailand, May 1-3, 2014.

2. Presented oral presentation on “The development of dimple shaped dry powder carrier for ethambutol dihydrochloride,” Inhalation Asia 2013, University of Hongkong, Hongkong, June 25-28, 2013.
3. Presented oral presentation on “The development of chitosan as a carrier for ethambutol dihydrochloride to target alveoli” The 2nd Current Drug Development (CDD 2012), Phuket, Thailand, May 2-4, 2012.